Instituto de Biociências

UNIVERSIDADE ESTADUAL PAULISTA
"JÚLIO DE MESQUITA FILHO"
Campus de Botucatu

PG-BGA

Perfil global de expressão de MicroRNAs na próstata ventral de ratos submetidos à restrição proteica materna: Efeitos perinatais e reflexos no envelhecimento

MS. FLÁVIA BESSI CONSTANTINO

Tese apresentada ao Instituto de Biociências, Campus de Botucatu, UNESP, para obtenção do título de Doutor no Programa de Pós-Graduação em Biologia Geral e Aplicada, Área de concentração Biologia Estrutural e Funcional.

BOTUCATU – SP

2021

UNIVERSIDADE ESTADUAL PAULISTA "Júlio de Mesquita Filho"

Instituto de Biociências-Departamento de Biologia Estrutural e Funcional

Perfil global de expressão de MicroRNAs na próstata ventral de ratos submetidos à restrição proteica materna: Efeitos perinatais e reflexos no envelhecimento

MS. FLÁVIA BESSI CONSTANTINO

PROF. DR. LUIS ANTONIO JUSTULIN JUNIOR

PROF. DR. ROBSON FRANCISCO CARVALHO

Tese apresentada ao Instituto de Biociências, Campus de Botucatu, UNESP, para obtenção do título de Doutor no Programa de Pós-Graduação em Biologia Geral e Aplicada, Área de concentração Biologia Estrutural e Funcional.

BOTUCATU – SP

2021

Ficha catalográfica

FICHA CATALOGRÁFICA ELABORADA PELA SEÇÃO TÉC. AQUIS. TRATAMENTO DA INFORM.
DIVISÃO TÉCNICA DE BIBLIOTECA E DOCUMENTAÇÃO - CÂMPUS DE BOTUCATU - UNESP
BIBLIOTECÁRIA RESPONSÁVEL: ROSEMEIRE APARECIDA VICENTE-CRB 8/5651

Constantino, Flavia Bessi.
Perfil global de expressão de MicroRNAs na próstata ventral de ratos submetidos à restrição proteica materna : efeitos perinatais e reflexos no envelhecimento / Flavia Bessi Constantino. - Botucatu, 2021

Tese (doutorado) - Universidade Estadual Paulista "Júlio de Mesquita Filho", Instituto de Biociências de Botucatu
Orientador: Luis Antonio Justulin Junior
Coorientador: Robson Francisco Carvalho
Capes: 20603002

1. Próstata - Câncer. 2. MicroRNAs. 3. Carcinogênese. 4. Ratos Sprague-Dawley. 5. Dieta de baixo teor proteico.

Palavras-chave: Cancer; DOHaD; Prostata; miRNAs.

A minha Família, Namorado e Amigos…

Dedico

Agradecimentos

Ao **Dr. Luis Antonio Justulin Junior**, pelo conhecimento compartilhado, pela confiança em meu trabalho, por sempre acreditar em meu potencial e me apoiar sempre, sem você não teria chegado tão longe. Obrigada por me receber de braços abertos no laboratório e me tornar uma amante da pesquisa.

Ao **Laboratório de Matriz Extracelular (Labmec)** e agregados, pelo companheirismo, conhecimento compartilhado, por todo apoio em momentos difíceis e pelas risadas.

Ao **Miguel Antunes,** por sempre acreditar em mim, me fazer buscar sempre mais, por todo apoio e carinho. Obrigada por além de ser meu técnico, ser meu amigo.

A **minha Família,** por sempre serem meu porto seguro e me fazerem alçar voos mais altos. Obrigada por sempre me apoiarem e estarem sempre presentes mesmo longe.

Ao **Renato Colenci**. por sempre estar ao meu lado, por me fazer uma pessoa melhor, por sempre me ouvir e dar conselhos, por fazer meus dias mais felizes. Obrigada, sem o seu apoio não teria conseguido.

As agencias de fomento **FAPESP** (processo nº2017/08716-6) e **CAPEs** pelo suporte financeiro.

E a **todos que contribuíram** de alguma forma para o meu crescimento e para a confecção desta tese.

"A tarefa não é tanto ver aquilo que ninguém viu, mas pensar o que ninguém ainda pensou sobre aquilo que todo mundo vê."

(Arthur Schopenhauer)

Sumário

Lista de abreviaturas

ACE2: angiotensin-converting enzyme 2

BPH: Benign prostatic hyperplasia

CaP: câncer de próstata

CEEA: Comissão de Ética na Experimentação Animal

COBEA: Colégio Brasileiro de Experimentação Animal

COVID-19: coronavirus disease 2019

CTR: Controle

CTSL: cathepsin L

CUG: complexo urogenital

DAG: distância ano genital

DEGs: differentially expressed genes

DG: Dia gestacional

DM2: Diabetes mellitus do tipo 2

DNMT: DNA metil transferases

DOHaD: Developmental Origins of Health and Disease

DPN: dias pós-natal

DPP4: dipeptidyl peptidase 4

GEO: Gene Expression Omnibus

GLLP: *Gestational and lactational low protein diet*

GSEA: Gene Set Enrichment Analysis

GSH: Glutationa Peroxidase

HAC: histona acetilase

HDAC: deacelilase

HE: hematoxilina-eosina

HPB: hiperplasia prostática benigna

IGF-1: Fator de crescimento semelhante à insulina tipo 1

KOBAS: *KEGG Orthology Based Annotation System*

LPD: Low protein diet

LR: Likelihood Ratio

miRNA: microRNAs

mRNAS: RNA mensageiro

ORF8: open reading frame 8

PA: lobo anterior

PCA: análise de componentes principais

PCa: Prostate cancer

PDL: lobo dorsolateral

PF: Programação Fetal

PND: Postnatal day

PPI: protein-protein interactions

PTHrP: *parathyroid hormone-related protein*

PV: lobo ventral

RBD: receptor-binding domain

RTKs: receptores de tirosina-quinase

SARS-CoV-2: severe acute respiratory syndrome coronavirus 2

Shh: Sonic hedgehog

SOD: Superóxido Dismutase

Tbx3: *T-box transcription factor*

TCGA: *The Cancer Genome Atlas*

TMPRSS2: cellular transmembrane serine protease 2

USG: seio urogenital

ZIKV: Zika virus

Lista de Figuras

Capítulo 1

Capítulo 2

Capítulo 3

Lista de tabelas

Supplementary Table 3. Functional enrichment analysis list generated in the Metascape tool (https://metascape.org) [DOI: 10.1038/s41467-019-09234-6] for DEGs in the placenta tissues (1º trimester x 2º trimester and 1º trimester x 2º trimester.

Supplementary Table 4. Human-SARS-CoV Interactome based on the in silico computational framework P-HIPSTer (http://phipster.org/).

Supplementary Table 5. Human-ZIKA Interactome based on the in silico computational framework P-HIPSTer (http://phipster.org/).

Supplementary Table6. The Human-SARS-CoV interactome obtained in the P-HIPSTer (http://phipster.org/) for placenta.

Supplementary Table 7. The Human-ZIKA interactome obtained in the P-HIPSTer (http://phipster.org/) for placenta.

Supplementary table 8. Human-SARs Interactome based on literature.

Resumo

Nas últimas décadas, foi observado aumento na incidência de câncer na população. Estudos mostram que o câncer pode se originar de insultos sofridos por indivíduos durante a vida intrauterina, visto que que este período é caracterizado pela capacidade do embrião/feto em se adaptar às mudanças ambientais, alterando a expressão gênica por mecanismos pós-transcricionais. Já foi demonstrado que a restrição proteica materna promove a carcinogênese da próstata em ratos idosos; No entanto, há falta de informações sobre o mecanismo molecular envolvido nesse processo. Assim, objetivamos identificar os possíveis microRNAs desregulados em ratos jovens programados e localizar seus possíveis alvos associados à carcinogênese da próstata. Para isso, ratos machos Sprague Dawley nascidos de mães alimentadas com dieta padrão (17% de proteína), grupo controle (CTR), ou dieta pobre em proteínas (6% de proteína), grupo *gestational and lactational low protein diet* (GLLP), durante a gestação e lactação foram sacrificados no dia pós-natal 21. O sangue foi coletado para analises hormonais e a próstata ventral foi processada para morfologia e por sequenciamento, HigSeq -2500 Illumina, para determinar o perfil do microRNoma. Dados de sequenciamento de miRNAs de pacientes com câncer de próstata, oriundos do *the cancer genome atlas* (TCGA), foram reanalisados para comparação com os resultados de ratos. Além disso, foi realizada a transfecção do miR-33 em células PNT-2 para avaliar a expressão de seus alvos e a viabilidade celular após tratamento através da técnica de MTT. Assim, foi observado atraso no desenvolvimento da próstata ventral e aumento dos níveis de testosterona e expressão de estrogênio em ratos GLLP. Além disso, 20 miRNAs foram identificados como diferencialmente expressos, 6 *down* regulados e 14 *up* regulados. Os resultados de enriquecimento para miRNAs *down* regulados estão relacionados às vias do câncer e da angiogênese, enquanto os miRNAs *up* regulados estão enriquecendo vias de retículo endoplasmático e de carcinoma. A reanálise do sequenciamento de miRNA de TCGA revelou 7 em comum com o grupo GLLP. Um deles é o miR-33 que, além de ser *down* regulado na próstata, também é desregulado no testículo, na glândula adrenal e no fígado, dados gerados através do RTq-PCR. Sua supra expressão nas células transfectadas causou uma diminuição na viabilidade celular e seu alvo, CYP1B1, é uma enzima importante no metabolismo do estrogênio, que pode levar à carcinogênese mediada por mudanças nos níveis hormonais e transformação do estradiol. Concluímos que o miR-33 é um alvo importante para explicar as alterações causadas pela LPD materna podendo, ser considerado um considerável biomarcador por ser desregulado em vários órgãos analisados.

Palavras-Chave: Programação Fetal, Câncer de Próstata e MicroRNAs

Capítulo 1: Revisão Bibliográfica

1.1 Programação Fetal

A boa nutrição é fundamental para a manutenção da saúde, sendo que nenhum país pode alcançar a cobertura universal de saúde sem investir em ações que garantam a nutrição essencial de sua população. A má alimentação é uma das maiores causas de comorbidade e morte no mundo, mais que o Tabaco e a hipertensão (AFSHIN et al., 2019). Além disso, está relacionada com o aumento do risco de doenças infecciosas, como pneumonia, diarreia, sarampo e tuberculose, assim como o aumento de doenças no coração, câncer, diabetes além de mortes neonatais (BLACK et al., 2013; CAULFIELD et al., 2004; HOFFMAN et al., 2020; PELLETIER et al., 1995; PORTELA et al., 2021). Em 2017, 56% das mortes de crianças com menos de 5 anos foram atribuídas à má nutrição materna (INSTITUTE FOR HEALTH METRICS AND EVALUATION (IHME), 2018). Estudos vem mostrando que a má nutrição materna pode estar relacionada com o aparecimento de doenças crônicas na vida adulta dos filhos, mostrando que a origem dessas doenças pode se dar a partir de insultos sofridos durante o período embrionário/fetal. Esse processo ficou conhecido como Programação Fetal (PF) (BARKER, 2007; MERICQ et al., 2017; PINHO et al., 2014; SANTOS et al., 2019).

Um dos primeiros pesquisadores a estudar a PF foi Ravelli e colaboradores em 1976 (RAVELLI; STEIN; SUSSER, 1976). Eles fizeram um estudo coorte retrospectivo com 300.000 pessoas que foram expostas à fome holandesa durante o período pré-natal e logo após o nascimento. A Fome Holandesa Aconteceu em 1944-45 durante a Segunda Guerra mundial que por conta da invasão alemã e pelo congelamento do mar impedindo a chegada de navios, a população ficou sem abastecimento de comida e passou a ter uma alimentação de 400-800 calorias diariamente. Ravelli e colaboradores (1976) observaram que se o feto foi exposto à restrição alimentar durante o último trimestre de gestação, ele apresentava uma menor probabilidade de obesidade por esse período ser um período crítico para o desenvolvimento de tecido adiposo. Porém, se a restrição alimentar acomete o feto durante a primeira metade da gestação o quadro muda, tendo maior probabilidade de obesidade pois a restrição alimentar afeta o centro hipotalâmico responsável pela saciedade e crescimento fetal. Após este período, a

alimentação deixou de ser restrita e levou a um excesso de gordura no organismo o que ocasiona um maior crescimento e aumento de células adiposas (RAVELLI; STEIN; SUSSER, 1976).

Além de Ravelli, o epidemiologista inglês David Barker também encontrou resultados pertinentes. Em 1989, BARKER e seus colaboradores relacionaram o baixo peso ao nascimento com mortes por doenças cardíacas na vida adulta (BARKER et al., 1989). Em outro estudo demonstraram que pacientes com baixo peso ao nascimento, associado com maior tamanho de placenta apresentam maior pressão arterial na vida adulta (BARKER et al., 1990). Além disso, estudos vem mostrando que a restrição alimentar materna pode levar a modificação do metabolismo de colesterol, afetar níveis de insulina podendo iniciar um estado de resistência à insulina e levar ao *Diabetes mellitus* do tipo 2 (DM2) na vida adulta (BARKER et al., 1993; BARKER, 1997). Por apresentar baixo peso ao nascimento elas passam por um período de crescimento acelerado (*catch-up growth*) (FITZHARDINGE; STEVEN, 1972), o que contribui para aumentar o risco de sobrepeso e obesidade já na infância. Ainda não se sabe quais fatores determinam o crescimento acelerado no período pós-natal. No entanto, alguns estudos sugerem que esse tipo de crescimento pode estar associado a fatores inerentes ao período intrauterino e, consequentemente, as características e hábitos maternos durante a gravidez.

Através destes e outros estudos se originou a Hipótese de Barker, e com o passar do tempo, a ideia de programação fetal se estendeu para outros períodos, além do período fetal, e não ficou restrita ao processo de doença, mas à saúde também, originando a denominada *Developmental Origins of Health and Disease* (DOHaD) (GLUCKMAN; HANSON; BUKLIJAS, 2010; SCHULZ, 2010).

1.2 Programação Fetal e baixa ingesta de Proteína

A organização alimentar e agrícola das nações unidas mostra que em países da Europa, Oceania e América do Norte as pessoas se alimentam em média de 100 gramas (g) de proteínas por dia. Os países do sul da Ásia, África Subsaariana e América do Sul tem uma média de 50 a 90 g de proteína. No entanto, a maioria dos países de baixa renda está dentro da faixa entre 30-60 g dia (UNITED NATIONS FOOD AND

AGRICULTURAL ORGANIZATION (FAO), 2020). A porcentagem mínima de proteína recomendada pela organização mundial de saúde é de no mínimo 0,8 g/dia de proteína por quilograma de peso para um indivíduo adulto, sendo que para gestantes e lactantes essa recomendação aumenta. Assim, um dos grandes fatores que levam a má nutrição é a ausência de proteína na alimentação, seja este um fator cultural ou socioeconômico. Além de que, diversos modelos tem sido utilizados para melhor conhecimento dos efeitos da PF, sendo o mais utilizado a dieta hipoproteica oferecida durante a gestação e lactação, principalmente utilizando-se de modelos com animais de laboratório (COLOMBELLI et al., 2017; DE BRITO ALVES et al., 2016; OZANNE; HALES, 2004; PINHO et al., 2014). Segundo o Instituto Americano de Nutrição para dietas de ratos o indicado é que a ração tenha pelo menos 12% de proteína. A maioria dos estudos com programação fetal por restrição proteica utiliza valores de 6-8% de proteína para os animais restritos contra 20-22% para os animais controle.

Estudos vem mostrando que a prole de mãe que se alimenta com baixa quantidade de proteína tem menor peso ao nascimento, seguido pelo conhecido *catch-up growth* (crescimento acelerado), resistência à insulina e DM2 na vida adulta, diminuindo a expectativa de vida destes individuos (EMBLETON et al., 2016; MCMILLEN; ADAM; MÜHLHÄUSLER, 2005; PETRY et al., 2001). Quando a dieta hipoproteica vem seguida de um estilo de vida desfavorável como o consumo de uma dieta hiperlipídica, sedentarismo e consumo de alimentos processado, os quadros clínicos são agravados (DEARDEN; OZANNE, 2014; KWON et al., 2012; OZANNE; HALES, 2004).

O consumo de uma dieta hipoproteica também exibe resistência à insulina em tecido adiposo (TARRY-ADKINS et al., 2015), fibrose e esteatose hepática e um processo inflamatório aumentado (KWON et al., 2012; TARRY-ADKINS et al., 2016). Há redução de crescimento de diferentes órgãos, dislipidemia, elevação da pressão sistólica (hipertensão), disfunção renal e vascular (BLACK et al., 2015; DE BRITO ALVES et al., 2016; FALCÃO-TEBAS et al., 2012; LEANDRO et al., 2012). Acarreta menor número de néfrons no rim (HABIB et al., 2012; SENE et al., 2013), menor quantidade de células beta-pancreática e de ilhotas de Langerhans no pâncreas (CALZADA et al., 2016; DAHRI

et al., 1991), proporção alterada entre os tipos celulares e aumento de estresse oxidativo (BURNS et al., 1997; TARRY-ADKINS et al., 2016; VEGA et al., 2016), menor número de neurônios que controlam o apetite no hipotálamo (PLAGEMANN et al., 2000) e menor número de alvéolos pulmonares (ZANA-TAIEB et al., 2013). Em conjunto, estes dados demonstram que o *status* nutricional durante o desenvolvimento pré e pós-natal alteram o metabolismo da prole e a morfofisiologia de diferentes órgãos e sistemas, sendo que as consequências podem ser observadas tanto ao nascimento, como a longo prazo.

1.3 Próstata e a programação Fetal por baixa ingesta de proteína

A próstata é uma glândula exócrina acessória do sistema genital cujo desenvolvimento e homeostasia encontram-se sob controle androgênico (BIANCARDI et al., 2017; CUNHA et al., 1985; ZAVIACIC; ABLIN, 2000). Ela secreta um complexo proteolítico composto por fosfatase ácida, ácido cítrico, fibrinolisina, enzimas específicas e outros componentes do fluido seminal que auxiliam no sucesso reprodutivo (AUMÜLLER; SEITZ, 1990; MARKER et al., 2003).

A próstata está localizada no compartimento subperitoneal, anterior ao reto e inferior à bexiga urinaria (SCHAUER; ROWLEY, 2011). Estudos mostram que ela possui três zonas morfologicamente distintas: (1) zona periférica (região com maior acometimento de câncer), (2) zona de transição e (3) zona central, além de uma região não glandular, o estroma fibromuscular anterior (Figura1.A) (LOWSLEY, 1912).

Já a próstata de roedores apresenta quatro lobos: lobo anterior (PA), lobo ventral (PV), lobo dorsal e lobo lateral, sendo os dois últimos também chamados de lobo dorsolateral (PDL) (Figura 1B). Cada lobo é localizado em posição específica em torno da uretra (LOWSLEY, 1912). Se fizermos uma homologia com a próstata humana, o lobo anterior corresponde á zona central da glândula e o lobo dorsolateral a zona periférica. O lobo ventral não apresenta nenhuma homologia com a próstata humana, porém, é o mais responsivo a andrógeno, de rápido e fácil acesso, além de geralmente não desenvolver prostatite, por essas e outras razões, este é o lobo mais estudado (ROY-BURMAN et al., 2004).

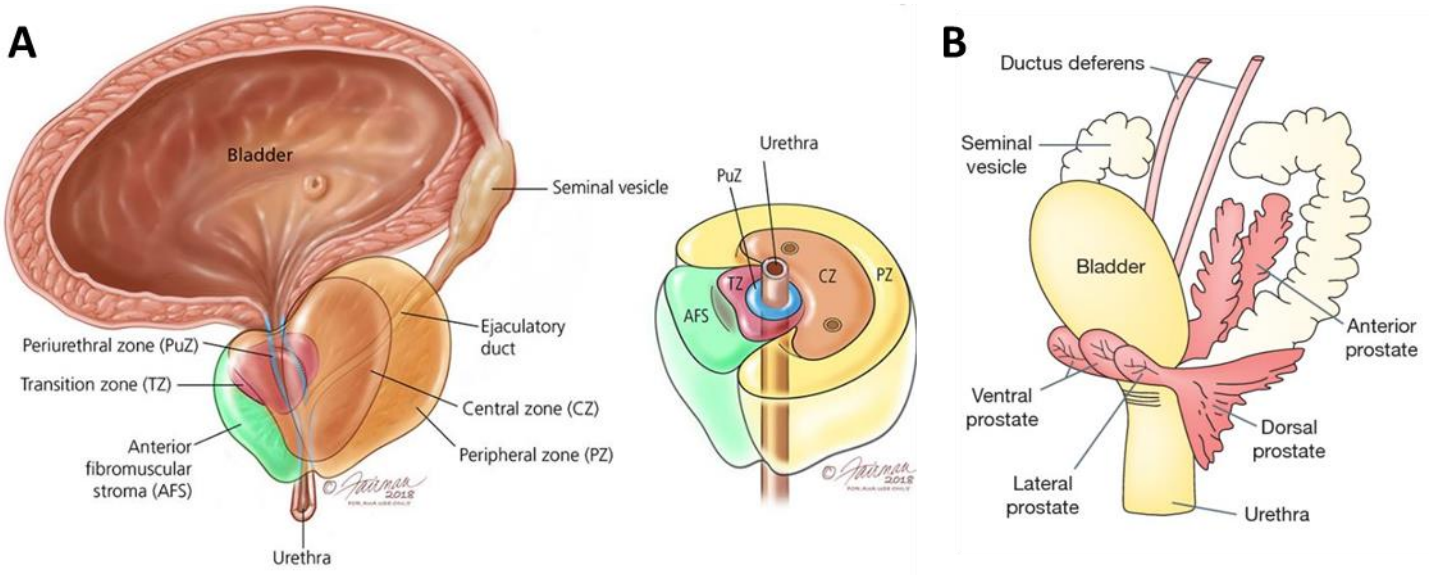

Figura 1. Organização anatômica da próstata. **A.** Próstata humana. **B.** Próstata de camundongo. Imagem A retirada do site https://www.urologyhealth.org/urologic-conditions/prostatitis-(infection-of-the-prostate) Acesso:03/08/2020 e imagem B adaptada de (AHMAD; SANSOM; LEUNG, 2008).

Nos camundongos e ratos, o desenvolvimento prostático tem início por volta do 17º dia de gestação e, no humano entre 9-10 semanas de gestação (WELSH et al., 2008). A próstata se desenvolve através de um processo conservador, denominado de morfogênese de ramificação, onde pequenos brotos se projetam a partir do epitélio do seio urogenital (USG). Particularmente no rato, a síntese de testosterona pelos testículos fetais tem início entre os dias 13-14 da gestação (DG) (WILSON et al., 1983). Em resposta aos andrógenos, o epitélio do UGS passa a expressar *Sonic hedgehog* (Shh), que por sua vez estimula expressão do gene homeobox *Nkx3.1* no DG15.5, dois dias antes de surgirem os primeiros brotos prostáticos (WILHELM; KOOPMAN, 2006). Depois do nascimento, ocorre alongamento dos brotos e início da morfogênese com a formação dos ductos glandulares (PRINS et al., 1992), visto que em ratos a maior parte do desenvolvimento acontece durante os primeiros 15 dias pós-natal (DPN) enquanto que, em humanos o desenvolvimento é quase todo durante a vida intrauterina (TIMMS; MOHS; DIDIO, 1994). Em ambos, esse processo se estende até que a maturidade sexual seja atingida com a puberdade (MARKER et al., 2003) (Figura 2).

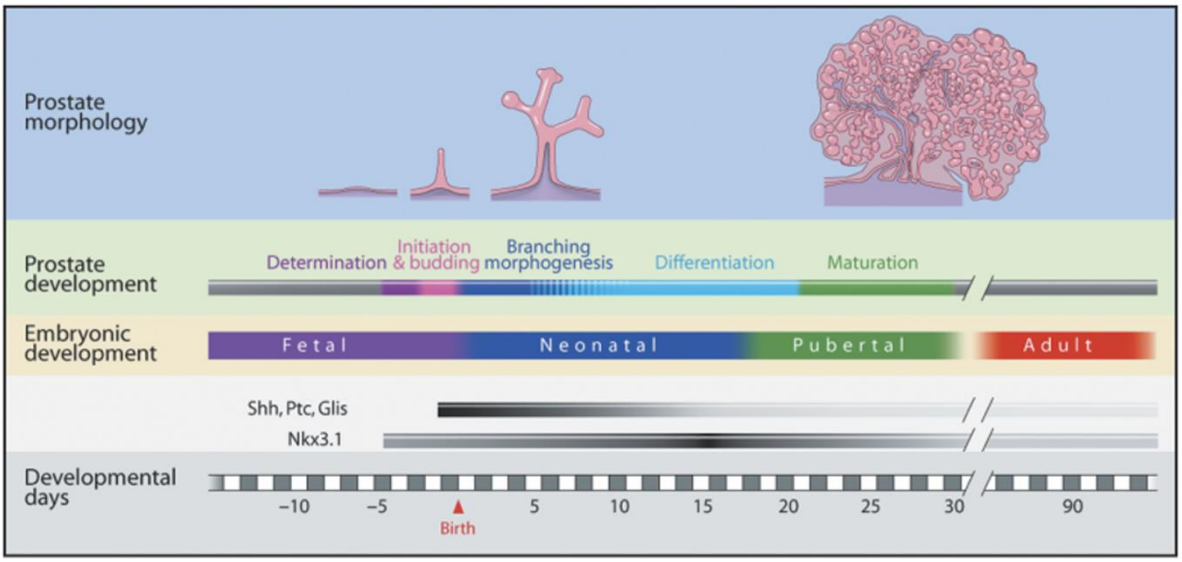

Figura 2. Estágios do desenvolvimento da próstata de rato e humano. Imagem de (PRINS; PUTZ, 2008).

A próstata apresenta uma complexa rede de ducto, que nada mais é do que uma região de lúmen revestido por células epiteliais secretoras, que possuem polaridade apical-basal e são responsáveis pela síntese e secreção de proteínas e fluidos para o lúmen prostático (MARKER et al., 2003). As células epiteliais se organizam de forma a dar a característica histológica de glândula túbulo-alveolar composta, o seu epitélio usualmente é colunar alto, porém pode haver alteração dependendo do estado funcional da glândula (DERMER, 1978) (Figura 3). O componente estromal engloba todos os elementos celulares e extracelulares que estão fora da lâmina basal epitelial como a camada fibromuscular que cerca a glândula. Além da camada muscular, o estroma também apresenta fibroblastos, vasos sanguíneos e os pericitos associados, células imunitárias, terminações nervosas e vasos linfáticos, os quais são incorporados a uma matriz extracelular colagenosa (AUMÜLLER; SEITZ, 1990).

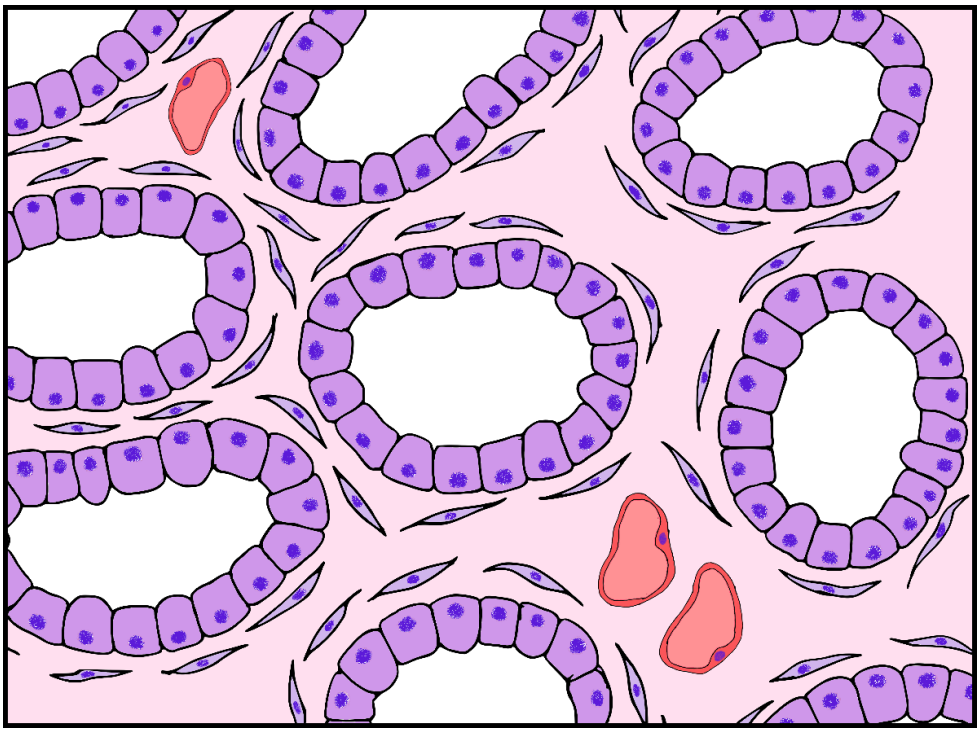

Figura 3. Esquema da glândula prostática. Imagem de Mateus Betta de Oliveira.

Portanto, além de sua importância para a fertilidade, nos últimos anos a próstata tem despertado grande interesse médico-científico pela alta incidência de distúrbios, principalmente a hiperplasia prostática benigna (HPB) e o câncer de próstata (CaP) (DASGUPTA; SRINIDHI; VISHWANATHA, 2012). O CaP é a terceira causa de óbitos por câncer entre homens no mundo e é o segundo mais incidente (Tabela 1)(“Global Cancer Observatory” acess:26/05/2021).

Frente a isso e considerando que o período intrauterino é caracterizado pela capacidade do embrião/feto em se adaptar às mudanças ambientais, alterando a expressão gênica por mecanismos pós-transcricionais, vários autores demonstraram o impacto negativo de alterações do ambiente intrauterino sobre o desenvolvimento e fisiologia prostática. Ratos do DPN 21 submetidos a restrição proteica materna apresentaram menor peso prostático, com diminuição do tamanho nos ácinos da PDL (RAMOS et al., 2010). Pinho et al. (2014) também observaram atraso no desenvolvimento prostático associado com diminuição de proliferação celular na prole de animais submetidos ao mesmo protocolo e analisados no DPN 1.

Tabela 1. Distribuição proporcional dos dez tipos de câncer mais incidentes estimados para 2020 em homens, exceto pele não melanoma, (https://gco.iarc.fr/) acesso: 26/05/2021.

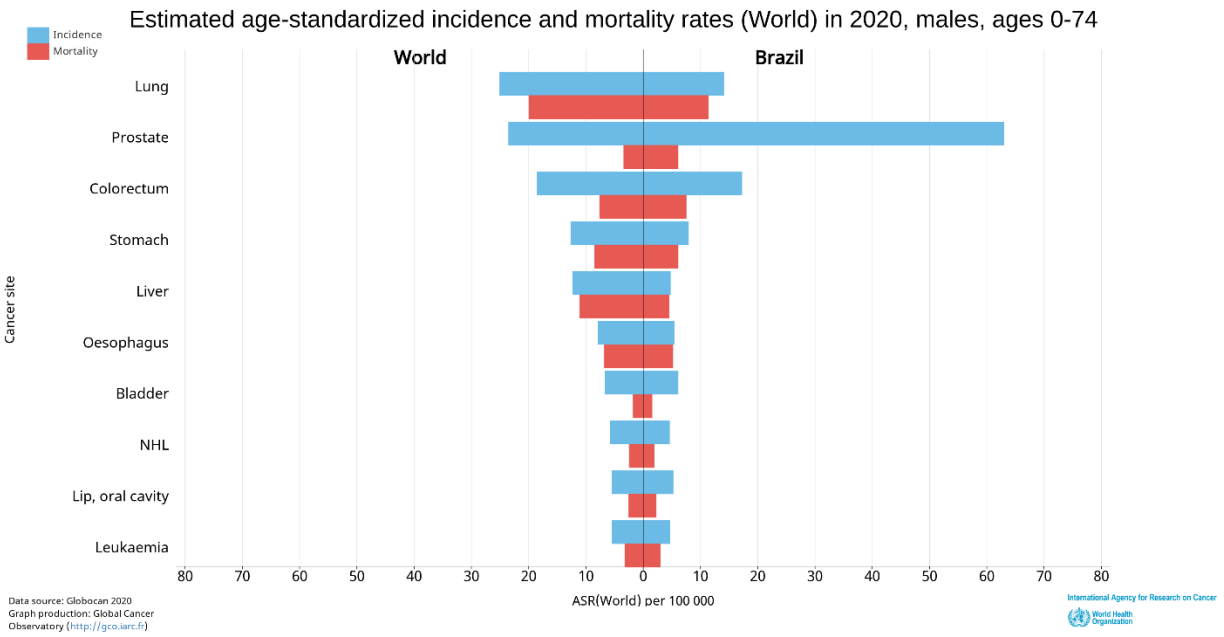

Nosso grupo de pesquisa demonstrou recentemente que a restrição proteica perinatal reduziu o processo de angiogênese prostática, levando a menor troca de moléculas entre os vasos e os compartimentos epitelial e estromal, impactando negativamente o desenvolvimento glandular. Estes resultados foram relacionados à menor concentração de testosterona, insulina e fator de crescimento semelhante à insulina tipo 1 (IGF-1) circulante, com efeitos negativos sobre os índices de proliferação e diferenciação do epitélio glandular (COLOMBELLI et al., 2017). Mais recentemente, observamos que ratos com 540 dias de idade que sofreram restrição proteica na gestação e lactação apresentaram maior incidência de lesões prostáticas, com aumento na incidência de neoplasia intraepitelial (SANTOS et al., 2019). Estes dados demonstram que a restrição proteica materna é suficiente para desencadear um aumento de incidência de lesões prostáticas na prole durante o envelhecimento. Entretanto, os mecanismos moleculares envolvidos neste processo ainda não foram totalmente esclarecidos.

1.4 Mecanismos Epigenéticos Envolvidos na Programação Fetal

O período de desenvolvimento intrauterino é caracterizado pela grande plasticidade e habilidade do embrião/feto em responder a alterações ambientais (dieta,

estresse e hormônios), modulando a expressão de genes envolvidos com o controle da proliferação e diferenciação celular em uma fase de morfogênese de órgãos e sistemas vitais (BURTON; FOWDEN; THORNBURG, 2016). Entretanto, pouco se sabe sobre os agentes envolvidos neste processo e as consequências para a prole. Nos últimos anos, mecanismos epigenéticos tem sido apontado como os principais moduladores da expressão gênica envolvidos em várias formas de programação fetal (JOUBERT et al., 2016), uma vez que mudanças ambientais podem alterar de forma persistente marcadores epigenéticos e desencadear respostas fenotípicas que afetam a estrutura e o funcionamento de órgãos de maneira permanente (SINCLAIR et al., 2007; WATERLAND; JIRTLE, 2003).

O termo "epigenética" foi utilizado pela primeira vez por Waddington (WADDINGTON, 2012) para definir as interações dos genes e o ambiente que levam ao desenvolvimento de um fenótipo. A partir de então, outros autores referem-se à epigenética como mudanças reversíveis e herdáveis no genoma capazes de afetar a expressão gênica e o fenótipo celular, sem, entretanto, alterar a sequência primária de nucleotídeos do DNA (DEANS; MAGGERT, 2015; FERNANDEZ-TWINN; CONSTÂNCIA; OZANNE, 2015). Estudos em modelo de programação fetal por restrição proteica tem demonstrado a participação de mecanismos epigenéticos e, apesar destes mecanismos terem sido bastante estudados no contexto do desenvolvimento embrionário e da biologia do câncer, o conhecimento sobre como a epigenética contribui para a programação fetal ainda é escasso. Isto se torna particularmente importante, uma vez que alterações em fatores ambientais, como a nutrição materna impacta fortemente os níveis de expressão gênica na prole (HEERWAGEN et al., 2010). Os principais mecanismos de regulação epigenética incluem metilação de DNA, por enzimas DNA metil transferases (DNMT), modificação pós-transcricional de histonas pelas enzimas histona acetilase (HAC) ou deacelilase (HDAC), além da participação de RNAs não codificantes, dentre estes, os microRNAs (miRNA) que também tem sido descritos no mecanismo epigenético de regulação da expressão gênica (ALLIS; JENUWEIN, 2016; HEERWAGEN et al., 2010).

miRNAs são uma classe de pequenos RNAs não codificantes com aproximadamente 22 nucleotídeos que têm como função a regulação pós-transcricional da expressão de genes. Os miRNAs se originam de uma longa molécula primária transcrita de um precursor pela RNA polimerase II em seu determinado gene *loci* com formato *hairpin* chamado de miRNA primário (pri-miRNA). A transcrição do pri-miRNAs pode ser controlado por fatores transcricionais da RNA Pol II (p53, Proteína de determinação de MYC, ZEB1 e ZEB2 e MYOD1) e por regulação epigenética (metilação de DNA e modificações de histonas)(CAI; HAGEDORN; CULLEN, 2004; DAVIS-DUSENBERY; HATA, 2010; KIM; HAN; SIOMI, 2009; KROL; LOEDIGE; FILIPOWICZ, 2010; LEE et al., 2004). Os pri-miRNAs passam por passos de maturação, ainda no núcleo. A Drosha, que possui dois domínios o RNase III (RIIIDs) e o dsRNA-binding (dsRBD), juntamente com seu cofator essencial a proteína DiGeorge Syndrome Critical Region Gene 8 (DGCR8) formam um complexo chamado Microprocessador (DENLI et al., 2004; GREGORY et al., 2004; HAN et al., 2004; LANDTHALER; YALCIN; TUSCHL, 2004) que inicia a maturação cortando a stem–loop para liberar um pequeno RNA em forma de *hairpin* com ~ 65 nucleotídeos de comprimento (pre-miRNA) (LEE et al., 2003). Após o processamento da Drosha, o pre-miRNA é exportado no citoplasma através de um complexo formado pela proteína Exportin 5 (EXP5), proteína nuclear de ligação GTP-RAN e o pre-miRNAs (BOHNSACK; CZAPLINSKI; GORLICH, 2004; LUND et al., 2004; YI et al., 2003). Após a passagem pelo complexo de poros nucleares, o GTP é hidrolisado sendo o complexo desmontado e ocorrendo a liberação do pre-miRNA no citoplasma, onde a maturação pode ser completada. No citoplasma o pre-miRNA é processado pela Dicer, uma outra enzima RNase III, que juntamente com a TAR RNA-*binding protein* (TRBP) reduz o pre-miRNA para uma fita dupla de aproximadamente 20 nucleotídeos que agora é denominado de miRNA maduro. Uma das fitas do pequeno duplex de RNA gerado pelo Dicer se liga com uma proteína AGO para formar um complexo efetor chamado complexo de silenciamento induzido por RNA (RISC) (HAMMOND et al., 2001; MOURELATOS et al., 2002; TABARA et al., 1999). Assim, os miRNAs funcionam como um guia, unindo-se ao seu alvo, enquanto a proteína AGO funciona como um recrutador de fatores que induzem a repressão translacional dos mRNA (Figura 3).

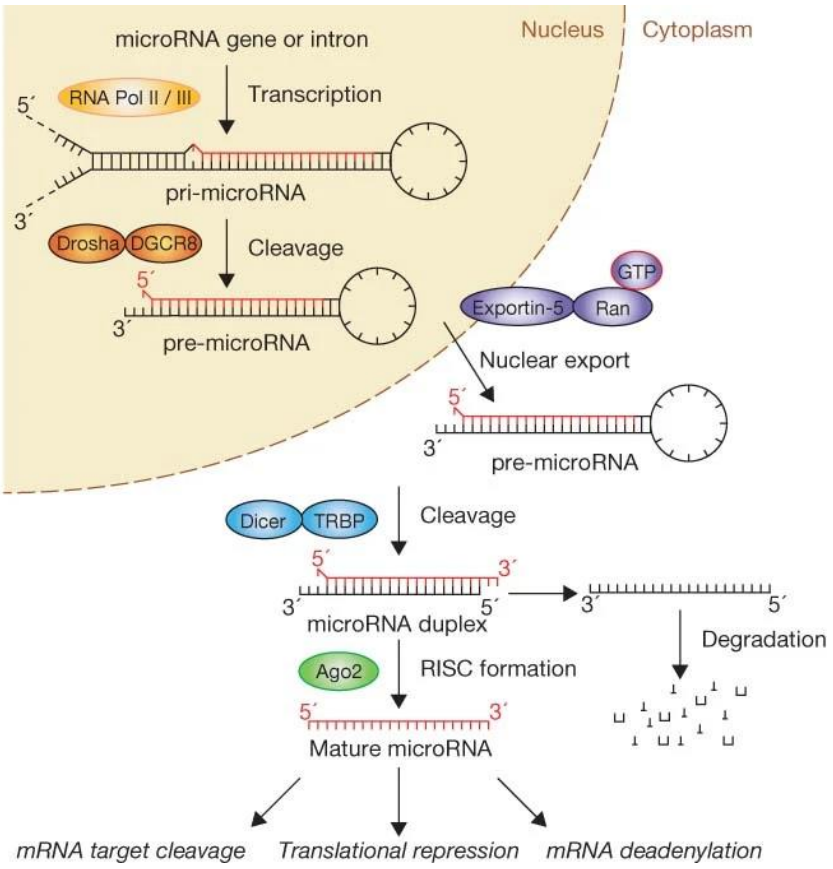

Figura 4. Esquema da biogênese dos miRNAs. (WINTER et al., 2009)

As primeiras publicações referentes a miRNAs foram publicadas em 1993 por Victor Ambros e Gary Ruvkun. Foram dois artigos publicados na mesma edição da Cell, cada um descrevendo o seu trabalho. Victor descreveu o primeiro miRNA, mesmo essa terminologia vindo a ser usada oito anos depois (LEE; FEINBAUM; AMBROS, 1993) e Gary descreveu o mecanismo regulatório do mRNA (lin-4 regulando lin-14) (WIGHTMAN; HA; RUVKUN, 1993). Desde então houve uma crescente no número de publicações, sendo que nos últimos 10 anos foram publicados mais de 100 mil estudos relacionados com miRNAs. Esses estudos são variados, porém uma grande parcela é relacionando a atuação dos miRNAs nos diversos tipos de canceres (CHAKRABORTY et al., 2020; MIN et al., 2014; PARASRAMKA et al., 2012; PIAN et al., 2020). Um dos pontos estudados é a expressão dos pri-miRNAs. Os genes dos miRNAs, muitas vezes, são localizados em regiões que possuem uma maior probabilidade de serem deletadas, amplificadas ou translocados (CALIN et al., 2004). Essa característica pode causar a desregulação da expressão dos pri-miRNAs e promover a iniciação ou progressão do câncer (ZHANG et

al., 2006). Esta desregulação pode ser causada pelo próprio câncer, que aumenta a expressão de fatores transcricionais e com isso desregular a expressão dos pri-miRNAs (BOMMER et al., 2007; LIN; GREGORY, 2015; RAVER-SHAPIRA et al., 2007). Outro ponto importante é o complexo Microprocessador que frequentemente está desregulado no câncer (MURALIDHAR et al., 2011; SUGITO et al., 2006). Mas as alterações podem ocorrer também no momento da exportação para o citoplasma (MELO et al., 2010) e na proteína Dicer (KUMAR et al., 2009). Assim, as alterações nos níveis de expressão dos miRNAs veem sendo muito estudas e correlacionadas com o surgimento ou progressão de diversos tipos de câncer.

Fatores dietéticos também estão sendo relacionados com a desregulação dos miRNAs induzidas pela nutrição materna durante a gestação e ou lactação que afeta a prole. A alta ingestão materna de gordura durante a gestação e lactação modulou o metabolismo lipídico hepático e a expressão de microRNA-122 (miR-122) e microRNA-370 (miR-370) na prole (BENATTI et al., 2014) além de alterar a expressão hepática da insulina como o fator de crescimento 2 e microRNAs importantes na prole adulta (miR-503, miR-379, miR-770-3p, miR-369-3p, miR-197, miR-21, miR-328, miR-471, miR-207, miR-667 *up* regulados e miR-410, miR-804, miR-323-5p, let-7c, miR-302a, miR-711, miR-26a, miR-122, miR-216b, miR-294, miR-185, miR-192, miR-29a, miR-194, miR-145, miR-126-3p, miR-762, miR-16, miR-1224, miR-22, miR-30c-2, miR-494, miR-483 *down* regulados)(ZHANG et al., 2009). Já a baixa ingestão de proteína na última semana de gravidez é crítica e suficiente para induzir efeitos na homeostase da glicose, causando alterações permanente no conjunto específico de miRNAs que podem contribuir para a vulnerabilidade geral de descendência para a obesidade, resistência à insulina e diabetes tipo 2 (ALEJANDRO et al., 2020). Alguns estudos mostram que a LPD maternal causa desregulação de miRNAs que causam mudanças metabólicas, inflamação crônica, aumento da pressão sanguínea e alterações na morfologia do coração (ASSALIN; GONTIJO; BOER, 2019; ZHENG et al., 2017). Além disso, um estudo publicado no *Journal of Hepatology* mostra que a dieta rica em gordura fornecida multigeracional aumenta a incidência de carcinoma hepatocelular por indução via a regulação do eixo miR-27a-3p-Acsl1/Aldh2 (SUN et al., 2020).

Referências Bibliográficas

As referências da revisão bibliográfica estão em conjunto com as do capítulo 2.

Capítulo 2: MiRNAome integrative analysis reveals molecular mechanisms associated with development of PCa in the offspring subjected to maternal low protein diet.

Constantino F.B.[1], Protela L.F.[1], Camargo A.C.L.[1], Colombelli K.T[1], Santos S.A[1], Fioretto M.N[1], Freire P.P.[4], Minatel B.C.[3], Barros-Filho M.C.[2,3], Kislinger T.[5], Moreno C.S.[6]. Lam W.L.[2], Carvalho R.F.[1], Justulin L.A[1*]

1. Department of Morphology, Institute of Biosciences, Sao Paulo State University (UNESP), Botucatu, SP, Brazil

2. Department of Integrative Oncology, British Columbia Cancer Research Centre, Vancouver, BC, Canada

3. International Research Center, A.C. Camargo Cancer Center, Sao Paulo, SP, Brazil

4. Department of Immunology - University of São Paulo (USP), São Paulo, SP, Brazil

5. Medical Biophisics, University of Toronto, Toronto, ON, Canada

6. Departments of Pathology & Laboratory Medicine, and Biomedical Informatics, Emory University School of Medicine, Atlanta, GA, United State

***Corresponding author:**

Prof. Dr. Luis A Justulin

Sao Paulo State University (UNESP), Institute of Biosciences of Botucatu, SP, Brazil.

Zip Code: 18618-689

Phone number: +551438800481

email: l.justulin@unesp.br

Abstract

In the last decades, there has been an increase in the incidence of cancer in the population. Studies show that cancer can originate through insults suffered by individuals during intrauterine life, a condition known as Fetal Programming. (PF). The perinatal period is characterized by the ability of the embryo / fetus to adapt to environmental changes, altering gene expression by post-transcriptional mechanisms. Recently, we demonstrated that maternal protein restriction promotes prostate carcinogenesis in elderly rats; However, information about the molecular mechanism involved in this process is lacking. Thus, we aimed at identifying possible deregulated microRNAs in young programmed rats and locate their possible targets associated with prostate carcinogenesis. For this, male Sprague Dawley rats born to mothers fed a standard diet (17% protein) - a control group (CTR) or a low protein diet (6% protein) - a gestational and lactational low protein diet (GLLP), during pregnancy and lactation were sacrificed on the postnatal day 21. We observed a delay in the development of the ventral prostate and increased levels of testosterone and estrogen expression in GLLP rats. In addition, 20 miRNAs were identified as differentially expressed, 6 downregulated and 14 upregulated. The enrichment results for downregulated miRNAs are related to cancer and angiogenesis pathways, while upregulated miRNAs are enriching endoplasmic reticulum and carcinoma pathways. The reanalysis of miRNA sequencing from TCGA revealed 7 in common with the GLLP group. One of them is miR-33 which, in addition to being down-regulated in the prostate, is also unregulated in the testis, adrenal gland and liver. Their overexpression in transfected cells caused a decrease in cell viability and your target, CYP1B1, which is an important enzyme in estrogen metabolism, leading to carcinogenesis mediated by changes in hormone levels. We concluded that miR-33 is an important target to explain the changes caused by maternal LPD and can also be considered the biomarker because it is unregulated in several organs.

1.0 Introduction

Inadequate diet is one of the main causes of comorbidities in the world, being related to diseases such as cancer, diabetes and neonatal deaths (AFSHIN et al., 2019; BLACK et al., 2013; CAULFIELD et al., 2004; PELLETIER et al., 1995). Studies show that maternal malnutrition in early life may be related to an increased likelihood of chronic diseases emergence in adulthood, showing that the origin of these diseases may be due to aggressions suffered during the embryo/fetal period. This is one of the themes studied by the international society named Developmental Origins of Health and Disease (DOHaD) (BARKER, 2007; MERICQ et al., 2017; PINHO et al., 2014; SANTOS et al., 2019; SCHULZ, 2010). Maternal exposure to low protein diet (LPD) during pregnancy and lactation has been widely performed in laboratory models, and it is an example of a metabolic programming that follows during the critical periods of development (COLOMBELLI et al., 2017; OZANNE; HALES, 2004; PINHO et al., 2014; SENE et al., 2013; VEGA et al., 2016). Studies show that offspring whose dams received LPD have lower birth weight, followed by accelerated growth (catch-up growth), insulin resistance and type 2 diabetes in adulthood and decreasing life expectancy (ALEJANDRO et al., 2020; EMBLETON et al., 2016; MCMILLEN; ADAM; MÜHLHÄUSLER, 2005; PETRY et al., 2001).

In addition, studies have aroused interest in the maternal LPD on the prostate (PINHO et al., 2014; PORTELA et al., 2021; RAMOS et al., 2010; SANTOS et al., 2020). Prostate is an exocrine accessory gland to the genital system whose development and homeostasis are under androgenic control (BIANCARDI et al., 2017; CUNHA et al., 1985). It is an important gland to the fertility (VERZE; CAI; LORENZETTI, 2016), and has

aroused, in recent years, medical-scientific interest, as it has a high incidence of benign prostatic hyperplasia (BPH) and prostate cancer (PCa), which is the third cancer that most kills the men in the world (DASGUPTA; SRINIDHI; VISHWANATHA, 2012; “Global Cancer Observatory”). In a previous study, Santos et al. related maternal LPD to the onset of prostate cancer (SANTOS et al., 2019). However, little is known about the epigenetic mechanisms involved in these changes, and studies show that epigenetic factors are the main modulators of gene expression involved in fetal programming-related risks of diseases at adulthood (JOUBERT et al., 2016).

Environmental changes can persistently alter epigenetic markers and trigger phenotypic responses that permanently affect the structure and functioning of the organs (SINCLAIR et al., 2007; WATERLAND; JIRTLE, 2003). The main mechanisms of epigenetic regulation include DNA methylation, by DNA methyltransferase enzymes (DNMT), post-transcriptional modification of histones by histone acetylase (HAC) or deacetylase (HDAC), in addition to the participation of non-coding RNAs. It is also included miRNA, which have been also been described as an epigenetic mechanism for the regulation of gene expression (ALLIS; JENUWEIN, 2016; HEERWAGEN et al., 2010). MiRNAs are small, single-stranded, evolutionarily conserved molecules (~ 17-25 nucleotides) which suppress the expression of genes that encode proteins, aiming at translational repression, mRNA degradation or both (SHYU; WILKINSON; VAN HOOF, 2008). Maternal LPD during gestation and lactation deregulated six miRNAs from offspring mice on postnatal day (PND) 21. Inflammatory pathways (including MAPK, TGF-beta and Toll-like receptor) have been associated with the six differentially expressed miRNAs, as well as increased levels of IL-6 and TNF-α in the liver (ZHENG et al., 2017).

Another study showed that maternal LPD leads to the dysregulation of two important miRNAs for the control of PPAR-γ and C/EBP-β expression, transcription factors involved in the differentiation of adipocytes and fat deposition, affecting lipid metabolism in the offspring in weaning age (PAN et al., 2013). Thus, maternal LPD have been linked to miRNA dysregulation, so our objective was to assess the profile of unregulated miRNAs after maternal LPD and relate them to PCa.

2.0 Material and Methods

2.1 Animals

Male and female Sprague Dawley rats were purchased at the State University of Campinas (Campinas, SP, Brazil) and kept at the Department of Structural and Functional Biology at the São Paulo State University (UNESP), Brazil. The animals were maintained under controlled temperature (22-25°C), photoperiod (12h), and relative humidity (55%) and received water and feed *ad libitum*. The animal design was performed according to SANTOS et al. (2019). Briefly, when 3 months old, weighing about 250-300g, the animals were placed to mate in a harem model (3 female rats for 1 male rat per box). The pregnancy confirmation was detected through vaginal washing.The pregnant rats were distributed into two groups: 1: Control (CTR) group, which received a standard diet (17% protein) during gestation and lactation; 2: Gestational and lactational low protein diet (GLLP) group, which received hypoprotein diet (6% protein) during gestation and lactation (Supplementary Figure 1). At birth, litters were adjusted to eight pups (4 males and 4 females). Male rat pups were weighed and euthanized in postnatal day (PND) 21 through anesthesia (ketamine and xilazin) followed by decapitation. The blood was collected for hormonal analysis and the ventral prostate lobe (VP) was collected, fixed for

morphological and stereological analysis, and frozen in liquid nitrogen for the extraction of total RNA to perform the techniques of miRNAs sequencing (microRNAome) and RT-qPCR. Testicle, adrenal gland, skin, and liver were collected to RT-qPCR.

The experimental procedures are according to the Ethical Principles on Animal Experimentation adopted by the Brazilian College of Animal Experimentation (COBEA) and were approved by the Ethics Committee on Animal Experimentation of the Institute of Biosciences of Botucatu (CEEA-949).

2.2 Morphological Analyses

The ventral prostates (VP) of six animals per litter/group from PND 21 were removed, and immediately fixed in the methacarn solution during approximately 4 hours (Puchtler et al 1970). Then, the samples were dehydrated by ethanol followed by diaphanization in xylene, and later the sample were embedded in Paraplast® Plus (Sigma-Aldrich Chemicals, St Louis, MO, USA). Consecutive 5 µm serial sections were obtained and the slides were stained with hematoxylin-eosin for morphological and stereological analysis. Stereological analysis was performed to analyze the relative proportions of the VP components (epithelium, lumen, and stroma). Results were expressed as a percentage of each component and a proportion of the total area analyzed (WEIBEL; KISTLER; SCHERLE, 1966).

2.3 Hormonal Analysis

The blood sample of 12 animals per litter/group from the PND 21 were collected, centrifuged and serum was stored until use. Analysis of hormone levels was performed by the colorimetric Elisa method following the manufacturers' protocol. The measured hormones were: Estrogen (17β-estradiol, Monobind®, 4925-300 CA, USA Sensitivity: 6.5

pg/mL) and Testosterone (17β-hydroxy-4-androsten-3-one, Monobind®, 3725-300A, USA. Sensitivity: 0.038 ng/mL).

2.4 Total RNA extraction and miRNA sequencing

Total RNA was extracted from prostate by Invitrogen™ Trizol® Reagent according to manufacturer's protocols (Thermo Fisher Scientific, MA, USA). The RNA samples were quantified by spectrophotometry using the Thermo Scientific™ NanoDrop (Thermo Fisher Scientific, MA, USA) and treated with Invitrogen™ DNase I (Thermo Fisher Scientific, MA, USA) to remove contamination with genomic DNA. The quality of the RNA was confirmed by Bioanalyzer 2100 Eukaryote Total RNA Pico (Agilent Tech, CA, USA) through the RNA integrity number (RIN), which must be greater than 8.

The libraries were prepared by TruSeq® Small RNA Library Prep Kit (Illumina, CA, USA). Small non-coding RNA sequencing were performed on the Illumina HiSeq2500 at Macrogen inc. After sequencing, FASTQ files were pre-processed by adapter trimming and quality filtering, based on the Phred quality score (≥20). Sequence reads were aligned to the current version of the Rattus Novegicus genome (Rnor_6.0) using the Spliced Transcripts Alignment to a Reference (STAR) aligner and annotated miRNA species quantified based on genomic loci. All these steps were performed at OASIS Platform (RAHMAN et al., 2018). Differential expression and exploratory analysis were performed using the DESeq package (Log2FC |0.4|; FDR< 0.05) (https://yanli.shinyapps.io/DEApp/).

2.5 Integrative analysis

The integrative analysis was carried out using the results of the transcriptome and proteome from another study of our group (data not published). These results were

obtained from the same animal model mentioned in this study. For the results of the transcriptome, mRNAs were considered differently expressed with p-value<0.05 and log2 Fold Change |0.66|. For proteome results, differential expressed proteins were considered with p-value<0.05 and log2 Fold Change |1|.

To perform the integrative analysis, we first find the target prediction of unregulated miRNAs using miRWalk 3.0 (http://mirwalk.umm.uni-heidelberg.de/) (DWEEP; GRETZ, 2015). Then, the correlation of miRNAs/mRNAs and miRNAs/proteins were observed considering values of inverted Fold Change (down/up or up/down).

2.6 Enrichment analysis

The enrichment analysis was done using the results of the Integrative analysis and was separately performed separately for targets upregulated and downregulated. For this we use the platform “KEGG Orthology Based Annotation System” (KOBAS) (http://kobas.cbi.pku.edu.cn/kobas3/?t=1) (XIE et al., 2011) was used. This platform generates an enrichment from several databases such as Gene Ontology, Panther, KEGG and Reactome. The pathways were considered enriched with p-adjusted <0.05.

2.7 Quantitative polymerase chain reaction (RT-qPCR)

RT-qPCR for miRNAs were performed according to the relevant literature (VARKONYI-GASIC et al., 2007).

The cDNA was synthesized using the Applied Biosystems™ High-Capacity cDNA Reverse Transcription Kit according to the manufacturer. For miRNAs, the stem-loop RT primer, designed according to (CHEN, 2005), was hybridized with the selected miRNA molecule giving rise to the reverse primer (Table 2). This reverse primer was used to

perform the miRNA cDNA instead of the Rondon primer used for mRNA cDNA. The cDNA reaction product was amplified using specific primers (Table 2) and Applied Biosystems™ SYBR™ Green PCR Master Mix system (Thermo Fisher Scientific, MA, USA). For miRNAs reaction was used the primer Forward and the primer universal described in table 2. The reactions were performed in duplicates for each target gene in the Applied Biosystems™ QuantStudio™ 12K Flex Real-Time PCR System (Thermo Fisher Scientific, MA, USA) in 96-well plates according to the manufacturer's instructions. The relative quantification of each gene was performed using the $2^{-\Delta\Delta CT}$ method (LIVAK; SCHMITTGEN, 2001). The values obtained for all samples were normalized by the reference miRNA (U6) and mRNA (actin). The values were calculated using the expression ratio of the GLLP/CTR groups. Student's “t” test was applied and considered statistically significant when $p < 0.05$. The sequences of the primers pair used are described in table 2.

Table 2. Sequences of primers.

	Foward	Reverse
miR-33-5p	CGGCGGGTGCATTGTAGTTGCATTGCA	GTCGTATCCAGTGCAGGGTCCGAGGTATTCGCACTGGATACGACTGCAAT
U6	GCAAATTCGTGAAGCGTTCC	GTCGTATCCAGTGCAGGGTCCGAGGTATTCGCACTGGATACGACAAAAATAT
Universal	GTGCAGGGTCCGAGGT	
CYP1B1 (rat)	GGGCTGGATTTGGAGGATGT	TCCTGGCTGGCTCCAAAG
SEMA6C (rat)	TCTGCAGTCTGCGCCTTCT	CCTTGAACTTGCCCTCAAAGC
CYP1B1 (Human)	TCCTCCTCTTCACCAGGTATCC	CTGGTCACCCATACAAGGCA
SEMA6C (Human)	CTCCGAGAGCCACACTTTGT	CGAGCATCCTCCACAGAGAC

2.8 TCGA data: a translational analysis

Raw prostate miRNA sequencing data from “The Cancer Genome Atlas” (TCGA) repository (https://portal.gdc.cancer.gov/repository), which contains 498 samples from patients with prostate cancer and 52 samples from a solid tissue (as a control group) were downloaded. Oasis platform (https://oasis.dzne.de/) was used to reanalyze this data with the same protocol used for rat data, but aligned with the most current construction of the

human genome (hg38) (RAHMAN et al., 2018). miRNAs were considered differentially expressed with FDR>0.05 and log_2 fold change |0.4|. The differentially expressed miRNAs of patients with prostate cancer were compared with unregulated miRNAs of the GLLP group.

Also, mRNAs results from GEPIA were also used to compare with target prediction of the miR-33a-5p. GEPIA is a Web Site that analyzed RNA sequencing expression data of 9,736 tumors (TCGA) and 8,587 normal samples (GTEx) using a standard processing pipeline (Cite GEPIA). mRNAs were considered differentially expressed with FDR>0.05 and log_2 fold change |0.4|.

2.9 Cellular Culture

Non-cancerous prostate cells, PNT2 cell line (Rio de Janeiro Cell Bank - BCRJ, Rio de Janeiro, Brazil), were maintained in Gibco™ RPMI 1640 Medium (Thermo Fisher Scientific, MA, USA). The cells were expanded in 25 cm^2 and 75 cm^2 polystyrene plates and kept in an oven with 5% CO_2 in a humid atmosphere at 37ºC. When the cells reached 80% confluence, they were subjected to 0.25% Gibco™ Trypsin-EDTA (0.5%), no phenol red (Thermo Fisher Scientific, MA, USA) and transferred to 12-well plates to compose the study groups. Each experimental group (explained in the next topic) was performed in triplicate and three biological repetitions.

2.9.1 Cellular Transfection

To form the different study groups, hsa-miR-33a-5p mimics were transfected into the cell. For this, two complexes were formed to be used in the final transfection solution. First, Invitrogen™ Lipofectamine™ RNAiMAX Transfection Reagent (Thermo Fisher Scientific, MA, USA) was diluted in Gibco™ Opti-MEM Reduced Serum Medium (Thermo

Fisher Scientific, MA, USA) to form the first complex. Then, the oligonucleotides were diluted in Opti-MEM® to form the second complex. The Lipofectamine+Opti-MEM complex was mixed with the oligos+Opti-MEM complex and incubated for 5 minutes at room temperature. After this period, 150 µl of the final transfection solution was added to each well containing PNT2 cells (80% confluence) and normal culture medium. The cells were incubated for a period of 15 hours and the medium with the treatment were exchanged by the specific medium. After 24 hours, the cells were collected and processed for extraction of total RNA using Invitrogen™ Trizol® Reagent according to manufacturer's protocols (Thermo Fisher Scientific, MA, USA) or added Invitrogen™ MTT (3-(4,5-Dimethylthiazol-2-yl)-2,5-Diphenyltetrazolium Bromide) (Thermo Fisher Scientific, MA, USA) solution to analyze cell viability after treatment.

2.9.2 Cell viability assay

PNT2 cells were seed in a 12-weel plates and treated with mimic as previously described. After 24, 48 or 72 hours of the treatment, the cell medium was removed and 200 µl of a 10% MTT solution (Invitrogen™ MTT (3-(4,5-Dimethylthiazol-2-yl)-2,5-Diphenyltetrazolium Bromide) (Thermo Fisher Scientific, MA, USA)) was added. 4 hours later, the medium containing MTT solution was removed and 300 µl DMSO was added directly to each well. We replaced the solution in a 96-well plate (each well in the 12-well plate becoming 3 in the 96-well plate). The optical density of each well was measured by spectrophotometer at the wavelength of 550 nm. The experiments were performed in triplicate.

2.10. Statistical Analysis

For global analyzes, specific statistical packages were used, as previously described. For the other parameters, the Shapiro-Wilk normality test was performed. For the data that passed the test, the comparison between the experimental groups was perform using the Student's T test. For data that did not pass the normality test, the Mann-Whitney test was performed. A statistically significant difference was considered when $p < 0.05$.

2.11. Making the images

The PCA graph was generated using the Clustvis tool (https://biit.cs.ut.ee/clustvis/) (METSALU; VILO, 2015) and the volcano graph on the VolcaNoseR website (https://huygens.science.uva.nl/VolcaNoseR/). Heatmap graphic was generated on the Morpheus platform (https://software.broadinstitute.org/morpheus/) and Sankey diagram using SankeyMATIC Web site (http://sankeymatic.com/).

3.0 Results

3.1 Animals of the GLLP group have lower body and prostate weight in addition to high levels of estrogen and testosterone.

The animals subjected to maternal low protein diet (LPD)during gestation and lactation had a lower birth weight that remained until PND 21 (Fig. 1A and Table 1). In addition, the prostate weights, normalized by the weight of the animal (relative) or not, were also lower in the GLLP group (Table 1).

The prostatic tissue morphometry of the CTR experimental animals present dilated acini, with ample light and full of secretion and with a cylindrical secretory epithelium associated with fibromuscular stroma (Fig. 1B). The GLLP animals, the animals in the GLLP group had smaller acini, with reduced light and more evident stroma when

compared with the CTR group (Fig. 1B). Stereological analyses were corroborated by histological data, where we observed a decrease in light and an increase in stroma in the GLLP group in relation to CTR (Table 1). The estrogen and testosterone levels were increased in the GLLP group (Fig. 1C).

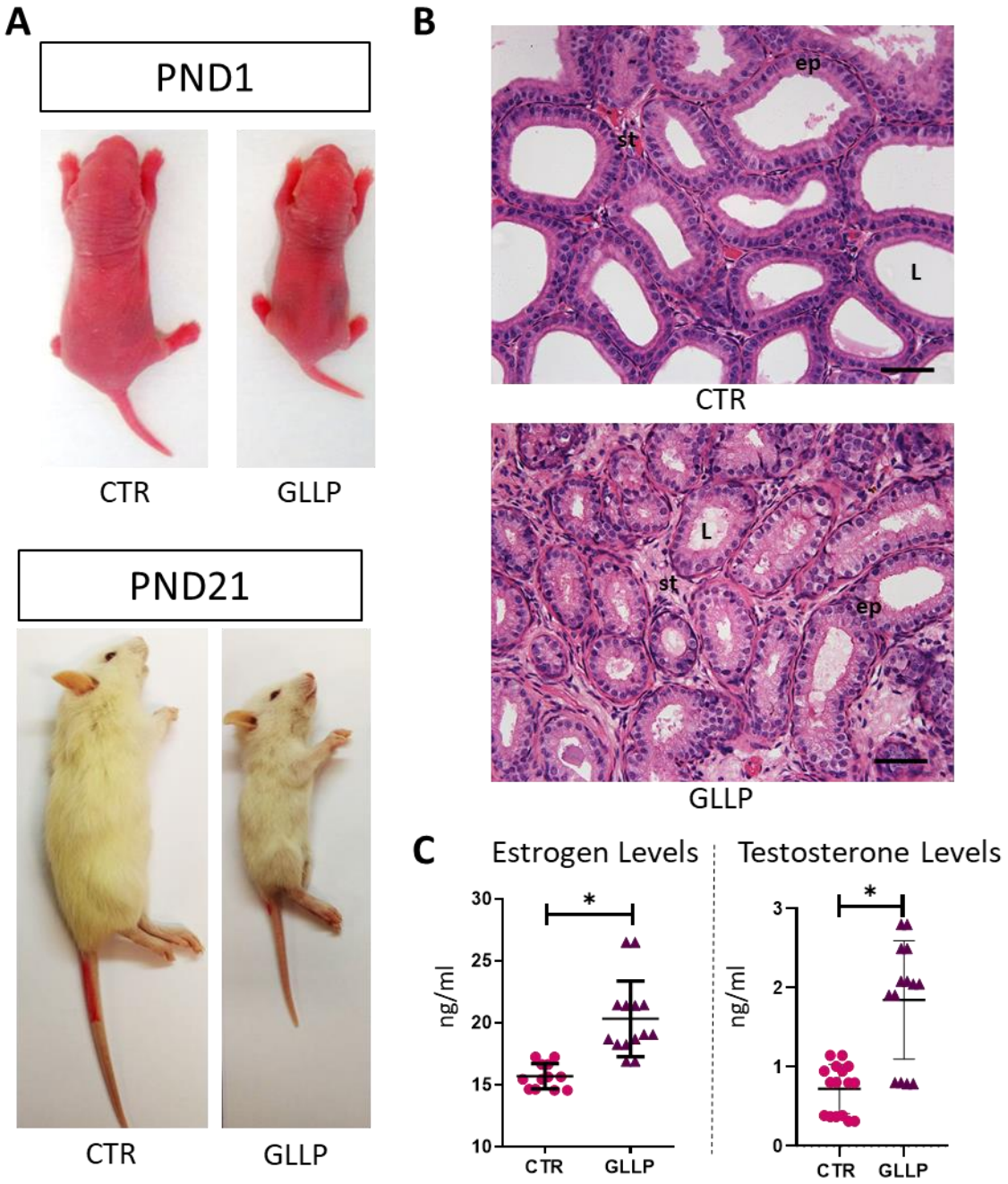

Figure 1. The GLLP group has lower weight, late prostate development and a higher level of testosterone and estrogen. **A.** Representative images of male rat pups from experimental groups at different ages. We can observe the difference between the groups: GLLP group is lower in both ages. **B.** Histological sections of the ventral prostate lobes (VP) stained with hematoxylin-eosin (HE) showing the delayed prostate development marked by smaller acinus and more evident stroma in GLLP group. **C.** Bar graph of blood hormone measurement (Estrogen and Testosterone) showing the high levels in GLLP group of both hormones. CTR: Control group; GLLP: Gestation and lactation low protein diet; PND: Postnatal day VP: Ventral prostate. ep: epithelium; st: stroma; L: lumen. * means statistical difference. Scale bar: 200 µm.

Table 1. Rat and prostate weight and stereological results.

	CTR	GLLP
PND1 Rat weight (g)	6.62 ± 0.4	6.02 ± 0.5 *
PND21 Rat weight (g)	39.25 ± 6.2	20.02 ± 2.9 *
VP weight (g)	0.03 ± 0.006	0.01 ± 0.003 *
VP relative weight (g)	0.0009 ± 0.0001	0.0007 ± 0.0001 *
Epithelium(%)	35.71 ± 5.8	48.05 ± 6.1 *
Lumen (%)	45.47 ± 9.8	30.50 ± 4.9 *
Stroma (%)	19.79± 5.4	29.63 ± 4.9 *
Glandular fraction	82.04 ± 5.2	67.58 ± 14.3 *

CTR: Control, GLLP: Gestation and lactation low protein diet, PND: Postnatal day, VP: Ventral prostate, g: grams. * means statistical difference

3.2 Performance of miRNAs differentially expressed in the GLLP group: Target prediction, integration analysis (transcriptome and proteome) and pathways enrichment analysis.

The 605 readings mapped for each sample were found after analysis on the Oasis platform and the raw data were sent to the database (unpublished data). We identified a differential expression profile between CTR and GLLP group by principal component analysis (PCA) (Figure 2A). Six miRNAs (rno-miR-33-5p, rno-miR-871-3p, rno-miR-3553, rno-miR-144-5p, rno-miR-99a-5p and rno-miR-7a-5p) have been identified that are at least 1.3 times less expressed in the GLLP group compared to CTR and fourteen miRNAs (rno-miR-708-5p, rno-miR-487b-3p, rno-miR-337-3p, rno-miR-411-3p, rno-miR-410-3p, rno-miR-496-3p, rno-miR-323-3p, rno-miR-299a-5p, rno-miR-412-3p,

rno-miR-493-5p, rno-miR-483-5p, rno-miR-6331, rno-miR-184, rno-miR-483-3p) are expressed at least 1.3 times more in the GLLP group as compared to the CTR (Figure 2B).

Target prediction for the 20 miRNAs resulted in 8172 potential targets (Supplementary Table 2). These predicted targets were compared with transcriptome and proteomic data (unpublished), which identified 708 differentially expressed mRNAs (525 regulated up and 183 down regulated) and 289 deregulated proteins (163 regulated up and 126 regulated down) in the GLLP group when compared with the CTR group (Supplementary Table 3). Thus, after integrative analysis of these data considering inverted fold changes levels, 80 targets with increased expression were identified (52 mRNAs, 28 proteins and 0 common) (Figure 2C) and 119 targets with decreased expression (64 mRNA, 53 proteins and 2 in common) (Figure 2D), totaling 199 possible targets of miRNAs (Supplementary Table 4).

The enrichment analysis for 80 upregulated targets enriched terms related to: Proteoglycans in cancer, positive regulation of angiogenesis, cellular response to tumor necrosis factor, Hepatocellular carcinoma, regulation of vascular endothelial growth factor production, response to estradiol, Pathways in cancer, Wnt signaling pathway (Figure 2.E and Supplementary Table 5). For the 119 down regulated targets, the enriched pathways are related to: Endoplasmic reticulum, Hepatocellular carcinoma, positive regulation of ERAD pathway (Figure 2.A and Supplementary Table 6).

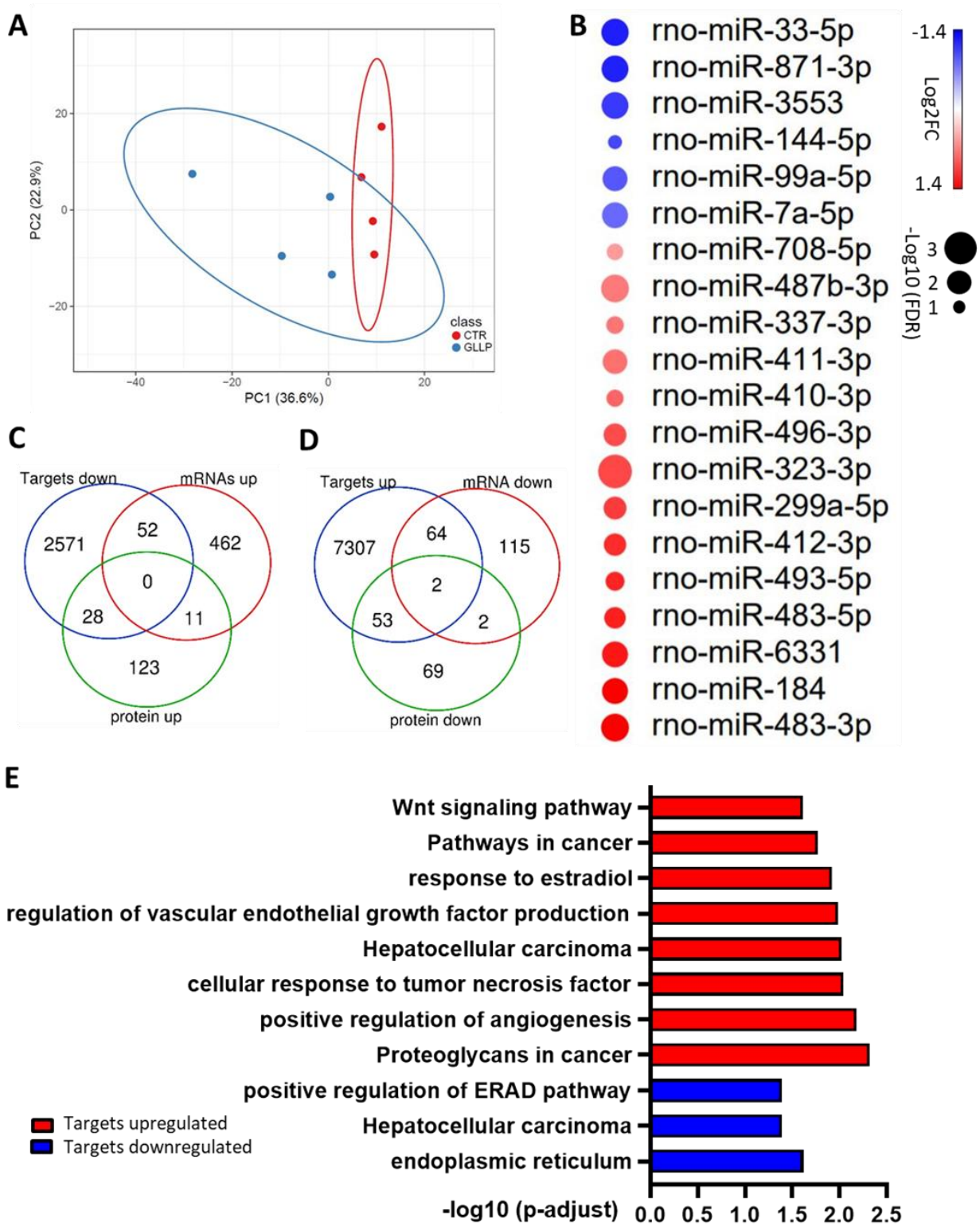

Figure 2. MiRNAs differentially expressed in the GLLP group have predicted targets related to interesting enriched pathways. **A.** Principal component analysis (PCA) show similarities between samples within each group. Red circle delimits the set of samples from the CTR group, and blue circle delimits the set of samples from the GLLP group. **B.** Heatmap showing the expression in log2 of Fold change (red up regulated, blue down regulated) and FDR (larger

circle size represents larger FDR value) of the differentially expressed miRNAs. **C.** Venn diagram showing the integration of predicted targets of downregulated miRNAs with upregulated mRNAs and proteins. **D** Venn diagram showing the integration of predicted targets of upregulated miRNAs with downregulated mRNAs and proteins. **E.** Bar graphs showing the ontological pathways and terms enriched of the miRNAs integrated predicted targets. Red bars refer to upregulated miRNAs integrated predicted targets; blue bars refer to downregulated miRNAs integrated predicted targets. The numbers below de bars represent the adjusted p-value shown in –log10. CTR: Control; GLLP: Gestational and lactational low protein intake.

3.5 Translational Analysis: Results of prostate cancer (TCGA) and correlation with rat data.

Using TCGA small-RNA sequencing, the expression of 1010 miRNAs was detected. The Differential expression profile was identified between the solid tissue group (CTR) and the Cancer group by principal component analysis (PCA) (Figure 3.A). The volcano graph (Fig. 3.B) identified 243 miRNAs that are downregulated in the Cancer group, and 248 miRNAs upregulated (Supplementary Table 7). Values of FDR> 0.05 and Log2 Fold Change of ± 0.4 were considered.

The correlation between the Rat and Human differentially expressed miRNAs resulted in 7 miRNAs in common (Figure 3.C and Supplementary Table 8). From this, five are upregulated in GLLP group but downregulated in cancer samples. The miR-708-5, are upregulated in both groups and the miR-33-5p, are downregulated in both groups.

Considering everything that has already been mentioned, from fold change values, enriched pathways and relationship with prostate cancer, mir-33-5p was evident in all criteria, proving to be a good miRNA to be studied.

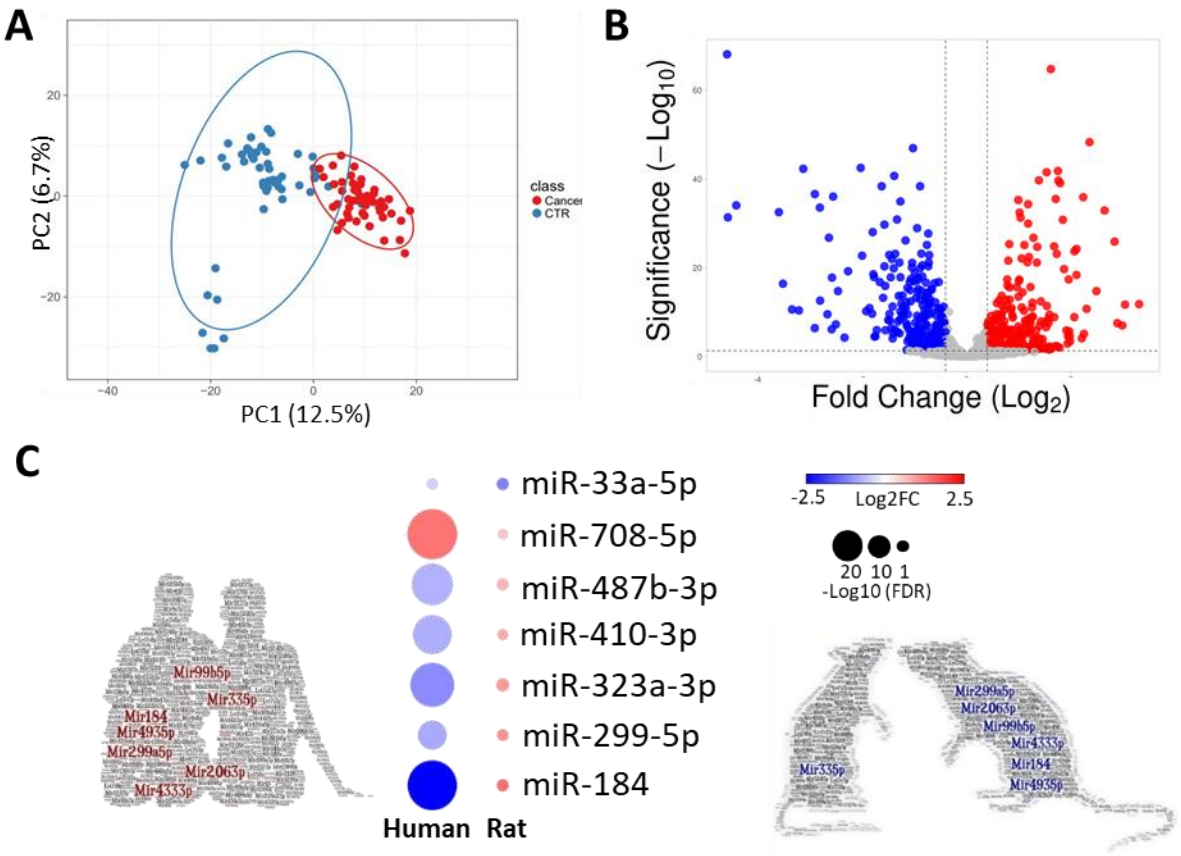

Figure 3. GLLP group presents some deregulated miRNAs in common with prostate cancer patients. **A.** Principal component analysis (PCA) shows similarities between samples within each group. Blue circle delimits the set of samples from the CTR group (n=52), and red circle delimits the set of samples from the cancer group (n=498). **B.** Volcano graph with the differential expression between the two experimental conditions. The vertical axis corresponds to log2 Fold Change <0.4> and the horizontal axis represents values of FDR <0.05 expressed in -log10. **C**. Heatmap showing the expression in log2 of Fold change (red upregulated, blue downregulated) and FDR (larger circle size represents larger FDR value) of the differentially expressed miRNAs in common between prostate cancer patients and GLLP group.

3.6 An exploratory analysis of miR-33a-5p

The first analysis performed with miR-33 was to prove its downregulation in the prostate of animals in the GLLP group using the RT-qPCR method (Fig. 4). In addition, the expression of this miRNA is also downregulated in the testis and liver. Furthermore, the expression of miR-33 was increased in the adrenal gland, on the GLLP group, and the expression levels of miR-33 were not different in the skin (Fig. 4).

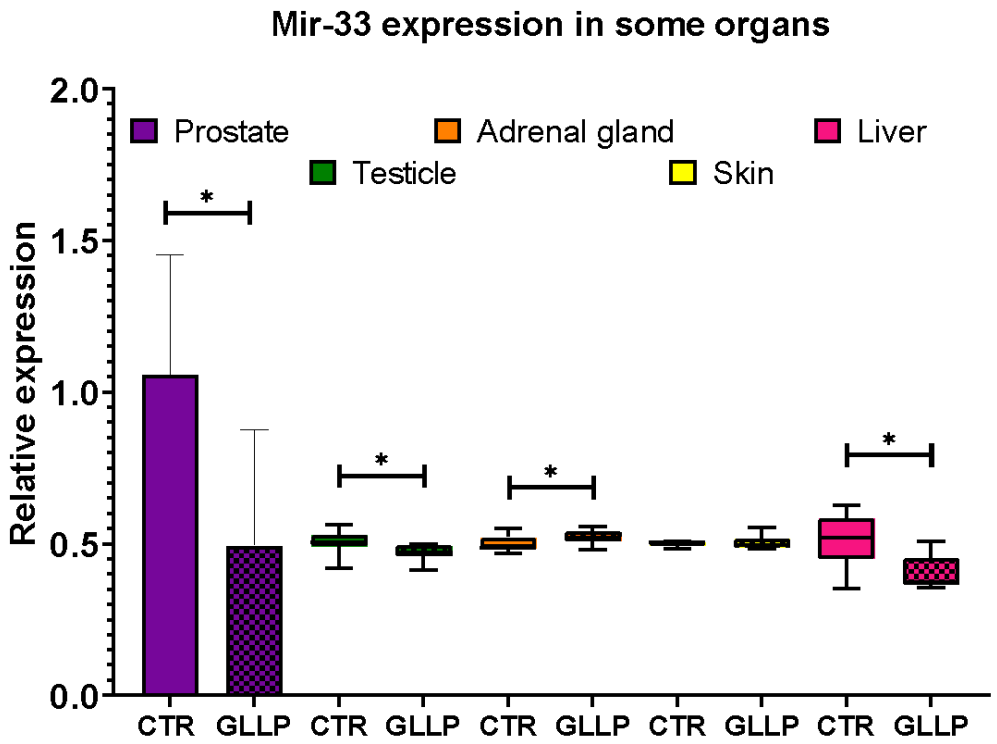

Figure 4. Expression of mir-33-5p using the RT-qPCR technique in different organs showing the lower expression in prostate, testicle and liver and a higher level in adrenal gland in GLLP group when compared to CTR. Prostate statistics was Student T test (bar graph) and the other organs Mann-Whitney test (box plot graph) CTR: Control group; GLLP: Gestation and lactation low protein diet. * means statistical difference.

The second analysis was to transfect the PNT2 cell line with miR-33, thereby increasing its expression. The technique was successfully performed, where the expression levels of cells treated with miR-33 MIMIC showed high expression levels while cells that were only treated with lipofectamine did not have their levels increased (Fig. 5A). This overexpression of miR-33 persisted significantly until at least 72 hours after the end of treatment, although expression levels have decreased (Fig. 5B).

To see the effect of mir-33a-5p overexpression on the culture cell line, we performed the MTT test to analyze cell viability. The result for this assay shows that the overexpression of mir-33a-5p decrease the cell viability levels (Fig. 5C).

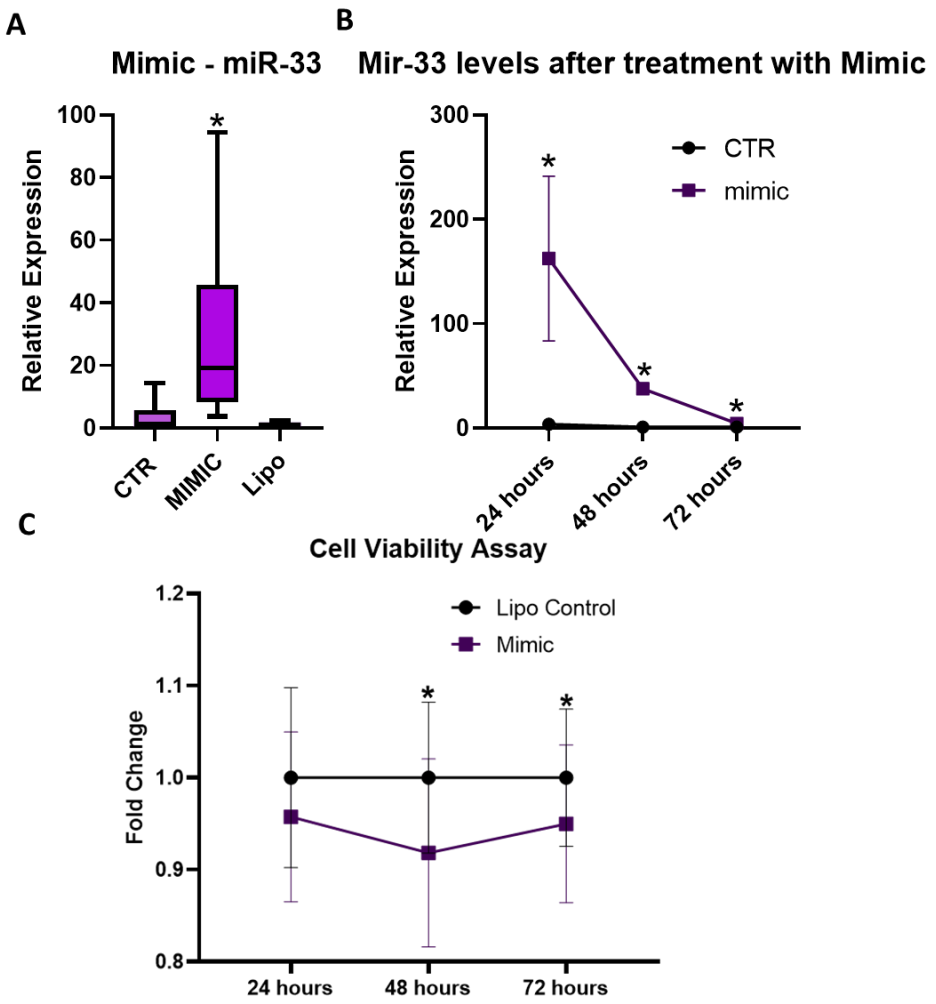

Figure 5. miR-33a-5p overexpression causes low levels of cell viability **A.** miR-33a-5p expression in PNT2 cell after treatment with Mimic (higher levels) or Lipofectamine alone (normal levels) represented by a Box plot. **B.** Line graph showing miR-33-5p expression levels after 24, 48 and 72 hours of treatment with Mimic. Expression levels in 24 hours are higher, but the difference remains significant until 72 hours, which was the last hour analyzed. **C.** Cell viability levels performed by MTT 24, 48 and 72 hours after the end of the treatment with mimic. The line graph shows the low levels of cell viability when miR-33a-5p is overexpressed. CTR: Control group; GLLP: Gestation and lactation low protein diet. * means statistical difference.

When we look at the enriched pathways of the downregulated miRNAs, we see that the targets of miR-33 are present in all of them, showing the importance of miR-33 for the regulation of the organism (Fig. 6A). In addition, we used RNA sequencing data results analyzed by Gepia from 9,736 tumors patientes (TCGA) and 8,587 normal

samples (GTEx) to compare with the miR-33 predicted targets and we observed 6 targets that is deregulated in both (Fig. 6B). From this results we choose two miR-33 targets predicted to validated, the SEMA6C and CYP1B.

The expression of both targets presented upregulated in GLLP animals (Fig. 6C) but there was no difference in the transfected cell line (Fig 6D).

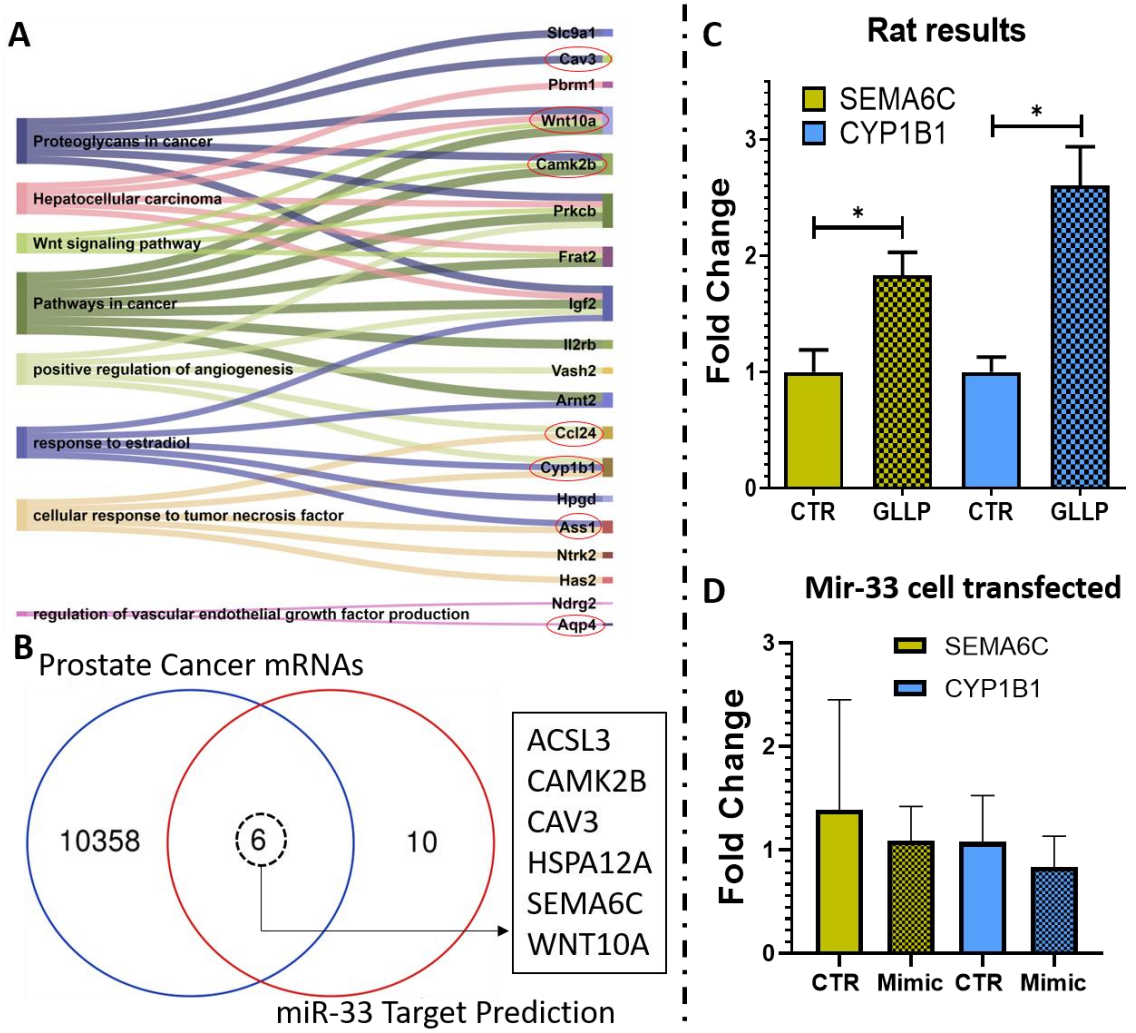

Figure 6. The predicted mir-33-5p targets are involved in all selected pathways and with prostate cancer. **A.** Sankey diagram showing the pathways enriched by predicted integrated targets of the upregulated miRNAs and the targets that are enriching the pathways. Red circle highlights the miR-33-5p targets. **B.** Venn diagram showing shared between deregulated mRNAs in prostate cancer with the predicted and integrated miR-33 targets. **C.** Expression levels of two predicted mir-33 targets (SEMAC and CYp1B1) in the prostate of rats in the CTR and GLLP group. The results

show that the downregulation of miR-33 leads to increased expression of the targets. **D.** Expression levels of two predicted mir-33 targets (SEMAC and CYp1B1) in PNT2 cells transfected with mimic miR-33a-5p.

4.0 Discussion

The term malnutrition is associated with the inadequate or insufficient intake of any food component, such as proteins. The minimum percentage of protein recommended by the American Institute of Nutrition for rat diets is 12% (NUTRITION, 1995). In our study, only 6% of the protein was made available to rats, that is, half of the recommended. Several authors have shown that feed intake with hypoproteins is associated with low birth weight and reduced growth of different organs in rodent models. (DE BRITO ALVES et al., 2016; FALCÃO-TEBAS et al., 2012; LEANDRO et al., 2012; LIMA et al., 2015; OZANNE; HALES, 2004). In our animals it was not different, the GLLP animals had a lower body weight at birth, in addition to a significant decrease weight in the prostate, which may be related to the delay in the development of this organ, which had smaller acini, with less light and increased stroma. These data corroborate the results of Santos et al. (2019) demonstrated a reduction in the prostate luminal fraction , as well as a decreased glandular secretion, produced by the quantification of the prostatein protein in LPD animals in PND 21. In addition, Ramos et al. (RAMOS et al., 2010) identified smaller amount and reduced size of acini in the dorsolateral prostate of rats exposed to intrauterine protein restriction and Pinho et al. (2014) also observed a delay in prostate development in the offspring of animals following the same protocol but with PND 1.

In addition to the morphological alterations, we found important hormonal changes, such as an increase in serum testosterone and estrogen in this PND 21 animal model. Studies show that prostate exposure to high testosterone levels is a potential carcinogen in the prostate, where 30% of animals with low doses but with chronic testosterone have

prostate cancer. However, estrogen has a synergistic effect with testosterone, 100% of animals exposed to testosterone doses associated with estrogen developed prostate cancer. (BOSLAND, 2005). Zambrano el al. (ZAMBRANO et al., 2014) observed that mothers who have low protein intake have high levels of estrogen in the gestational period. Thus, this may be one of the mechanisms that assist in the appearance of prostate cancer in aging animals, since studies show that the development of the prostate is sensitive to hormonal changes and exposure in the early stages of life can play a significant role in the appearance of precancerous lesions and carcinogenesis in adulthood through epigenetic changes (PRINS et al., 2008).

Epigenetics are inherited changes in gene expression without undergoing changes in DNA sequences. Interestingly, miRNAs are also considered an important epigenetic component, as they are targets for methylation of their DNA and for regulating epigenetic modifiers such as DNMTs and deacetylated histones (SALIMINEJAD et al., 2019). Some studies have already shown that maternal LPD causes the dysregulation of miRNAs that can lead to metabolic changes, chronic inflammation, increased blood pressure and morphological changes in the heart (ASSALIN; GONTIJO; BOER, 2019; ZHENG et al., 2017). In our study, maternal LPD caused alteration of 20 miRNAs and after integrating predicted targets with protein and mRNA data, we observed that miRNAs are enriching many cancer-related pathways. When we compared the 20 unregulated miRNAs with the 491 unregulated miRNAs of prostate cancer patients (TCGA data) we find 7 miRNAs in common. Our data suggest that miRNAs deregulated by fetal programming due to LPD may be influencing the microenvironment in order to predispose to the onset of cancer.

Among miRNAs, miR-33 has been widely studied both for its tumor suppressive effect, considering that its positive regulation decreases proliferation inhibiting tumor growth, and reducing the chance of metastasis by affecting cell migration, which can be a powerful strategy for the treatment of cancer (CIRERA-SALINAS et al., 2012; FRIEDMAN et al., 2012; KUO et al., 2013; RICE et al., 2013; THOMAS et al., 2012; ZHOU et al., 2015), and for its role in regulating cholesterol / lipid metabolism, being an important therapeutic target for atherosclerosis (HORIE et al., 2010; MARQUART et al., 2010; NAJAFI-SHOUSHTARI et al., 2010; RAYNER et al., 2010, 2011a, 2011b; ROTLLAN NOEMI et al., 2013; ROTTIERS et al., 2013). In addition, studies have shown that miR-33 inhibition leads to the development of obesity, insulin resistance and increased food intake, in organs such as liver, white adipose tissue and skeletal muscle, suggesting that the metabolic regulation by miR-33 is more complex than was known (NÄÄR, 2018; PRICE et al., 2018). The low-protein maternal diet offered at the end of pregnancy affects the fraction of offspring pancreatic β cells at birth, increasing their susceptibility to metabolic disorders and type 2 diabetes in adulthood. In addition to increasing glucose intolerance and reducing insulin sensitivity in aging male offspring (ALEJANDRO et al., 2020; BERENDS et al., 2018). Putting all information about miR-33 together, we can suggest that it is an important miRNA for fetal programming. In addition, miR-33 is deregulated not only in the prostate, but also in the testicle, adrenal and liver shown that it can be a biological marker for programming low protein intake.

Among the targets of miR-33, we chose 2 to perform the validation, SEMA6C and CYP1B1. Semaphorins are a family of proteins that, in addition to being important for the immune response because they have receptors in most defense cells, also play an

important role in the tumor microenvironment (FRANZOLIN; TAMAGNONE, 2019). For example, SEMA6D has been described as being associated with tumor progression and angiogenesis in gastric cancer (LU et al., 2016; ZHAO, 2006). SEMA7A expression is positively regulated in breast cancers and is associated with shorter survival (BLACK et al., 2016). In certain tumors, SEMA3E has been associated with progression due to the promotion of cell invasion, metastatic spread and tumor angiogenesis. (CASAZZA et al., 2010, 2012; LUCHINO et al., 2013; TAMAGNONE; MAZZONE, 2011).

Cytochrome P450 1B1 (CYP1B1) is an important enzyme in estrogen metabolism (DAWLING et al., 2004; HAYES et al., 1996; LI; ZHU; GONZALEZ, 2017). Studies have shown that high levels of CYP1B1 can lead to carcinogenesis mediated by changes in hormone levels and the transformation of estradiol into semiquinones and quinones, which can form DNA adducts resulting in oncogenic mutations (GAJJAR; MARTIN-HIRSCH; MARTIN, 2012; HAYES et al., 1996; SPINK et al., 1997). In addition, quinones / semiquinones also undergo a redox cycle and generate reactive oxygen species, resulting in oxidative damage (PARL et al., 2009). Thus, high levels of estrogen, associated with low levels of miR-33 (suppressor CIP1B1) and high levels of CIP1B1 and SEMA6C may be combined, leading to a carcinogenic microenvironment that associated with other factors may be the origin of the cancer found in these animals at age adult.

CYP1B1 is an important fatty acid modulator that suppresses the expression of the target genes PPARγ and PPARα, receptors for fatty acid metabolism, which play important roles in energy maintenance homeostasis. Cancer and obesity are closely related to disruption of fatty acid metabolism. Santos et al. showed that animals programmed by maternal LPD during pregnancy and lactation have low levels of

triglycerides, total protein, albumin, and glucose in the DPN21 (SANTOS et al., 2019). These results show that in addition to the action of CYP1B1 on hormone levels, it may also be regulating fatty acid metabolism.

Thus, we conclude that the effect of maternal LPD during pregnancy and lactation cause changes in miRNAs important for the tumor microenvironment been one of them the miR-33. We also proved the regulation of this miRNA in two targets, SEMA6C and CYP1B1 in rat samples. We also observed that miR-33 can be an important biomarker for fetal programming due to maternal protein restriction, being deregulated in other organs such as the liver, testis, and adrenal gland.

5.0 Reference

AFSHIN, A. et al. Health effects of dietary risks in 195 countries, 1990–2017: a systematic analysis for the Global Burden of Disease Study 2017. **The Lancet**, v. 393, n. 10184, p. 1958–1972, maio 2019.

AHMAD, I.; SANSOM, O. J.; LEUNG, H. Y. Advances in mouse models of prostate cancer. **Expert Reviews in Molecular Medicine**, v. 10, p. e16, 9 jun. 2008.

ALEJANDRO, E. U. et al. Maternal low-protein diet on the last week of pregnancy contributes to insulin resistance and β-cell dysfunction in the mouse offspring. **American Journal of Physiology-Regulatory, Integrative and Comparative Physiology**, v. 319, n. 4, p. R485–R496, 1 out. 2020.

ALLIS, C. D.; JENUWEIN, T. The molecular hallmarks of epigenetic control. **Nature Reviews Genetics**, v. 17, n. 8, p. 487–500, ago. 2016.

ASSALIN, H. B.; GONTIJO, J. A. R.; BOER, P. A. miRNAs, target genes expression and morphological analysis on the heart in gestational protein-restricted offspring. **PLOS ONE**, v. 14, n. 4, p. e0210454, 29 abr. 2019.

AUMÜLLER, G.; SEITZ, J. Protein secretion and secretory processes in male accessory sex glands. **International Review of Cytology**, v. 121, p. 127–231, 1990.

BARKER, D. J. et al. Weight in infancy and death from ischaemic heart disease. **Lancet (London, England)**, v. 2, n. 8663, p. 577–580, 9 set. 1989.

BARKER, D. J. et al. Fetal and placental size and risk of hypertension in adult life. **BMJ : British Medical Journal**, v. 301, n. 6746, p. 259–262, 4 ago. 1990.

BARKER, D. J. et al. Fetal nutrition and cardiovascular disease in adult life. **Lancet (London, England)**, v. 341, n. 8850, p. 938–941, 10 abr. 1993.

BARKER, D. J. P. Maternal nutrition, fetal nutrition, and disease in later life. **Nutrition**, v. 13, n. 9, p. 807–813, set. 1997.

BARKER, D. J. P. The origins of the developmental origins theory. **Journal of Internal Medicine**, v. 261, n. 5, p. 412–417, maio 2007.

BENATTI, R. O. et al. Maternal high-fat diet consumption modulates hepatic lipid metabolism and microRNA-122 (miR-122) and microRNA-370 (miR-370) expression in offspring. **British Journal of Nutrition**, v. 111, n. 12, p. 2112–2122, jun. 2014.

BERENDS, L. M. et al. Programming of central and peripheral insulin resistance by low birthweight and postnatal catch-up growth in male mice. **Diabetologia**, v. 61, n. 10, p. 2225–2234, 2018.

BIANCARDI, M. F. et al. Female prostate: historical, developmental, and morphological perspectives. **Cell Biology International**, v. 41, n. 11, p. 1174–1183, nov. 2017.

BLACK, M. J. et al. Accelerated age-related decline in renal and vascular function in female rats following early-life growth restriction. **American Journal of Physiology. Regulatory, Integrative and Comparative Physiology**, v. 309, n. 9, p. R1153-1161, 1 nov. 2015.

BLACK, R. E. et al. Maternal and child undernutrition and overweight in low-income and middle-income countries. **The Lancet**, v. 382, n. 9890, p. 427–451, ago. 2013.

BLACK, S. A. et al. Semaphorin 7a exerts pleiotropic effects to promote breast tumor progression. **Oncogene**, v. 35, n. 39, p. 5170–5178, 29 set. 2016.

BOHNSACK, M. T.; CZAPLINSKI, K.; GORLICH, D. Exportin 5 is a RanGTP-dependent dsRNA-binding protein that mediates nuclear export of pre-miRNAs. **RNA (New York, N.Y.)**, v. 10, n. 2, p. 185–191, fev. 2004.

BOMMER, G. T. et al. p53-mediated activation of miRNA34 candidate tumor-suppressor genes. **Current biology: CB**, v. 17, n. 15, p. 1298–1307, 7 ago. 2007.

BOSLAND, M. C. The Role of Estrogens in Prostate Carcinogenesis: A Rationale for Chemoprevention. **Reviews in Urology**, v. 7, n. Suppl 3, p. S4–S10, 2005.

BURNS, S. P. et al. Gluconeogenesis, glucose handling, and structural changes in livers of the adult offspring of rats partially deprived of protein during pregnancy and lactation. **The Journal of Clinical Investigation**, v. 100, n. 7, p. 1768–1774, 1 out. 1997.

BURTON, G. J.; FOWDEN, A. L.; THORNBURG, K. L. Placental Origins of Chronic Disease. **Physiological Reviews**, v. 96, n. 4, p. 1509–1565, 2016.

CAI, X.; HAGEDORN, C. H.; CULLEN, B. R. Human microRNAs are processed from capped, polyadenylated transcripts that can also function as mRNAs. **RNA (New York, N.Y.)**, v. 10, n. 12, p. 1957–1966, dez. 2004.

CALIN, G. A. et al. Human microRNA genes are frequently located at fragile sites and genomic regions involved in cancers. **Proceedings of the National Academy of Sciences of the United States of America**, v. 101, n. 9, p. 2999–3004, 2 mar. 2004.

CALZADA, L. et al. Maternal protein restriction during gestation impairs female offspring pancreas development in the rat. **Nutrition Research (New York, N.Y.)**, v. 36, n. 8, p. 855–862, 2016.

CASAZZA, A. et al. Sema3E–Plexin D1 signaling drives human cancer cell invasiveness and metastatic spreading in mice. **Journal of Clinical Investigation**, v. 120, n. 8, p. 2684–2698, 2 ago. 2010.

CASAZZA, A. et al. Tumour growth inhibition and anti-metastatic activity of a mutated furin-resistant Semaphorin 3E isoform. **EMBO Molecular Medicine**, v. 4, n. 3, p. 234–250, mar. 2012.

CAULFIELD, L. E. et al. Undernutrition as an underlying cause of child deaths associated with diarrhea, pneumonia, malaria, and measles. **The American Journal of Clinical Nutrition**, v. 80, n. 1, p. 193–198, jul. 2004.

CHAKRABORTY, C. et al. The Interplay among miRNAs, Major Cytokines, and Cancer-Related Inflammation. **Molecular Therapy - Nucleic Acids**, v. 20, p. 606–620, 5 jun. 2020.

CHEN, C. Real-time quantification of microRNAs by stem-loop RT-PCR. **Nucleic Acids Research**, v. 33, n. 20, p. e179–e179, 27 nov. 2005.

CIRERA-SALINAS, D. et al. Mir-33 regulates cell proliferation and cell cycle progression. **Cell Cycle**, v. 11, n. 5, p. 922–933, mar. 2012.

COLOMBELLI, K. T. et al. Impairment of microvascular angiogenesis is associated with delay in prostatic development in rat offspring of maternal protein malnutrition. **General and Comparative Endocrinology**, v. 246, p. 258–269, maio 2017.

CUNHA, G. R. et al. Stromal-epithelial interactions in adult organs. **Cell Differentiation**, v. 17, n. 3, p. 137–148, set. 1985.

DAHRI, S. et al. Islet function in offspring of mothers on low-protein diet during gestation. **Diabetes**, v. 40 Suppl 2, p. 115–120, dez. 1991.

DASGUPTA, S.; SRINIDHI, S.; VISHWANATHA, J. K. Oncogenic activation in prostate cancer progression and metastasis: Molecular insights and future challenges. **Journal of Carcinogenesis**, v. 11, p. 4, 2012.

DAVIS-DUSENBERY, B. N.; HATA, A. Mechanisms of control of microRNA biogenesis. **Journal of Biochemistry**, v. 148, n. 4, p. 381–392, out. 2010.

DAWLING, S. et al. In Vitro Model of Mammary Estrogen Metabolism: Structural and Kinetic Differences between Catechol Estrogens 2- and 4-Hydroxyestradiol. **Chemical Research in Toxicology**, v. 17, n. 9, p. 1258–1264, set. 2004.

DE BRITO ALVES, J. L. et al. Maternal protein restriction induced-hypertension is associated to oxidative disruption at transcriptional and functional levels in the medulla oblongata. **Clinical and Experimental Pharmacology and Physiology**, v. 43, n. 12, p. 1177–1184, dez. 2016.

DEANS, C.; MAGGERT, K. A. What Do You Mean, “Epigenetic”? **Genetics**, v. 199, n. 4, p. 887–896, abr. 2015.

DEARDEN, L.; OZANNE, S. E. The road between early growth and obesity: new twists and turns. **The American Journal of Clinical Nutrition**, v. 100, n. 1, p. 6–7, jul. 2014.

DENLI, A. M. et al. Processing of primary microRNAs by the Microprocessor complex. **Nature**, v. 432, n. 7014, p. 231–235, 11 nov. 2004.

DERMER, G. B. Basal cell proliferation in benign prostatic hyperplasia. **Cancer**, v. 41, n. 5, p. 1857–1862, maio 1978.

DWEEP, H.; GRETZ, N. miRWalk2.0: a comprehensive atlas of microRNA-target interactions. **Nature Methods**, v. 12, n. 8, p. 697, ago. 2015.

EMBLETON, N. D. et al. Catch-up growth and metabolic outcomes in adolescents born preterm. **Archives of Disease in Childhood**, v. 101, n. 11, p. 1026–1031, 2016.

FALCÃO-TEBAS, F. et al. Maternal low-protein diet-induced delayed reflex ontogeny is attenuated by moderate physical training during gestation in rats. **British Journal of Nutrition**, v. 107, n. 3, p. 372–377, 14 fev. 2012.

FERNANDEZ-TWINN, D. S.; CONSTÂNCIA, M.; OZANNE, S. E. Intergenerational epigenetic inheritance in models of developmental programming of adult disease. **Seminars in Cell & Developmental Biology**, v. 43, p. 85–95, jul. 2015.

FITZHARDINGE, P. M.; STEVEN, E. M. The Small-for-Date Infant I. Later Growth Patterns. **Pediatrics**, v. 49, n. 5, p. 671–681, 1 maio 1972.

FRANZOLIN, G.; TAMAGNONE, L. Semaphorin Signaling in Cancer-Associated Inflammation. **International Journal of Molecular Sciences**, v. 20, n. 2, p. 377, 17 jan. 2019.

FRIEDMAN, E. B. et al. Serum microRNAs as biomarkers for recurrence in melanoma. **Journal of Translational Medicine**, v. 10, n. 1, p. 155, 2012.

GAJJAR, K.; MARTIN-HIRSCH, P. L.; MARTIN, F. L. CYP1B1 and hormone-induced cancer. **Cancer Letters**, v. 324, n. 1, p. 13–30, nov. 2012.

Global Cancer Observatory. Disponível em: <https://gco.iarc.fr/>. Acesso em: 26 maio. 2021.

GLUCKMAN, P. D.; HANSON, M. A.; BUKLIJAS, T. A conceptual framework for the developmental origins of health and disease. **Journal of Developmental Origins of Health and Disease**, v. 1, n. 1, p. 6–18, fev. 2010.

GREGORY, R. I. et al. The Microprocessor complex mediates the genesis of microRNAs. **Nature**, v. 432, n. 7014, p. 235–240, nov. 2004.

HABIB, S. L. et al. Diabetes and risk of renal cell carcinoma. **Journal of Cancer**, v. 3, p. 42–48, 2012.

HAMMOND, S. M. et al. Argonaute2, a link between genetic and biochemical analyses of RNAi. **Science (New York, N.Y.)**, v. 293, n. 5532, p. 1146–1150, 10 ago. 2001.

HAN, J. et al. The Drosha-DGCR8 complex in primary microRNA processing. **Genes & Development**, v. 18, n. 24, p. 3016–3027, 15 dez. 2004.

HAYES, C. L. et al. 17 beta-estradiol hydroxylation catalyzed by human cytochrome P450 1B1. **Proceedings of the National Academy of Sciences**, v. 93, n. 18, p. 9776–9781, 3 set. 1996.

HEERWAGEN, M. J. R. et al. Maternal obesity and fetal metabolic programming: a fertile epigenetic soil. **American Journal of Physiology-Regulatory, Integrative and Comparative Physiology**, v. 299, n. 3, p. R711–R722, set. 2010.

HOFFMAN, D. J. et al. Developmental Origins of Metabolic Disease. **Physiological Reviews**, 3 dez. 2020.

HORIE, T. et al. MicroRNA-33 encoded by an intron of sterol regulatory element-binding protein 2 (Srebp2) regulates HDL in vivo. **Proceedings of the National Academy of Sciences**, v. 107, n. 40, p. 17321–17326, 5 out. 2010.

INSTITUTE FOR HEALTH METRICS AND EVALUATION (IHME). **Findings from the Global Burden of Disease Study 2017**. Seattle: [s.n.].

JOUBERT, B. R. et al. DNA Methylation in Newborns and Maternal Smoking in Pregnancy: Genome-wide Consortium Meta-analysis. **American Journal of Human Genetics**, v. 98, n. 4, p. 680–696, 7 abr. 2016.

KIM, V. N.; HAN, J.; SIOMI, M. C. Biogenesis of small RNAs in animals. **Nature Reviews Molecular Cell Biology**, v. 10, n. 2, p. 126–139, fev. 2009.

KROL, J.; LOEDIGE, I.; FILIPOWICZ, W. The widespread regulation of microRNA biogenesis, function and decay. **Nature Reviews. Genetics**, v. 11, n. 9, p. 597–610, set. 2010.

KUMAR, M. S. et al. Dicer1 functions as a haploinsufficient tumor suppressor. **Genes & Development**, v. 23, n. 23, p. 2700–2704, 1 dez. 2009.

KUO, P.-L. et al. MicroRNA-33a functions as a bone metastasis suppressor in lung cancer by targeting parathyroid hormone related protein. **Biochimica et Biophysica Acta (BBA) - General Subjects**, v. 1830, n. 6, p. 3756–3766, 1 jun. 2013.

KWON, D.-H. et al. Dietary protein restriction induces steatohepatitis and alters leptin/signal transducers and activators of transcription 3 signaling in lactating rats. **The Journal of Nutritional Biochemistry**, v. 23, n. 7, p. 791–799, jul. 2012.

LANDTHALER, M.; YALCIN, A.; TUSCHL, T. The human DiGeorge syndrome critical region gene 8 and Its D. melanogaster homolog are required for miRNA biogenesis. **Current biology: CB**, v. 14, n. 23, p. 2162–2167, 14 dez. 2004.

LEANDRO, C. G. et al. Maternal Moderate Physical Training during Pregnancy Attenuates the Effects of a Low-Protein Diet on the Impaired Secretion of Insulin in Rats: Potential Role for Compensation of Insulin Resistance and Preventing Gestational Diabetes Mellitus. **Journal of Biomedicine and Biotechnology**, v. 2012, p. 1–7, 2012.

LEE, R. C.; FEINBAUM, R. L.; AMBROS, V. The C. elegans heterochronic gene lin-4 encodes small RNAs with antisense complementarity to lin-14. **Cell**, v. 75, n. 5, p. 843–854, 3 dez. 1993.

LEE, Y. et al. The nuclear RNase III Drosha initiates microRNA processing. **Nature**, v. 425, n. 6956, p. 415–419, 25 set. 2003.

LEE, Y. et al. MicroRNA genes are transcribed by RNA polymerase II. **The EMBO journal**, v. 23, n. 20, p. 4051–4060, 13 out. 2004.

LI, F.; ZHU, W.; GONZALEZ, F. J. Potential role of CYP1B1 in the development and treatment of metabolic diseases. **Pharmacology & Therapeutics**, v. 178, p. 18–30, out. 2017.

LIMA, R. F. DE et al. Bisphenol-A promotes antiproliferative effects during neonatal prostate development in male and female gerbils. **Reproductive Toxicology**, v. 58, p. 238–245, dez. 2015.

LIN, S.; GREGORY, R. I. MicroRNA biogenesis pathways in cancer. **Nature Reviews Cancer**, v. 15, n. 6, p. 321–333, jun. 2015.

LIVAK, K.; SCHMITTGEN, T. **Analysis of relative gene expression data using real-time quantitative PCR and the 2(-Delta Delta C(T)) Method**. Disponível em: <https://pubmed.ncbi.nlm.nih.gov/11846609/>. Acesso em: 14 ago. 2020.

LOWSLEY, O. S. The development of the human prostate gland with reference to the development of other structures at the neck of the urinary bladder. **American Journal of Anatomy**, v. 13, n. 3, p. 299–349, 1912.

LU, Y. et al. Expression of semaphorin 6D and its receptor plexin-A1 in gastric cancer and their association with tumor angiogenesis. **Oncology Letters**, v. 12, n. 5, p. 3967–3974, nov. 2016.

LUCHINO, J. et al. Semaphorin 3E Suppresses Tumor Cell Death Triggered by the Plexin D1 Dependence Receptor in Metastatic Breast Cancers. **Cancer Cell**, v. 24, n. 5, p. 673–685, nov. 2013.

LUND, E. et al. Nuclear export of microRNA precursors. **Science (New York, N.Y.)**, v. 303, n. 5654, p. 95–98, 2 jan. 2004.

MARKER, P. C. et al. Hormonal, cellular, and molecular control of prostatic development. **Developmental Biology**, v. 253, n. 2, p. 165–174, 15 jan. 2003.

MARQUART, T. J. et al. miR-33 links SREBP-2 induction to repression of sterol transporters. **Proceedings of the National Academy of Sciences**, v. 107, n. 27, p. 12228–12232, 6 jul. 2010.

MCMILLEN, I. C.; ADAM, C. L.; MÜHLHÄUSLER, B. S. Early origins of obesity: programming the appetite regulatory system. **The Journal of Physiology**, v. 565, n. Pt 1, p. 9–17, 15 maio 2005.

MELO, S. A. et al. A genetic defect in exportin-5 traps precursor microRNAs in the nucleus of cancer cells. **Cancer Cell**, v. 18, n. 4, p. 303–315, 19 out. 2010.

MERICQ, V. et al. Long-term metabolic risk among children born premature or small for gestational age. **Nature Reviews Endocrinology**, v. 13, n. 1, p. 50–62, jan. 2017.

MIN, W. et al. The expression and significance of five types of miRNAs in breast cancer. **Medical Science Monitor Basic Research**, v. 20, p. 97–104, 21 jul. 2014.

MOURELATOS, Z. et al. miRNPs: a novel class of ribonucleoproteins containing numerous microRNAs. **Genes & Development**, v. 16, n. 6, p. 720–728, 15 mar. 2002.

MURALIDHAR, B. et al. Functional evidence that Drosha overexpression in cervical squamous cell carcinoma affects cell phenotype and microRNA profiles. **The Journal of Pathology**, v. 224, n. 4, p. 496–507, ago. 2011.

NÄÄR, A. M. miR-33: A Metabolic Conundrum. **Trends in Endocrinology & Metabolism**, v. 29, n. 10, p. 667–668, out. 2018.

NAJAFI-SHOUSHTARI, S. H. et al. MicroRNA-33 and the SREBP Host Genes Cooperate to Control Cholesterol Homeostasis. **Science**, v. 328, n. 5985, p. 1566–1569, 18 jun. 2010.

NUTRITION, N. R. C. (US) S. ON L. A. **Nutrient Requirements of the Laboratory Rat**. [s.l.] National Academies Press (US), 1995.

OZANNE, S. E.; HALES, C. N. Catch-up growth and obesity in male mice. **Nature**, v. 427, n. 6973, p. 411–412, jan. 2004.

PAN, S. et al. MicroRNA-130b and microRNA-374b mediate the effect of maternal dietary protein on offspring lipid metabolism in Meishan pigs. **British Journal of Nutrition**, v. 109, n. 10, p. 1731–1738, 28 maio 2013.

PARASRAMKA, M. A. et al. A role for low-abundance miRNAs in colon cancer: the miR-206/Krüppel-like factor 4 (KLF4) axis. **Clinical Epigenetics**, v. 4, n. 1, p. 16, 24 set. 2012.

PARL, F. F. et al. Estrogen Exposure, Metabolism, and Enzyme Variants in a Model for Breast Cancer Risk Prediction. **Cancer Informatics**, v. 7, p. CIN.S2262, jan. 2009.

PELLETIER, D. L. et al. The Effects of malnutrition on child mortality in developing countries. **Bulletin of the World Health Organization 1995 ; 73(4) : 443-448**, 1995.

PETRY, C. et al. Diabetes in Old Male Offspring of Rat Dams Fed a Reduced Protein Diet. **International journal of experimental diabetes research**, v. 2, p. 139–43, 1 fev. 2001.

PIAN, C. et al. Discovering Cancer-Related miRNAs from miRNA-Target Interactions by Support Vector Machines. **Molecular Therapy - Nucleic Acids**, v. 19, p. 1423–1433, 6 mar. 2020.

PINHO, C. F. et al. Gestational protein restriction delays prostate morphogenesis in male rats. **Reproduction, Fertility and Development**, v. 26, n. 7, p. 967, 2014.

PLAGEMANN, A. et al. Hypothalamic neuropeptide Y levels in weaning offspring of low-protein malnourished mother rats. **Neuropeptides**, v. 34, n. 1, p. 1–6, fev. 2000.

PORTELA, L. MF. et al. Increased oxidative stress and cancer biomarkers in the ventral prostate of older rats submitted to maternal malnutrition. **Molecular and Cellular Endocrinology**, v. 523, p. 111148, mar. 2021.

PRICE, N. L. et al. Genetic Ablation of miR-33 Increases Food Intake, Enhances Adipose Tissue Expansion, and Promotes Obesity and Insulin Resistance. **Cell Reports**, v. 22, n. 8, p. 2133–2145, 20 2018.

PRINS, G. S. et al. Androgen receptor expression and 5 alpha-reductase activity along the proximal-distal axis of the rat prostatic duct. **Endocrinology**, v. 130, n. 5, p. 3066–3073, maio 1992.

PRINS, G. S. et al. Perinatal Exposure to Oestradiol and Bisphenol A Alters the Prostate Epigenome and Increases Susceptibility to Carcinogenesis. **Basic & clinical pharmacology & toxicology**, v. 102, n. 2, p. 134, fev. 2008.

PRINS, G. S.; PUTZ, O. Molecular signaling pathways that regulate prostate gland development. **Differentiation; Research in Biological Diversity**, v. 76, n. 6, p. 641–659, jul. 2008.

RAHMAN, R.-U. et al. Oasis 2: improved online analysis of small RNA-seq data. **BMC Bioinformatics**, v. 19, n. 1, p. 54, 14 fev. 2018.

RAMOS, C. DA F. et al. The prostate of weaned pups is altered by maternal malnutrition during lactation in rats. **Asian Journal of Andrology**, v. 12, n. 2, p. 180–185, mar. 2010.

RAVELLI, G. P.; STEIN, Z. A.; SUSSER, M. W. Obesity in young men after famine exposure in utero and early infancy. **The New England Journal of Medicine**, v. 295, n. 7, p. 349–353, 12 ago. 1976.

RAVER-SHAPIRA, N. et al. Transcriptional activation of miR-34a contributes to p53-mediated apoptosis. **Molecular Cell**, v. 26, n. 5, p. 731–743, 8 jun. 2007.

RAYNER, K. J. et al. MiR-33 Contributes to the Regulation of Cholesterol Homeostasis. **Science**, v. 328, n. 5985, p. 1570–1573, 18 jun. 2010.

RAYNER, K. J. et al. Antagonism of miR-33 in mice promotes reverse cholesterol transport and regression of atherosclerosis. **The Journal of Clinical Investigation**, v. 121, n. 7, p. 2921–2931, 1 jul. 2011a.

RAYNER, K. J. et al. Inhibition of miR-33a/b in non-human primates raises plasma HDL and lowers VLDL triglycerides. **Nature**, v. 478, n. 7369, p. 404–407, out. 2011b.

RICE, S. J. et al. MicroRNA-33a Mediates the Regulation of High Mobility Group AT-Hook 2 Gene (HMGA2) by Thyroid Transcription Factor 1 (TTF-1/NKX2–1)*. **Journal of Biological Chemistry**, v. 288, n. 23, p. 16348–16360, jun. 2013.

ROTLLAN NOEMI et al. Therapeutic Silencing of MicroRNA-33 Inhibits the Progression of Atherosclerosis in Ldlr−/− Mice—Brief Report. **Arteriosclerosis, Thrombosis, and Vascular Biology**, v. 33, n. 8, p. 1973–1977, 1 ago. 2013.

ROTTIERS, V. et al. Pharmacological inhibition of a microRNA family in nonhuman primates by a seed-targeting 8-mer antimiR. **Science Translational Medicine**, v. 5, n. 212, p. 212ra162, 20 nov. 2013.

ROY-BURMAN, P. et al. Genetically defined mouse models that mimic natural aspects of human prostate cancer development. **Endocrine-Related Cancer**, v. 11, n. 2, p. 225–254, jun. 2004.

SALIMINEJAD, K. et al. An overview of microRNAs: Biology, functions, therapeutics, and analysis methods: SALIMINEJAD ET AL. **Journal of Cellular Physiology**, v. 234, n. 5, p. 5451–5465, maio 2019.

SANTOS, S. A. A. et al. Maternal Low-Protein Diet Impairs Prostate Growth in Young Rat Offspring and Induces Prostate Carcinogenesis With Aging. **The Journals of Gerontology: Series A**, v. 74, n. 6, p. 751–759, 16 maio 2019.

SANTOS, S. A. A. et al. Identification of potential molecular pathways involved in prostate carcinogenesis in offspring exposed to maternal malnutrition. **Aging**, v. 12, 13 out. 2020.

SCHAUER, I. G.; ROWLEY, D. R. The functional role of reactive stroma in benign prostatic hyperplasia. **Differentiation; Research in Biological Diversity**, v. 82, n. 4–5, p. 200–210, dez. 2011.

SCHULZ, L. C. The Dutch Hunger Winter and the developmental origins of health and disease. **Proceedings of the National Academy of Sciences of the United States of America**, v. 107, n. 39, p. 16757–16758, 28 set. 2010.

SENE, A. et al. Impaired cholesterol efflux in senescent macrophages promotes age-related macular degeneration. **Cell Metabolism**, v. 17, n. 4, p. 549–561, 2 abr. 2013.

SHYU, A.-B.; WILKINSON, M. F.; VAN HOOF, A. Messenger RNA regulation: to translate or to degrade. **The EMBO journal**, v. 27, n. 3, p. 471–481, 6 fev. 2008.

SINCLAIR, K. D. et al. DNA methylation, insulin resistance, and blood pressure in offspring determined by maternal periconceptional B vitamin and methionine status. **Proceedings of the National Academy of Sciences of the United States of America**, v. 104, n. 49, p. 19351–19356, 4 dez. 2007.

SPINK, D. C. et al. Induction of cytochrome P450 1B1 and catechol estrogen metabolism in ACHN human renal adenocarcinoma cells. **The Journal of Steroid Biochemistry and Molecular Biology**, v. 62, n. 2–3, p. 223–232, jun. 1997.

SUGITO, N. et al. RNASEN regulates cell proliferation and affects survival in esophageal cancer patients. **Clinical Cancer Research: An Official Journal of the American Association for Cancer Research**, v. 12, n. 24, p. 7322–7328, 15 dez. 2006.

SUN, Y. et al. Multigenerational maternal obesity increases the incidence of HCC in offspring via miR-27a-3p. **Journal of Hepatology**, v. 73, n. 3, p. 603–615, set. 2020.

TABARA, H. et al. The rde-1 gene, RNA interference, and transposon silencing in C. elegans. **Cell**, v. 99, n. 2, p. 123–132, 15 out. 1999.

TAMAGNONE, L.; MAZZONE, M. Semaphorin Signals on the Road of Endothelial Tip Cells. **Developmental Cell**, v. 21, n. 2, p. 189–190, ago. 2011.

TARRY-ADKINS, J. L. et al. Coenzyme Q10 Prevents Insulin Signaling Dysregulation and Inflammation Prior to Development of Insulin Resistance in Male Offspring of a Rat Model of Poor Maternal Nutrition and Accelerated Postnatal Growth. **Endocrinology**, v. 156, n. 10, p. 3528–3537, out. 2015.

TARRY-ADKINS, J. L. et al. Coenzyme Q10 prevents hepatic fibrosis, inflammation, and oxidative stress in a male rat model of poor maternal nutrition and accelerated postnatal growth. **The American Journal of Clinical Nutrition**, v. 103, n. 2, p. 579–588, fev. 2016.

THOMAS, M. et al. The proto-oncogene Pim-1 is a target of miR-33a. **Oncogene**, v. 31, n. 7, p. 918–928, fev. 2012.

TIMMS, B. G.; MOHS, T. J.; DIDIO, L. J. Ductal budding and branching patterns in the developing prostate. **The Journal of Urology**, v. 151, n. 5, p. 1427–1432, maio 1994.

UNITED NATIONS FOOD AND AGRICULTURAL ORGANIZATION (FAO). PROTEIN SUPPLY QUANTITY. **Our World in Data**, 2020.

VARKONYI-GASIC, E. et al. Protocol: a highly sensitive RT-PCR method for detection and quantification of microRNAs. **Plant Methods**, v. 3, n. 1, p. 12, 2007.

VEGA, C. C. et al. Resveratrol partially prevents oxidative stress and metabolic dysfunction in pregnant rats fed a low protein diet and their offspring. **The Journal of Physiology**, v. 594, n. 5, p. 1483–1499, 1 mar. 2016.

VERZE, P.; CAI, T.; LORENZETTI, S. The role of the prostate in male fertility, health and disease. **Nature Reviews Urology**, v. 13, n. 7, p. 379–386, jul. 2016.

WADDINGTON, C. H. The epigenotype. 1942. **International Journal of Epidemiology**, v. 41, n. 1, p. 10–13, fev. 2012.

WATERLAND, R. A.; JIRTLE, R. L. Transposable elements: targets for early nutritional effects on epigenetic gene regulation. **Molecular and Cellular Biology**, v. 23, n. 15, p. 5293–5300, ago. 2003.

WEIBEL, E. R.; KISTLER, G. S.; SCHERLE, W. F. Practical stereological methods for morphometric cytology. **The Journal of Cell Biology**, v. 30, n. 1, p. 23–38, jul. 1966.

WELSH, M. et al. Identification in rats of a programming window for reproductive tract masculinization, disruption of which leads to hypospadias and cryptorchidism. **Journal of Clinical Investigation**, v. 118, n. 4, p. 1479–1490, 1 abr. 2008.

WIGHTMAN, B.; HA, I.; RUVKUN, G. Posttranscriptional regulation of the heterochronic gene lin-14 by lin-4 mediates temporal pattern formation in C. elegans. **Cell**, v. 75, n. 5, p. 855–862, 3 dez. 1993.

WILHELM, D.; KOOPMAN, P. The makings of maleness: towards an integrated view of male sexual development. **Nature Reviews. Genetics**, v. 7, n. 8, p. 620–631, ago. 2006.

WILSON, J. D. et al. The endocrine control of male phenotypic development. **Australian Journal of Biological Sciences**, v. 36, n. 2, p. 101–128, 1983.

WINTER, J. et al. Many roads to maturity: microRNA biogenesis pathways and their regulation. **Nature Cell Biology**, v. 11, n. 3, p. 228–234, mar. 2009.

XIE, C. et al. KOBAS 2.0: a web server for annotation and identification of enriched pathways and diseases. **Nucleic Acids Research**, v. 39, n. Web Server issue, p. W316-322, jul. 2011.

YI, R. et al. Exportin-5 mediates the nuclear export of pre-microRNAs and short hairpin RNAs. **Genes & Development**, v. 17, n. 24, p. 3011–3016, 15 dez. 2003.

ZAMBRANO, E. et al. Fetal programming of sexual development and reproductive function. **Molecular and Cellular Endocrinology**, v. 382, n. 1, p. 538–549, 25 jan. 2014.

ZANA-TAIEB, E. et al. Effect of two models of intrauterine growth restriction on alveolarization in rat lungs: morphometric and gene expression analysis. **PloS One**, v. 8, n. 11, p. e78326, 2013.

ZAVIACIC, M.; ABLIN, R. J. The female prostate and prostate-specific antigen. Immunohistochemical localization, implications of this prostate marker in women and reasons for using the term “prostate” in the human female. **Histology and Histopathology**, v. 15, n. 1, p. 131–142, 2000.

ZHANG, J. et al. Maternal high fat diet during pregnancy and lactation alters hepatic expression of insulin like growth factor-2 and key microRNAs in the adult offspring. **BMC genomics**, v. 10, p. 478, 16 out. 2009.

ZHANG, L. et al. microRNAs exhibit high frequency genomic alterations in human cancer. **Proceedings of the National Academy of Sciences of the United States of America**, v. 103, n. 24, p. 9136–9141, 13 jun. 2006.

ZHAO, X.-Y. Expression of semaphorin 6D in gastric carcinoma and its significance. **World Journal of Gastroenterology**, v. 12, n. 45, p. 7388, 2006.

ZHENG, J. et al. Maternal Low-Protein Diet Modulates Glucose Metabolism and Hepatic MicroRNAs Expression in the Early Life of Offspring †. **Nutrients**, v. 9, n. 3, p. 205, 27 fev. 2017.

ZHOU, J. et al. miR-33a functions as a tumor suppressor in melanoma by targeting HIF-1α. **Cancer Biology & Therapy**, v. 16, n. 6, p. 846–855, 3 jun. 2015.

Funding

This research was supported by the National Council for Scientific and Technological Development, CNPq (Process 310663/2018-0 to LAJ,), by Coordenação de Aperfeiçoamento de Pessoal de Nível Superior (CAPES) and by Fundação de Amparo à Pesquisa do Estado de São Paulo (Process 2017/01063-7 to LAJ, and scholarship 2017/08716-6 to FBC).

Author contributions

Conceptualization, F.B.C, L.A.J.; methodology, F.B.C., L.M.F.P., A.C.L.C., K.T.C., S.A.A.S, M.N.F., P.P.F., B.C.M, M.C.B., T.K., C.S.M., W.L.L., R.F.C., L.A.J. ; formal analysis, F.B.C., R.F.C., L.A.J; investigation, F.B.C., R.F.C., L.A.J.; resources, F.B.C., L.A.J.; data curation, F.B.C., R.F.C., L.A.J.; writing—original draft preparation, F.B.C., writing—review and editing, all authors; supervision, R.F.C., L.A.J; project administration, L.A.J; funding acquisition, L.A.J.

Competing interests

The author declares no competing interests.

Ethical Approval

Ethics Committee on Animal Experimentation of the Institute of Biosciences of Botucatu (CEEA-949).

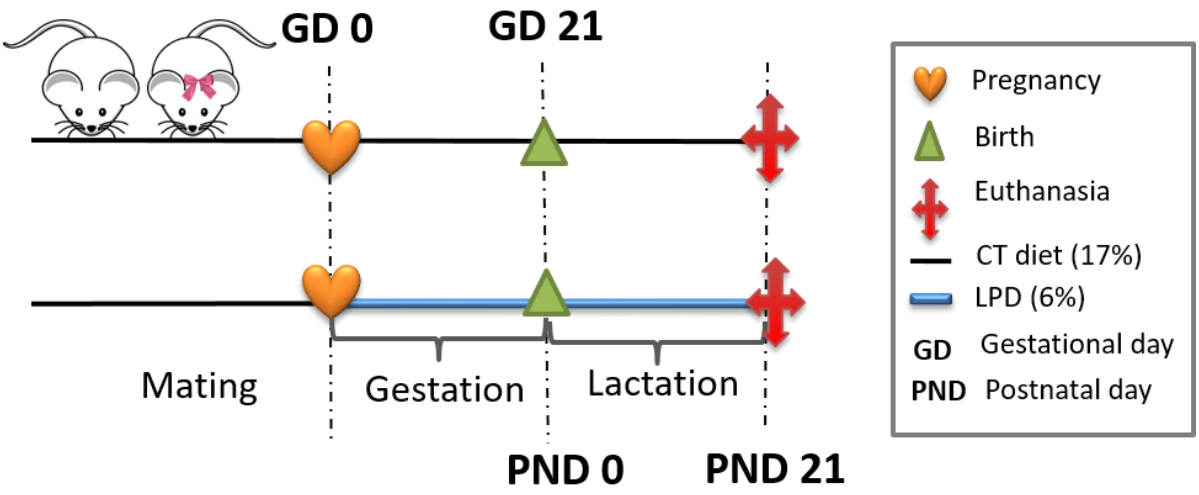

Supplementary Figure 1. Scheme of the experimental design of the animals.

Carta: O artigo presente no Anexo 1 desta tese, contempla um assunto totalmente diferente do trabalho até então explorado por esse grupo de pesquisa. No final de 2019 um vírus teve o seu primeiro caso em humano e por conta do seu contágio rápido e mortal para uma parcela da humanidade, um Pandemia se estende até hoje, dia 24 de maio de 2021. Assim, este próximo artigo teve como objetivo utilizar os conhecimentos adquiridos durante o meu doutorado, conhecimento estes de técnicas *in-silico* e contribuir de alguma forma para a ciência. Cabe ressaltar, que no momento específico em que ele foi realizado estávamos passando por um período de isolamento social, onde os Laboratórios estavam fechados.

Anexo 1: Prediction of non-canonical routes for SARS-CoV-2 infection in human placenta cells – submitted to Science Signaling.

F. B. Constantino [1†], S. S. Cury [1†], C. R. Nogueira [2], R. F. Carvalho [1*], L. A. Justulin [1*]

Affiliations

[1] Department of Structural and Functional Biology, Institute of Biosciences, São Paulo State University (UNESP), Botucatu, São Paulo, Brazil.

[2] São Paulo State University (UNESP), Botucatu Medical School, Botucatu, São Paulo, Brazil.

†These authors contributed equally.

*Corresponding authors

Corresponding author´s information:

Luis Antonio Justulin

Department of Structural and Functional Biology

Institute of Biosciences, São Paulo State University (UNESP)

CEP: 18.618-689, Botucatu, São Paulo – Brazil

Telephone number: +55 14 3880 0481

l.justulin@unesp.br

Robson Francisco Carvalho

Department of Structural and Functional Biology

Institute of Biosciences, São Paulo State University (UNESP)

CEP: 18.618-689, Botucatu, São Paulo – Brazil

Telephone number: +55 14 3880 0473

robson.carvalho@unesp.br

Abstract

The data available about COVID-19 during pregnancy have demonstrated that SARS-CoV-2 infects placenta cells, despite these cells express low levels of the canonical virus entry genes (ACE2 and TMPRSS2). Here we analyzed the transcriptional profile (microarray and single-cell RNA-Seq) of proteins potentially interacting with coronaviruses to identify non-canonical mediators of SARS-CoV-2 infection and replication in the placenta. We show that, despite low levels of the canonical cell entry mediators ACE2 and TMPRSS2, cells of the syncytiotrophoblast, villous cytotrophoblast, and extravillous trophoblast co-express high levels of the potential non-canonical cell-entry mediators DPP4 and CTSL. We also found changes in the expression of DAAM1 and PAICS genes during pregnancy, which are translated into proteins also predicted to interact with coronaviruses proteins. These results provide new insight into the interaction between SARS-CoV-2 and host proteins that may act as non-canonical routes for SARS-CoV-2 infection and replication in the placenta cells.

1. Introduction

The severe acute respiratory syndrome coronavirus 2 (SARS-CoV-2) is the causative agent of the coronavirus disease 2019 (COVID-19) *(1, 2)*. It was first notified at the end of 2019, in Wuhan, China, and become a worldwide pandemic *(3)*. At the beginning of June, five months later, COVID-19 infected over seven million people and is the cause of approximately 404,000 deaths worldwide (https://coronavirus.jhu.edu/).

Older age, laboratory abnormalities, and several comorbidities are associated with the more severe cases of COVID-19 *(4,5)*. For specific groups of COVID-19 patients, for example, pregnant women, the potential impacts of SARS-CoV-2 infection remains mostly unknown, and data are limited. However, considering previous works reporting coronaviruses infections *(6)*, pregnant women are at higher risk of SARS-CoV-2 infection due to physiological changes in the immune, cardiorespiratory, and metabolic systems *(7)*.

Although only a small number of maternal viruses infections are transmitted to the fetus, some may cause life-threatening diseases *(8)*. These viruses use cellular host entry mediators expressed by placenta cells, as described for the cytomegalovirus and the Zika virus *(9, 10)*, to infect these cells. The Zika virus (ZIKV) outbreak, associated with causes fetal brain damage, emphasizes the necessity of further characterization and understanding placental infection or intrauterine (vertical) transmission of SARS-CoV-2, as well as the possible adverse fetal outcomes. The few studies on the subject have provided contradictory findings, with some reports suggesting no evidence of placental infection or vertical transmission of SARS-CoV-2 *(11–13)*. Conversely, multiple lines of evidence have shown placental SARS-CoV-2 infection in pregnant women diagnosed with moderate to severe COVID-19. Neonates born from mothers with COVID-19 presented a positive serological test for SARS-CoV-2 immunoglobulin (Ig)M and IgG *(14, 15)*. While the IgG can be transferred from mother to fetus across the placenta, the detection of IgM in newborns suggests a vertical transmission of the virus, since IgM can not cross the placental barrier due to its high molecular mass *(16)*. Accordingly, SARS-CoV-2 RNA was detected through RT-qPCR in mother, neonate, and placental tissues *(17)*. These authors further demonstrated the SARS-CoV-2 in syncytiotrophoblast by *in*

situ hybridization assay and transmission electron microscopy. Also, it was recently shown SARS-CoV-2 particles in syncytiotrophoblasts with generalized inflammation, diffuse perivillous fibrin depositions, and tissue damage in an asymptomatic woman *(18)*. Remarkably, these placental alterations due to the SARS-CoV-2 infection lead to fetal distress and neonatal multi-organ failure. These results highlight the importance of exploring the expression profile of potential host mediators of the SARS-CoV-2 that may create a permissive microenvironment to placental infection and possible vertical transmission of the virus.

In fact, like other viruses, SARS-CoV-2 requires diverse host cellular factors for infection and replication. The angiotensin-converting enzyme 2 *(ACE2)* is the canonical receptor for the SARS-CoV-2 spike protein receptor-binding domain (RBD) for viral attachment *(19, 20)*. This process is followed by S protein priming by cellular transmembrane serine protease 2 (*TMPRSS2*) that allows the fusion of the virus with host cellular membranes *(19, 20)*. Single-cell RNA sequencing (scRNA-Seq) has demonstrated that both *ACE2* and *TMPRSS2* are co-expressed in multiple tissues affected by COVID-19, including airway epithelial cells, cornea, digestive and urogenital systems *(21)*. Few cells express *ACE2* and *TMPRSS2* in the placenta *(21, 22)*, suggesting that SARS-CoV-2 is unlikely to infect the placenta through the canonical cell entry mediators. Therefore, other host interacting proteins may play a role in the biological cycle of the virus and contribute to the pathogenesis of SARS-CoV-2 in the placenta. In this paper, we demonstrate, through transcriptomic (microarray and scRNA-Seq) analysis and in silico predictions of virus-host protein-protein interactions, that cells of the syncytiotrophoblast, villous cytotrophoblast, and extravillous trophoblast express high levels of potential non-canonical cell-entry mediators dipeptidyl peptidase 4 *(DPP4)* and cathepsin L *(CTSL)*, despite low-levels of ACE2 and TMPRSS2. These results open new avenues of investigation of the human placenta infection by the SARS-CoV-2.

2. Results

2.2 Prediction of non-canonical routes for SARS-CoV-2 infection in human placenta cells

We first investigated the gene expression in placental tissues of classical host-virus interacting proteins described in the literature. The canonical entry receptors *ACE2* and *TMPRSS2* were low expressed throughout gestation. *CTSL*, which is translated into a lysosomal cysteine proteinase that plays a role in intracellular protein catabolism - presented the highest level of expression in the placenta during the first, second, and third trimester. Similarly, *DPP4*, which is translated into an intrinsic membrane glycoprotein, was highly expressed throughout gestation (Figure 1A).

Next, we analyzed the gene expression profile during gestation in placental tissues. We found 25 differentially expressed genes (DEGs) in the second trimester, and 687 DEGs in the third, when they were independently compared to the first trimester (Supplementary Table 1). All DEGs were divided into three clusters by the K-means clustering analysis (Supplementary Figure 1A). Cluster 1 includes genes that increase expression during pregnancy, and these genes enriched terms related to blood vessels morphogenesis, complement cascade, extracellular matrix organization, and cellular response to nitrogen compounds. Cluster 2 encompasses genes that increase expression specifically in the third trimesters, which are related to female pregnancy, growth hormone signaling pathway, homeostasis, and steroid biosynthetic process. Cluster 3 includes genes that decrease expression during pregnancy. and these genes enriched terms related to cell division, sulfur compounds biosynthetic process, chromosomal segregation, PID MYC active pathway (Supplementary Figure 1B and Supplementary Table 2). The gene expression changes in the course of pregnancy revealed that the second and third trimesters enriched genes that are associated with the placental growth, mainly in the third trimester (Supplementary Figure 1C and Supplementary Table 3). Even with a high discrepancy between the number of DEGs in second and third trimesters (25 and 687, respectively), we identified similarities in the enriched terms between gene

clusters (Supplementary Figure 1D) and between the second and third trimesters of gestation (Supplementary Figure 1E).

We further asked whether the DEGs in the placenta during gestation are translated into proteins that potentially interact with SARS-CoV proteins. Considering that the current cases of SARS-CoV-2 placental infection are mainly related to the third trimester of pregnancy (17, 23), we selected the 687 DEGs in the placenta in the third trimester compared to the first trimester and, among them, 474 and 213 were up- and down-regulated, respectively (Supplementary Table 1). Next, we selected the human proteins potentially interacting with SARS-CoV using the P-HIPSter database. We found 32 virus-host interacting proteins of SARS-CoV (Supplementary Table 4), and nine virus-host interacting proteins of the ZIKV (Supplementary Table 5). We also found that, from these list of virus-host interacting proteins, 10 DEGs *(DAAM1, FRMD3, STX3, HBD, PRKCZ, CTK3, PAICS, EVL, TREM2, and HBE1)* are translated into proteins that interact with SARS-CoV proteins, and one with the ZIKV (Supplementary Figures 1F and 1G). Among these 10 DEGs, six were up-regulated *(DAAM1, FRMD3, STX3, HBD, PRKCZ, and CTK3)* and four *(PAICS, EVL, TREM2, and HBE1)* were down-regulated in the third trimester (Figure 1B). The gene *DAAM1*, which is translated into an intrinsic membrane glycoprotein implicated in cell motility, adhesion, cytokinesis, and cell polarity - showed the highest level of fold change in the third trimester of gestation compared to the first (logFC= 1.43; Figure 1B). The host-virus protein-protein interactions (PPI) predicted for these 10 DEGs presented a Likelihood Ratio (LR) > 100 (Supplementary Table 6), according to P-HIPSTer (24). Noteworthy, *PAICS* transcript, which is translated into an enzyme that catalyzes the sixth and seventh steps of the novo purine biosynthesis, were predicted to interact with both SARS-CoV and ZIKV (Figure 1B and Supplementary Table 7). We observed a significant interaction of placental proteins predicted to interact with SARS-CoV-2 (based on the DEGs or not), and *PAICS* was also predicted to interact with other proteins in the PPI network with the highest degree (Figure 1C and Supplementary Table 8).

We next used single-cell RNA sequencing to analyze the expression of the 10 DEGs translated into proteins that potentially interact with SARS-CoV in human placental

cells (Supplementary Figures 1H and 1I). We selected the genes *ACE2, TMPRSS2, CTSL, DPP4, PAICS,* and *DAAM1* for further investigations using scRNA-seq transcriptome data from cells of the syncytiotrophoblast (n=1144), villous cytotrophoblast (n=8244), and extravillous trophoblast (n=2170) of non-disease human placental tissues, considering the potential relevance of these genes for SARS-CoV infection and replication in the organ (Figure 1D). We noticed that the expression of the classical SARS-CoV-2 entry receptor genes *(ACE2 and TMPRSS2)* was minimally expressed in these cells. In contrast, potential non-canonical cell entry mediator genes *DPP4* and *CTSL*, as well as, the genes for the predicted virus-host interaction proteins *DAAM1,* and *PAICS* were expressed at higher levels (Figure 1E and Supplementary Figure 2A). We also looked for the co-expression of *ACE2* and *TMPRSS2* with *DPP4, CTSL, DAAM1,* and *PAICS* by using scRNA-Seq in these same cells (Figure 2). This analysis revealed that *DPP4, CTSL, DAAM1*, and *PAICS* are co-expressed at high-levels, while these genes are co-express at low levels with *ACE2* and *TMPRSS2* (Figure 2). Remarkably, we found only three cells co-expressing *ACE2* and *TMPRSS2*. For this reason, we consider that *DPP4, CTSL, DAAM1, and PAICS* may represent candidates of an alternative route for SARS-CoV-2 infection in human placentas. We used The Human Protein Atlas to predict the subcellular location of proteins encoded by our candidates. *DPP4* is predicted as intracellular, membrane, and secreted protein; *CTSL* is a protein located in the Golgi apparatus and additionally in vesicles; *PAICS* is a protein found in the cytosol while *DAAM1* is located in the plasma membrane and cytosol (Figure 1E). Finally, we analyzed the gene expression profile of *ACE2, TMPRSS2, CTSL, DPP4, DAAM1,* and *PAICS* genes on publicly available scRNA-Seq datasets of lung, liver, and thymus fetal tissues. *CTSL, DPP4,* and *DAAM1* were found as highly expressed in fetal cells compared to *ACE2* and *TMPRSS2* in all tissues analyzed (Supplementary Figure 2). Additional investigations may determine the generality and impact of these findings, including the confirmation of vertical transmission.

3. Discussion

Recent literature has shown placenta cells infected with SARS-CoV-2 in pregnant women diagnosed with moderate to severe COVID-19 (*17*, *25*) with findings supporting

the possibility of vertical transmission of SARS-CoV-2 (*17*, *26*). However, few placenta cells express *ACE2* and *TMPRSS2* (*21*, *22*) required for virus entry, raising the question about whether potential non-canonical molecular mechanisms may be involved in the biological cycle of the virus in these cells. Here, we demonstrated by transcriptomic analyses (microarray and scRNA-Seq) and *in silico* predictions of virus-host protein-protein interactions that, despite low-levels of *ACE2* and *TMPRSS2*, villous trophoblast cells express high levels of the potential non-canonical cell-entry mediators *DPP4* and *CTSL*. We also found changes in the expression of *DAAM1* and *PAICS* genes that code for proteins predicted to interact with SARS-CoV proteins during pregnancy. These results provide evidence of potential host-virus PPI that may lead to SARS-CoV-2 infection and replication in the human placenta.

Firstly, we characterized the expression of SARS-CoV-2/SARS-CoV entry-associated receptors and proteases genes, which revealed that *DPP4* and *CTSL* are highly expressed in villous trophoblast cells during pregnancy. DPP4 has a high affinity to the SARS-CoV-2 spike receptor-binding domain, (*27*) and critical DPP4 residues share the SARS-CoV-2-S/DPP4 binding as found for MERS-CoV-S/DPP4 (*27*). In a pioneer study based on SARS-CoV cell entry mechanisms, Simmons et al. (*28*) described a three-step method for host-virus membrane fusion, involving receptor-binding and induced conformational changes in S glycoprotein with subsequent CTSL proteolysis and activation of membrane fusion within endosomes. During the COVID-19 pandemic, it has been further demonstrated that SARS-CoV-2 can use CTSB and CTSL as well as TMPRSS2 for priming host cells (*29*, *30*). These data provide evidence that CTSL is a potentially promising treatment for COVID-19 by blocking coronavirus host cell entry and intracellular replication (*31*). Secondly, we analyzed whether placental development and growth are associated with transcriptional changes in proteins that potentially interact with SARS-CoV. Among the transcripts translated into proteins predicted as interacting with SARS-CoV, *DAAM1* increased with placental development and growth. DAAM1 was previously identified as a regulator of bacteria phagocytosis by regulating filopodia formation and phagocytic uptake in primary human macrophages (*32*). We predicted that DAAM1 potentially interact with the viral protein encoded from open reading frame 8 (ORF8) and the hypothetical protein sars7a of SARS-CoV. The SARS-CoV ORF8 shares

the lowest homology with all SARS-CoV-2 proteins; however, it was previously demonstrated that SARS-CoV-2 ORF8 expression was able to selectively target MHC-I for lysosomal degradation by an autophagy-dependent mechanism in different cell types (*33*). We found that *PAICS* transcript, which is also translated into a protein predicted as interacting with the Nsp3 of SARS-CoV, decreased its levels with placental development and growth. PAICS is an enzyme of de novo purine biosynthesis pathway, which was previously predicted as having a putative interaction with the human influenza A virus (IAV) nucleoprotein and was up-regulated during IAV infection (*34*). The putative interaction of Nsp3 with PAICS is relevant. Nsp3 is one of the 16 non-structural proteins in the replicase ORF1ab gene of SARS-CoV and SARS-CoV-2 (*2*, *35*), and binds to virus RNA and proteins, including the nucleocapsid protein (*36*). Considering the low-levels of *ACE2* and *TMPRSS2* that we found in villous trophoblast cells, our results provide evidence of alternatives cell-entry mediators in the placenta. Moreover, the description of the potential interaction between host and SARS-CoV-2 may provide insights into the mechanisms of placental infection in women with COVID-19.

Cellular and molecular composition play a role in placenta infection and intrauterine transmission of viruses (*37*, *38*). Thus, we finally used single-cell analysis of the syncytiotrophoblast, villous cytotrophoblast, and extravillous trophoblasts - the fetal component of the placenta - that confirmed the low-levels of expression of the canonical entry receptor *ACE2* and *TMPRSS2* genes (*21*, *22*). Conversely, we found that these cells express high-levels of *DPP4* and *CTSL*, two potential mediators of SARS-Cov-2 host cell entry (*27*, *30*) that may contribute to the SARS-CoV-2 infection (*17*, *25*, *26*). It is essential to highlight that our scRNA-Seq analysis showed that the non-canonical *DPP4* and *CTSL* entry genes (*27*, *30*) are highly co-expressed in syncytiotrophoblast, villous cytotrophoblast, and extravillous trophoblasts cells. The transcripts *DAAM1* and *PAICS*, which are translated into proteins predicted as potentially interacting with SARS-CoV-2, were also highly co-expressed with *DPP4* and *CTSL.* These results demonstrate that, although *ACE2* and *TMPRSS2* are poorly expressed in the placenta, other mediators that potentially interact with the virus are highly co-expressed in villous trophoblast cells and, therefore, may represent a valuable alternative route for infection and viral replication.

Although our *in silico* analyses are a starting point, they have limitations. We reanalyzed published placenta datasets with a limited number of samples (microarray = 12 individuals, and scRNA-seq = 5 individuals) and, consequently, validations in a large cohort of samples must be performed. The predicted interactions presented here should also be experimentally validated in infected cells or placenta to circumvent these limitations. Moreover, the analyses of single-cell data should be conducted for the entire period of gestation, considering that we only evaluated single-cell data from the first trimester of pregnancy. The detection of SARS-CoV-2 in the placenta needs to be performed in a large cohort of pregnant women with COVID-19, including asymptomatics. Considering that vertical transmission of SARS-CoV-2 is still debated, the follow-up of newborns from mothers with COVID-19 during pregnancy should be necessary since, if it occurs even in the non-asymptomatic, the long-term consequences are mostly unknown.

In conclusion, despite low-levels of *ACE2* and *TMPRSS2*, our analyses demonstrate that villous trophoblast cells express high levels of potential non-canonical cell-entry mediators *DDP4* and *CTSL*. We also found changes in the expression of the *DAAM1* and *PAICS* genes coding for proteins predicted to interact with SARS-CoV proteins during pregnancy. These results provide new insight into the interaction between SARS-CoV-2 and the host proteins, and indicate that coronaviruses may use multiple mediators for virus infection and replication.

4. Materials and Methods

4.1 Differential expression analysis of the placenta during pregnancy trimesters

We reanalyzed microarray data from villous trophoblast tissues of first (45-59 days, n = 4), second trimester (109-115 days, n = 4), and third trimesters (n = 4) available in Gene Expression Omnibus (GEO), under the accession number GSE9984 (*39*). Next, we identified the DEGs during the pregnancy, by comparing the second trimester and third trimester with the first trimester using the GEO2R tool (https://www.ncbi.nlm.nih.gov/geo/geo2r). Genes with Log2 of Fold Change ≥ |0.5| and False Discovery Rate (FDR) < 0.05 were considered as DEGs. We further grouped the

gene expression profiles during pregnancy by using the K-means clustering analysis based on One Minus Pearson Correlation (Robust Multi-array Average, RMA, normalization log2, K-means = 3).

4.2 Enrichment analysis

We used the Metascape tool (https://metascape.org) (*40*) to perform functional enrichment analysis of the genes lists generated in the clustering and differential expression analyses.

4.3 Placenta proteins that potentially interact with coronaviruses and Zika virus

SARS-CoV-2 cell entry mediators were selected for first screening using the human proteins already described in the COVID-19 Cell Atlas (https://www.covid19cellatlas.org/) and the literature (*1*, *21*, *27*, *30*). Next, we used gene expression data to generated a list of PPIs that potentially interact with human coronaviruses and the ZIKV from the Pathogen–Host Interactome Prediction using Structure Similarity (P-HIPSTer, http://phipster.org/) database (*23*) (Supplementary Table 4 and 5, respectively). SARS-CoV was included in the analysis considering the evolutionary relationship between the novel SARS-CoV-2 (*1*), and ZIKV considering its impact on placental infection and fetal microcephaly (*9*, *37*).

4.4 Tissue-specific gene networks of potential virus-host placenta interactome

The HumanBase webtool (https://hb.flatironinstitute.org) (*41*) was used to generate the tissue-specific gene network of placental genes coding for proteins that potentially interact with SARS-CoV-2 based on P-HIPSTER or that we identified as either associated with COVID-19 or that we hypothesized may be associated with the disease, based on the literature (Supplementary Table 8). We considered co-expression, interaction, transcriptional factor binding, Gene Set Enrichment Analysis (GSEA) perturbations as active interaction sources, applying minimum interaction confidence of 0.07, and a maximum number of 15 genes.

4.5 Single-cell transcriptome analysis of human placentas and fetal tissues

We used the functionalities of the COVID-19 Cell Atlas (https://www.covid19cellatlas.org) to explore single-cell RNA sequencing (scRNA-Seq) data from five samples from first-trimester placentas, previously described by Vento-Tormo et al., (*42*). The expression of placental candidates genes potentially interacting with SARS-CoVs was visualized in placental cell types using the "interactive viewer" developed by cellxgene v0.15.0 (https://cellxgene.cziscience.com). We also characterized the gene expression profile of canonical and non-canonical placental mediators of viruses interaction per cell using cellxgene v0.15.0 bar plots. The placental single-cell transcriptome is available for re-analysis at Human Cell Atlas Data Portal (https://data.humancellatlas.org) or E- MTAB-6701 (https://www.ebi.ac.uk/arrayexpress). We applied this same strategy to investigate the gene expression of our candidates using scRNA-seq in human fetal tissues: lung (*43*), liver (*44*), and thymus (*45*). Last accessed June 2020.

4.6 Data representation and analysis

Morpheus (https://software.broadinstitute.org/morpheus/) was used to generate the heatmaps and to perform the clustering analyses. The Venn diagram was constructed using the Van de Peer Lab software (http://bioinformatics.psb.ugent.be/webtools/Venn/). Biorender was used to design cell images (https://app.biorender.com/).

Data Availability Statement

All data is available in the manuscript.

References

1. P. Zhou, X.-L. Yang, X.-G. Wang, B. Hu, L. Zhang, W. Zhang, H.-R. Si, Y. Zhu, B. Li, C.-L. Huang, H.-D. Chen, J. Chen, Y. Luo, H. Guo, R.-D. Jiang, M.-Q. Liu, Y. Chen, X.-R. Shen, X. Wang, X.-S. Zheng, K. Zhao, Q.-J. Chen, F. Deng, L.-L. Liu, B. Yan, F.-X. Zhan, Y.-Y. Wang, G.-F. Xiao, Z.-L. Shi, A pneumonia outbreak associated with a new coronavirus of probable bat origin. *Nature*. 579, 270–273 (2020).

2. F. Wu, S. Zhao, B. Yu, Y.-M. Chen, W. Wang, Z.-G. Song, Y. Hu, Z.-W. Tao, J.-H. Tian, Y.-Y. Pei, M.-L. Yuan, Y.-L. Zhang, F.-H. Dai, Y. Liu, Q.-M. Wang, J.-J. Zheng, L. Xu, E. C. Holmes, Y.-Z. Zhang, A new coronavirus associated with human respiratory disease in China. *Nature*. 579, 265–269 (2020).

3. E. Dong, H. Du, L. Gardner, An interactive web-based dashboard to track COVID-19 in real time. *Lancet Infect. Dis.* 20, 533–534 (2020).

4. The OpenSAFELY Collaborative, E. Williamson, A. J. Walker, K. J. Bhaskaran, S. Bacon, C. Bates, C. E. Morton, H. J. Curtis, A. Mehrkar, D. Evans, P. Inglesby, J. Cockburn, H. I. Mcdonald, B. MacKenna, L. Tomlinson, I. J. Douglas, C. T. Rentsch, R. Mathur, A. Wong, R. Grieve, D. Harrison, H. Forbes, A. Schultze, R. T. Croker, J. Parry, F. Hester, S. Harper, R. Perera, S. Evans, L. Smeeth, B. Goldacre, "OpenSAFELY: factors associated with COVID-19-related hospital death in the linked electronic health records of 17 million adult NHS patients." (preprint, Epidemiology, 2020), , doi:10.1101/2020.05.06.20092999.

5. J. Zhang, X. Dong, Y. Cao, Y. Yuan, Y. Yang, Y. Yan, C. A. Akdis, Y. Gao, *Allergy*, in press, doi:10.1111/all.14238.

6. D. A. Schwartz, A. L. Graham, Potential Maternal and Infant Outcomes from Coronavirus 2019-nCoV (SARS-CoV-2) Infecting Pregnant Women: Lessons from SARS, MERS, and Other Human Coronavirus Infections. *Viruses*. 12, 194 (2020).

7. F. Qadri, F. Mariona, Pregnancy affected by SARS-CoV-2 infection: a flash report from Michigan. *J. Matern. Fetal Neonatal Med.*, 1–3 (2020).

8. L. Pereira, Congenital Viral Infection: Traversing the Uterine-Placental Interface. *Annu. Rev. Virol.* 5, 273–299 (2018).

9. T. C. Pierson, M. S. Diamond, The emergence of Zika virus and its new clinical syndromes. *Nature*. 560, 573–581 (2018).

10. Y. Hashimoto, X. Sheng, L. A. Murray-Nerger, I. M. Cristea, Temporal dynamics of protein complex formation and dissociation during human cytomegalovirus infection. *Nat. Commun.* 11, 806 (2020).

11. H. Chen, J. Guo, C. Wang, F. Luo, X. Yu, W. Zhang, J. Li, D. Zhao, D. Xu, Q. Gong, J. Liao, H. Yang, W. Hou, Y. Zhang, Clinical characteristics and intrauterine vertical transmission potential of COVID-19 infection in nine pregnant women: a retrospective review of medical records. *The Lancet*. 395, 809–815 (2020).

12. Z. Yang, Y. Liu, *Am. J. Perinatol.*, in press, doi:10.1055/s-0040-1712161.

13. O. Celik, A. Saglam, B. Baysal, I. E. Derwig, N. Celik, M. Ak, S. N. Aslan, M. Ulas, A. Ersahin, A. T. Tayyar, B. Duran, S. Aydin, Factors preventing materno-fetal transmission of SARS-CoV-2. *Placenta*. 97, 1–5 (2020).

14. L. Dong, J. Tian, S. He, C. Zhu, J. Wang, C. Liu, J. Yang, Possible Vertical Transmission of SARS-CoV-2 From an Infected Mother to Her Newborn. *JAMA* (2020), doi:10.1001/jama.2020.4621.

15. H. Zeng, C. Xu, J. Fan, Y. Tang, Q. Deng, W. Zhang, X. Long, Antibodies in Infants Born to Mothers With COVID-19 Pneumonia. *JAMA* (2020), doi:10.1001/jama.2020.4861.

16. D. W. Kimberlin, S. Stagno, Can SARS-CoV-2 Infection Be Acquired In Utero?: More Definitive Evidence Is Needed. *JAMA* (2020), doi:10.1001/jama.2020.4868.

17. L. Patanè, D. Morotti, M. R. Giunta, C. Sigismondi, M. G. Piccoli, L. Frigerio, G. Mangili, M. Arosio, G. Cornolti, Vertical transmission of COVID-19: SARS-CoV-2 RNA on the fetal side of the placenta in pregnancies with COVID-19 positive mothers and neonates at birth. *Am. J. Obstet. Gynecol. MFM*, 100145 (2020).

18. S. Schoenmakers, P. Snijder, R. Verdijk, T. Kuiken, S. Kamphuis, L. Koopman, T. Krasemann, M. Rousian, M. Broekhuizen, E. Steegers, M. Koopmans, P. Fraaij, I. Reiss, "SARS-CoV-2 placental infection and inflammation leading to fetal distress and neonatal multi-organ failure in an asymptomatic woman" (preprint, Infectious Diseases (except HIV/AIDS), 2020), , doi:10.1101/2020.06.08.20110437.

19. Y. Wan, J. Shang, R. Graham, R. S. Baric, F. Li, Receptor Recognition by the Novel Coronavirus from Wuhan: an Analysis Based on Decade-Long Structural Studies of SARS Coronavirus. *J. Virol.* 94, e00127-20, /jvi/94/7/JVI.00127-20.atom (2020).

20. M. Letko, A. Marzi, V. Munster, Functional assessment of cell entry and receptor usage for SARS-CoV-2 and other lineage B betacoronaviruses. *Nat. Microbiol.* 5, 562–569 (2020).

21. HCA Lung Biological Network, W. Sungnak, N. Huang, C. Bécavin, M. Berg, R. Queen, M. Litvinukova, C. Talavera-López, H. Maatz, D. Reichart, F. Sampaziotis, K. B. Worlock, M. Yoshida, J. L. Barnes, SARS-CoV-2 entry factors are highly expressed in nasal epithelial cells together with innate immune genes. *Nat. Med.* 26, 681–687 (2020).

22. R. Pique-Regi, R. Romero, A. L. Tarca, F. Luca, Y. Xu, A. Alazizi, Y. Leng, C.-D. Hsu, N. Gomez-Lopez, "Does the human placenta express the canonical cell entry mediators for SARS-CoV-2?" (preprint, Genomics, 2020), , doi:10.1101/2020.05.18.101485.

23. E. D. Shanes, L. B. Mithal, S. Otero, H. A. Azad, E. S. Miller, J. A. Goldstein, Placental Pathology in COVID-19. *Am. J. Clin. Pathol.* 154, 23–32 (2020).

24. G. Lasso, S. V. Mayer, E. R. Winkelmann, T. Chu, O. Elliot, J. A. Patino-Galindo, K. Park, R. Rabadan, B. Honig, S. D. Shapira, A Structure-Informed Atlas of Human-Virus Interactions. *Cell*. 178, 1526-1541.e16 (2019).

25. C. A. Penfield, S. G. Brubaker, M. A. Limaye, J. Lighter, A. J. Ratner, K. M. Thomas, J. A. Meyer, A. S. Roman, Detection of severe acute respiratory syndrome coronavirus 2 in placental and fetal membrane samples. *Am. J. Obstet. Gynecol. MFM*, 100133 (2020).

26. H. Hosier, S. Farhadian, R. Morotti, U. Deshmukh, A. Lu-Culligan, K. Campbell, Y. Yasumoto, C. Vogels, A. Casanovas-Massana, P. Vijayakumar, B. Geng, C. Odio, J. Fournier, A. Brito, J. Fauver, F. Liu, T. Alpert, R. Tal, K. Szigeti-Buck, S. Perincheri, C. Larsen, A. Gariepy, G. Aguilar, K. Fardelmann, M. Harigopal, H. Taylor, C. Pettker, A. Wyllie, C. Dela Cruz, A. Ring, N. Grubaugh, A. Ko, T. Horvath, A. Iwasaki, U. Reddy, H. Lipkind, “SARS-CoV-2 Infection of the Placenta” (preprint, Sexual and Reproductive Health, 2020), , doi:10.1101/2020.04.30.20083907.

27. Y. Li, Z. Zhang, L. Yang, X. Lian, Y. Xie, S. Li, S. Xin, P. Cao, J. Lu, The MERS-CoV Receptor DPP4 as a Candidate Binding Target of the SARS-CoV-2 Spike. *iScience*. 23, 101160 (2020).

28. G. Simmons, D. N. Gosalia, A. J. Rennekamp, J. D. Reeves, S. L. Diamond, P. Bates, Inhibitors of cathepsin L prevent severe acute respiratory syndrome coronavirus entry. *Proc. Natl. Acad. Sci.* 102, 11876–11881 (2005).

29. X. Ou, Y. Liu, X. Lei, P. Li, D. Mi, L. Ren, L. Guo, R. Guo, T. Chen, J. Hu, Z. Xiang, Z. Mu, X. Chen, J. Chen, K. Hu, Q. Jin, J. Wang, Z. Qian, Characterization of spike glycoprotein of SARS-CoV-2 on virus entry and its immune cross-reactivity with SARS-CoV. *Nat. Commun.* 11, 1620 (2020).

30. M. Hoffmann, H. Kleine-Weber, S. Schroeder, N. Krüger, T. Herrler, S. Erichsen, T. S. Schiergens, G. Herrler, N.-H. Wu, A. Nitsche, M. A. Müller, C. Drosten, S. Pöhlmann, SARS-CoV-2 Cell Entry Depends on ACE2 and TMPRSS2 and Is Blocked by a Clinically Proven Protease Inhibitor. *Cell*. 181, 271-280.e8 (2020).

31. T. Liu, S. Luo, P. Libby, G.-P. Shi, Cathepsin L-selective inhibitors: A potentially promising treatment for COVID-19 patients. *Pharmacol. Ther.*, 107587 (2020).

32. A. Hoffmann, X. Naj, S. Linder, Daam1 is a regulator of filopodia formation and phagocytic uptake of *Borrelia burgdorferi* by primary human macrophages. *FASEB J.* 28, 3075–3089 (2014).

33. Y. Zhang, J. Zhang, Y. Chen, B. Luo, Y. Yuan, F. Huang, T. Yang, F. Yu, J. Liu, B. Liu, Z. Song, J. Chen, T. Pan, X. Zhang, Y. Li, R. Li, W. Huang, F. Xiao, H. Zhang, “The ORF8 Protein of SARS-CoV-2 Mediates Immune Evasion through Potently Downregulating MHC-I” (preprint, Microbiology, 2020), , doi:10.1101/2020.05.24.111823.

34. A. Generous, M. Thorson, J. Barcus, J. Jacher, M. Busch, H. Sleister, Identification of putative interactions between swine and human influenza A virus nucleoprotein and human host proteins. *Virol. J.* 11, 228 (2014).

35. L. Enjuanes, L. Enjuanes, *Coronavirus replication and reverse genetics* (Springer, Berlin; New York, 2005).

36. J. Lei, Y. Kusov, R. Hilgenfeld, Nsp3 of coronaviruses: Structures and functions of a large multi-domain protein. *Antiviral Res.* 149, 58–74 (2018).

37. J. Barbeito-Andrés, P. Pezzuto, L. M. Higa, A. A. Dias, J. M. Vasconcelos, T. M. P. Santos, J. C. C. G. Ferreira, R. O. Ferreira, F. F. Dutra, A. D. Rossi, R. V. Barbosa, C. K. N. Amorim, M. P. C. De Souza, L. Chimelli, R. S. Aguiar, P. N. Gonzalez, F. A. Lara, M. C. Castro, Z. Molnár, R. T. Lopes, M. T. Bozza, J. L. S. G. Vianez, C. G. Barbeito, P. Cuervo, M. Bellio, A. Tanuri, P. P. Garcez, Congenital Zika syndrome is associated with maternal protein malnutrition. *Sci. Adv.* 6, eaaw6284 (2020).

38. H. Koi, J. Zhang, S. Parry, The Mechanisms of Placental Viral Infection. *Ann. N. Y. Acad. Sci.* 943, 148–156 (2001).

39. A. M. Mikheev, T. Nabekura, A. Kaddoumi, T. K. Bammler, R. Govindarajan, M. F. Hebert, J. D. Unadkat, Profiling Gene Expression in Human Placentae of Different Gestational Ages: An OPRU* Network and UW SCOR Study. *Reprod. Sci.* 15, 866–877 (2008).

40. Y. Zhou, B. Zhou, L. Pache, M. Chang, A. H. Khodabakhshi, O. Tanaseichuk, C. Benner, S. K. Chanda, Metascape provides a biologist-oriented resource for the analysis of systems-level datasets. *Nat. Commun.* 10, 1523 (2019).

41. C. S. Greene, A. Krishnan, A. K. Wong, E. Ricciotti, R. A. Zelaya, D. S. Himmelstein, R. Zhang, B. M. Hartmann, E. Zaslavsky, S. C. Sealfon, D. I. Chasman, G. A. FitzGerald, K. Dolinski, T. Grosser, O. G. Troyanskaya, Understanding multicellular function and disease with human tissue-specific networks. *Nat. Genet.* 47, 569–576 (2015).

42. R. Vento-Tormo, M. Efremova, R. A. Botting, M. Y. Turco, M. Vento-Tormo, K. B. Meyer, J.-E. Park, E. Stephenson, K. Polański, A. Goncalves, L. Gardner, S. Holmqvist, J.

Henriksson, A. Zou, A. M. Sharkey, B. Millar, B. Innes, L. Wood, A. Wilbrey-Clark, R. P. Payne, M. A. Ivarsson, S. Lisgo, A. Filby, D. H. Rowitch, J. N. Bulmer, G. J. Wright, M. J. T. Stubbington, M. Haniffa, A. Moffett, S. A. Teichmann, Single-cell reconstruction of the early maternal–fetal interface in humans. *Nature*. 563, 347–353 (2018).

43. A. J. Miller, Q. Yu, M. Czerwinski, Y.-H. Tsai, R. F. Conway, A. Wu, E. M. Holloway, T. Walker, I. A. Glass, B. Treutlein, J. G. Camp, J. R. Spence, In Vitro and In Vivo Development of the Human Airway at Single-Cell Resolution. *Dev. Cell*. 53, 117-128.e6 (2020).

44. D.-M. Popescu, R. A. Botting, E. Stephenson, K. Green, S. Webb, L. Jardine, E. F. Calderbank, K. Polanski, I. Goh, M. Efremova, M. Acres, D. Maunder, P. Vegh, Y. Gitton, J.-E. Park, R. Vento-Tormo, Z. Miao, D. Dixon, R. Rowell, D. McDonald, J. Fletcher, E. Poyner, G. Reynolds, M. Mather, C. Moldovan, L. Mamanova, F. Greig, M. D. Young, K. B. Meyer, S. Lisgo, J. Bacardit, A. Fuller, B. Millar, B. Innes, S. Lindsay, M. J. T. Stubbington, M. S. Kowalczyk, B. Li, O. Ashenberg, M. Tabaka, D. Dionne, T. L. Tickle, M. Slyper, O. Rozenblatt-Rosen, A. Filby, P. Carey, A.-C. Villani, A. Roy, A. Regev, A. Chédotal, I. Roberts, B. Göttgens, S. Behjati, E. Laurenti, S. A. Teichmann, M. Haniffa, Decoding human fetal liver haematopoiesis. *Nature*. 574, 365–371 (2019).

45. J.-E. Park, R. A. Botting, C. Domínguez Conde, D.-M. Popescu, M. Lavaert, D. J. Kunz, I. Goh, E. Stephenson, R. Ragazzini, E. Tuck, A. Wilbrey-Clark, K. Roberts, V. R. Kedlian, J. R. Ferdinand, X. He, S. Webb, D. Maunder, N. Vandamme, K. T. Mahbubani, K. Polanski, L. Mamanova, L. Bolt, D. Crossland, F. de Rita, A. Fuller, A. Filby, G. Reynolds, D. Dixon, K. Saeb-Parsy, S. Lisgo, D. Henderson, R. Vento-Tormo, O. A. Bayraktar, R. A. Barker, K. B. Meyer, Y. Saeys, P. Bonfanti, S. Behjati, M. R. Clatworthy, T. Taghon, M. Haniffa, S. A. Teichmann, A cell atlas of human thymic development defines T cell repertoire formation. *Science*. 367 (2020), doi:10.1126/science.aay3224.

Funding

This research was supported by the National Council for Scientific and Technological Development, CNPq (Process 311530/2019-2 to RFC, and Process 310663/2018-0 to LAJ, and scholarship #870415/1997-2 to SSC), and by Fundação de Amparo à Pesquisa do Estado de São Paulo (Process 2012/13961-6 to RFC, Process 2017/01063-7 to LAJ, and scholarship 2017/08716-6 to FBC).

Author contributions

Conceptualization, F.B.C, L.A.J.; methodology, F.B.C., R.F.C., S.S.C., L.A.J.; formal analysis, F.B.C., C.R.N., R.F.C., S.S.C., L.A.J; investigation, F.B.C., C.R.N., R.F.C., S.S.C., L.A.J.; resources, R.F.C., L.A.J.; data curation, F.B.C., C.R.N., R.F.C., S.S.C., L.A.J.; writing—original draft preparation, F.B.C., R.F.C., S.S.C., L.A.J.; writing—review and editing, all authors; supervision, R.F.C., L.A.J; project administration, R.F.C., L.A.J; funding acquisition, R.F.C., L.A.J.

Competing interests

The author declares no competing interests.

Ethical Approval

Not applicable as we used publicly available data.

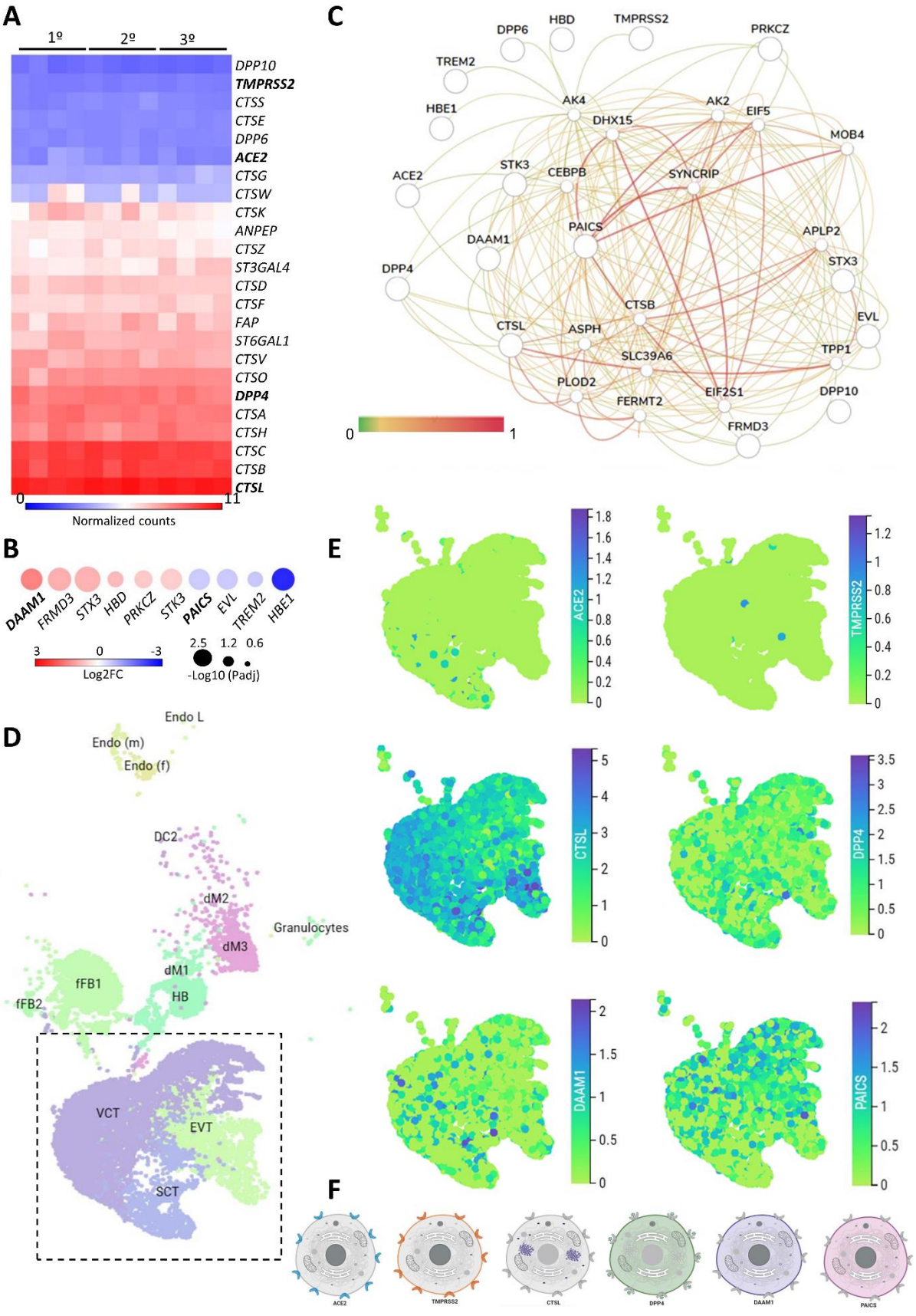
A
1º
2º
3º
DPP10
TMPRSS2
CTSS
CTSE
DPP6
ACE2
CTSG
CTSW
CTSK
ANPEP
CTSZ
ST3GAL4
CTSD
CTSF
FAP
ST6GAL1
CTSV
CTSO
DPP4
CTSA
CTSH
CTSC
CTSB
CTSL
0
11
Normalized counts
B
DAAM1
FRMD3
STX3
HBD
PRKCZ
STK3
PAICS
EVL
TREM2
HBE1
3
0
-3
Log2FC
2.5
1.2
0.6
-Log10 (Padj)
C
DPP6
HBD
TMPRSS2
PRKCZ
TREM2
HBE1
AK4
AK2
EIF5
DHX15
MOB4
ACE2
STK3
CEBPB
SYNCRIP
PAICS
DAAM1
APLP2
DPP4
STX3
CTSB
EVL
CTSL
ASPH
SLC39A6
TPP1
PLOD2
EIF2S1
DPP10
FERMT2
FRMD3
0
1
D
Endo L
Endo (m)
Endo (f)
DC2
dM2
Granulocytes
dM3
dM1
fFB1
HB
fFB2
VCT
EVT
SCT
E
ACE2
TMPRSS2
CTSL
DPP4
DAAM1
PAICS
F
ACE2
TMPRSS2
CTSL
DPP4
DAAM1
PAICS

Figure 1. The expression landscape of human placenta proteins potentially interacting with SARS-CoV-2. A. Heatmap illustrating gene expression (counts RMA normalized) of SARS-CoV-2 interacting proteins from placental samples in the first, second and third trimester of gestation (GSE9984)(*39*). B. Heat-scatter plot presenting ten differentially expressed genes in the placenta that encode proteins potentially interacting with SARS-CoV as predicted by the P-HIPSter (http://phipster.org/) database. The color and size of the circles correspond to the log2FC and -log10 transformed FDR adjusted P-value, respectively. Fold change represents the gene expression of placenta samples from the third trimester of gestation compared with the first trimester. Bolded genes represent the six candidates selected for the further scRNA-seq evaluations. C. Tissue-specific gene network of placenta proteins predicted to interact with coronaviruses. The network was generated using the HumanBase (https://hb.flatironinstitute.org/) online tool. D. Dimensionality reduction demonstrates different cell populations identified in five first-trimester human placental samples in a Uniform Manifold Approximation and Projection (UMAP) plot, by using scRNA-Seq data from Vento-Tormo et al., (*42*). The images were generated using the COVID-19 Cell Atlas (https://www.covid19cellatlas.org) functionalities. E. UMAP plots representing the gene expression (log-transformed normalized counts) of *ACE2*, *TMPRSS2*, *CTSL*, *DPP4*, *DAAM1,* and *PAICS* in human placental cells from the syncytiotrophoblast, villous cytotrophoblast, and extravillous trophoblast. The images were generated using COVID-19 Cell Atlas (https://www.covid19cellatlas.org) functionalities. F. Cell illustrations depicting the protein localization of ACE2, TMPRSS2, CTSL, DPP4, DAAM1, and PAICS in cell compartments, as described in the Human Protein Atlas database (http://www.proteinatlas.org). Illustrations were created using BioRender App (https://biorender.com/). RMA: Robust Multichip Average; FC: Fold Change; FDR: false discovery rate; Padj: adjusted P-value; SCT, syncytiotrophoblast; VCT, villous cytotrophoblast; EVT, extravillous trophoblast; HB, Hofbauer cells; FB: fibroblasts; dM, decidual macrophages; Endo, endothelial cells; l, lymphatic; m, maternal; f, fetal.

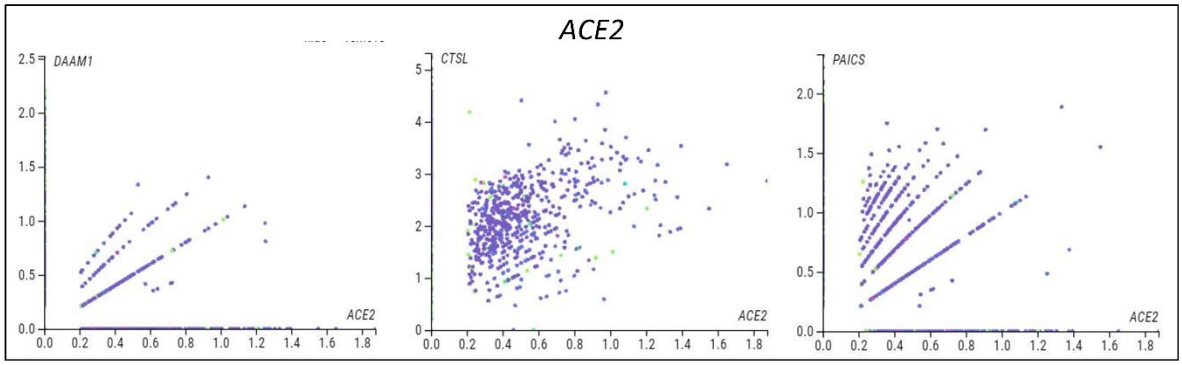
ACE2
DAAM1
ACE2
CTSL
ACE2
PAICS
ACE2

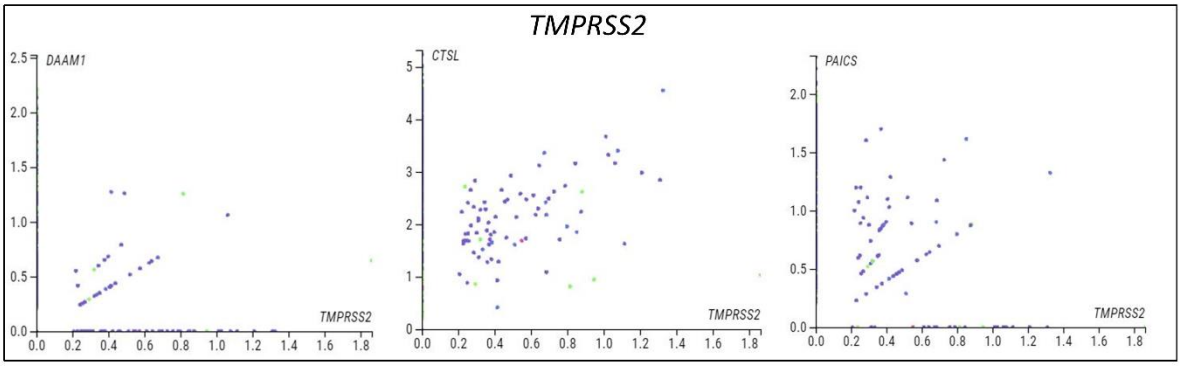
TMPRSS2
DAAM1
TMPRSS2
CTSL
TMPRSS2
PAICS
TMPRSS2

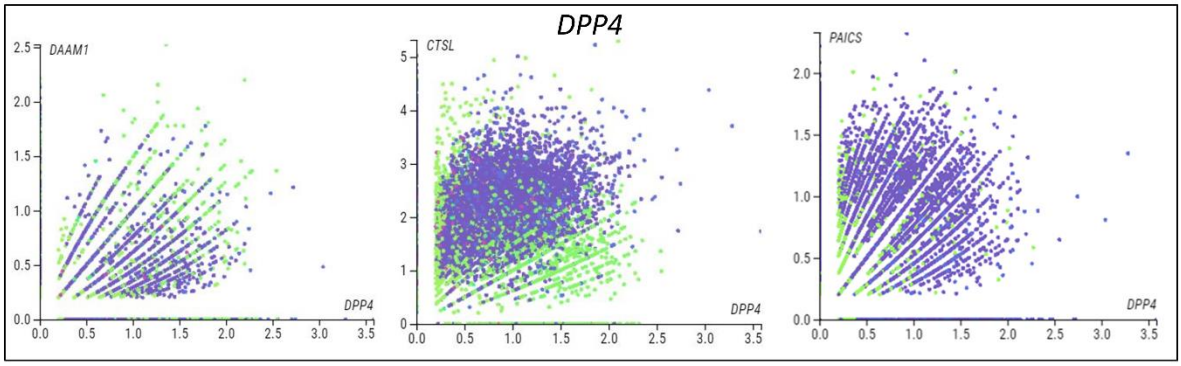
DPP4
DAAM1
DPP4
CTSL
DPP4
PAICS
DPP4

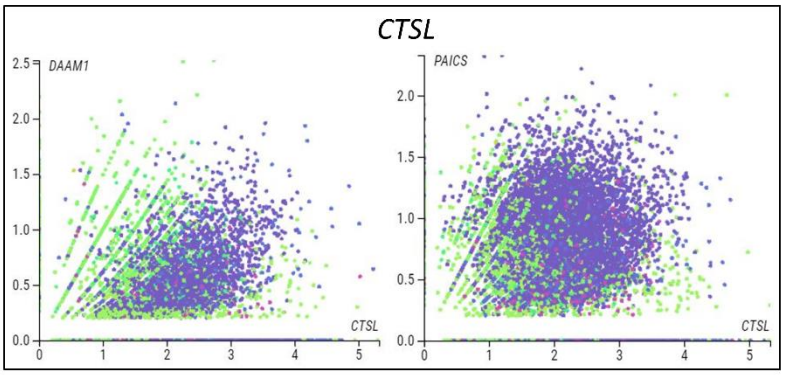
CTSL
DAAM1
CTSL
PAICS
CTSL

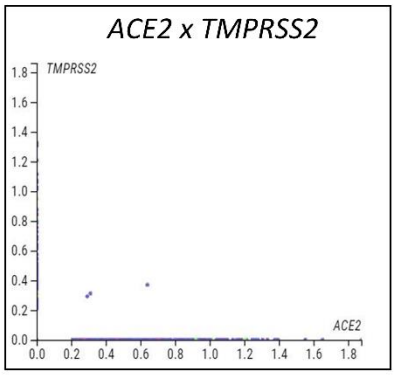
ACE2 x TMPRSS2
TMPRSS2
ACE2

Figure 2. Single-cell analysis of the human placenta indicates potential non-canonical routes of SARS-CoV-2. A. Co-expression analysis of *DAAM1*, *CTSL*, DPP4, and *PAICS* with the canonical virus entry-associated genes *ACE2* and *TMPRSS2*. B. Co-expression analysis of *DAAM1* and *PAICS* with the non-canonical virus entry genes *DPP4* and *CTLS*. The images were generated using COVID-19 Cell Atlas (https://www.covid19cellatlas.org) functionalities.

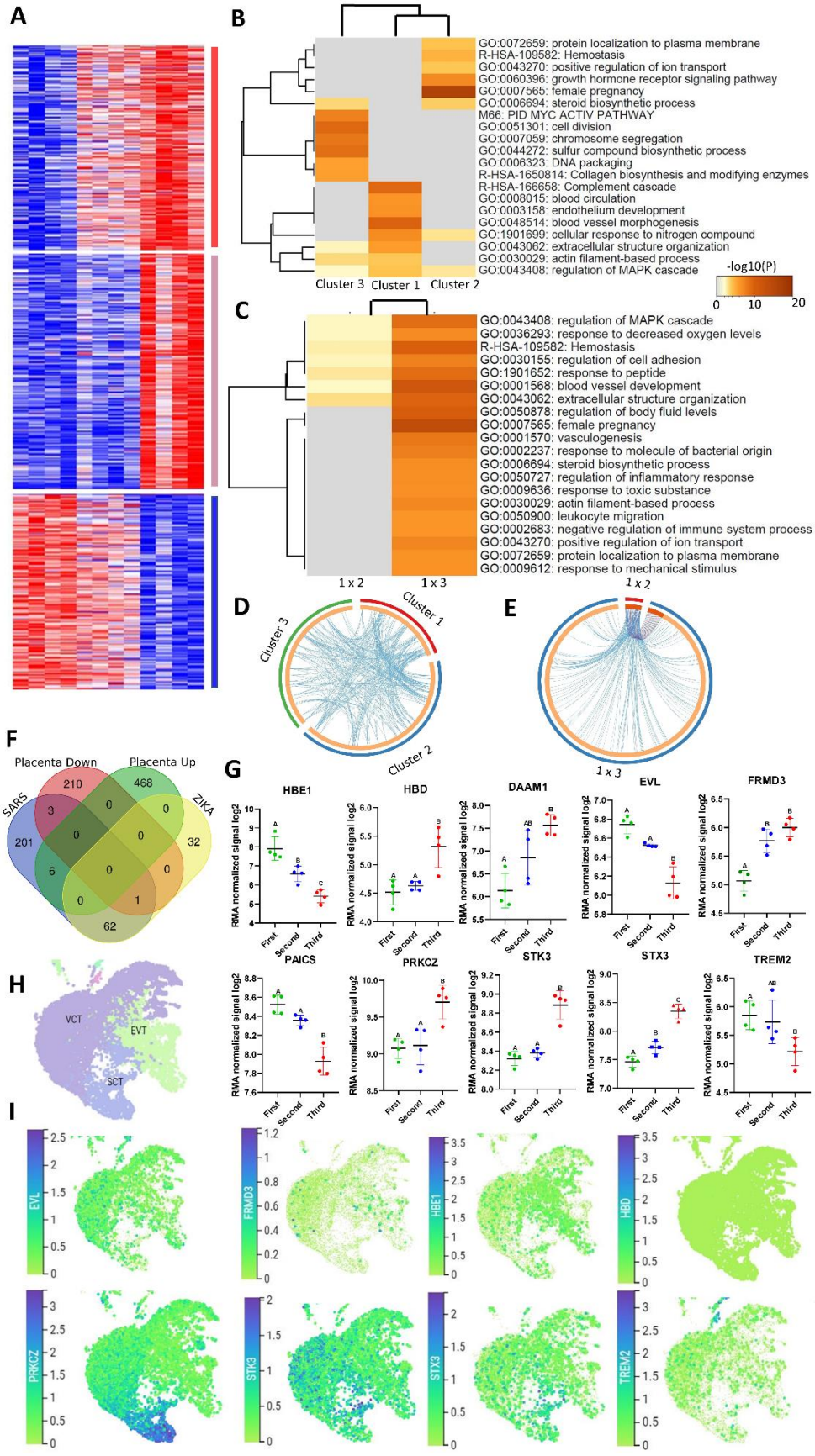
A
B
GO:0072659: protein localization to plasma membrane
R-HSA-109582: Hemostasis
GO:0043270: positive regulation of ion transport
GO:0060396: growth hormone receptor signaling pathway
GO:0007565: female pregnancy
GO:0006694: steroid biosynthetic process
M66: PID MYC ACTIV PATHWAY
GO:0051301: cell division
GO:0007059: chromosome segregation
GO:0044272: sulfur compound biosynthetic process
GO:0006323: DNA packaging
R-HSA-1650814: Collagen biosynthesis and modifying enzymes
R-HSA-166658: Complement cascade
GO:0008015: blood circulation
GO:0003158: endothelium development
GO:0048514: blood vessel morphogenesis
GO:1901699: cellular response to nitrogen compound
GO:0043062: extracellular structure organization
GO:0030029: actin filament-based process
GO:0043408: regulation of MAPK cascade
Cluster 3
Cluster 1
Cluster 2
-log10(P)
0
10
20
C
GO:0043408: regulation of MAPK cascade
GO:0036293: response to decreased oxygen levels
R-HSA-109582: Hemostasis
GO:0030155: regulation of cell adhesion
GO:1901652: response to peptide
GO:0001568: blood vessel development
GO:0043062: extracellular structure organization
GO:0050878: regulation of body fluid levels
GO:0007565: female pregnancy
GO:0001570: vasculogenesis
GO:0002237: response to molecule of bacterial origin
GO:0006694: steroid biosynthetic process
GO:0050727: regulation of inflammatory response
GO:0009636: response to toxic substance
GO:0030029: actin filament-based process
GO:0050900: leukocyte migration
GO:0002683: negative regulation of immune system process
GO:0043270: positive regulation of ion transport
GO:0072659: protein localization to plasma membrane
GO:0009612: response to mechanical stimulus
1 x 2
1 x 3
D
Cluster 3
Cluster 1
Cluster 2
E
1 x 2
1 x 3
F
Placenta Down
Placenta Up
SARS
ZIKA
210
468
201
32
3
0
6
62
1
G
HBE1
HBD
DAAM1
EVL
FRMD3
PAICS
PRKCZ
STK3
STX3
TREM2
RMA normalized signal log2
First
Second
Third
H
VCT
EVT
SCT
I
EVL
FRMD3
HBE1
HBD
PRKCZ
STK3
STX3
TREM2

Supplementary Figure 1. Gene expression profile of gestational trimesters and its potential to interact with SARS-CoV-2 proteins. A. Heatmap illustrates the expression (counts RMA normalized) of placenta differentially expressed genes (DEGs) from the three trimesters (GSE9984). Clustering analysis was performed based on One Minus Pearson Correlation and k-means analysis generated three clusters related to the increase or decrease of the gene expression during the gestation. Cluster 1 is represented by the red bar, cluster 2 by the pink bar, and cluster 3 by the blue bar. B. Functional enrichment analysis generated in the Metascape tool (https://metascape.org) [DOI: 10.1038/s41467-019-09234-6] from each cluster found in the placenta DEGs. C. Functional enrichment analysis generated in the Metascape tool from DEGs belonging to the comparison of first versus second trimester and first versus term placentas. D. Circus plot showing overlapped functional enriched terms from the gene lists of the clusters (1, 2 and 3). E. Circus plot showing the overlapping between the functional enriched terms generated from DEGs of first versus second trimester and DEGs from first trimester versus term placentas. F. Venn Diagram showing the DEGs shared by the placenta (up and down), human protein of expected interaction with SARS-CoV, and human protein of expected interaction with ZIKA virus. G. Box plot showing the expression of the 10 DEGs encoding for proteins with expected interaction with SARS-CoV. H-I. Single-cell gene expression analyses in placental cells types using scRNA-Seq data from Vento-Tormo et al, 20181. Dimensionality reduction demonstrates different cell populations identified in five human placental samples in a Uniform Manifold Approximation and Projection (UMAP) plot. SCT, syncytiotrophoblast; VCT, villous cytotrophoblast; EVT, extravillous trophoblast. The images were generated using COVID-19 Cell Atlas (https://www.covid19cellatlas.org) functionalities. RMA: Robust Multichip Average.

A

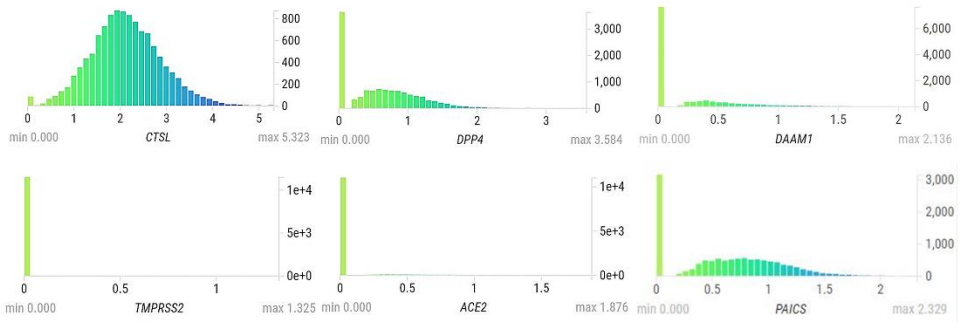
min 0.000 CTSL max 5.323
min 0.000 DPP4 max 3.584
min 0.000 DAAM1 max 2.136
min 0.000 TMPRSS2 max 1.325
min 0.000 ACE2 max 1.876
min 0.000 PAICS max 2.329

B

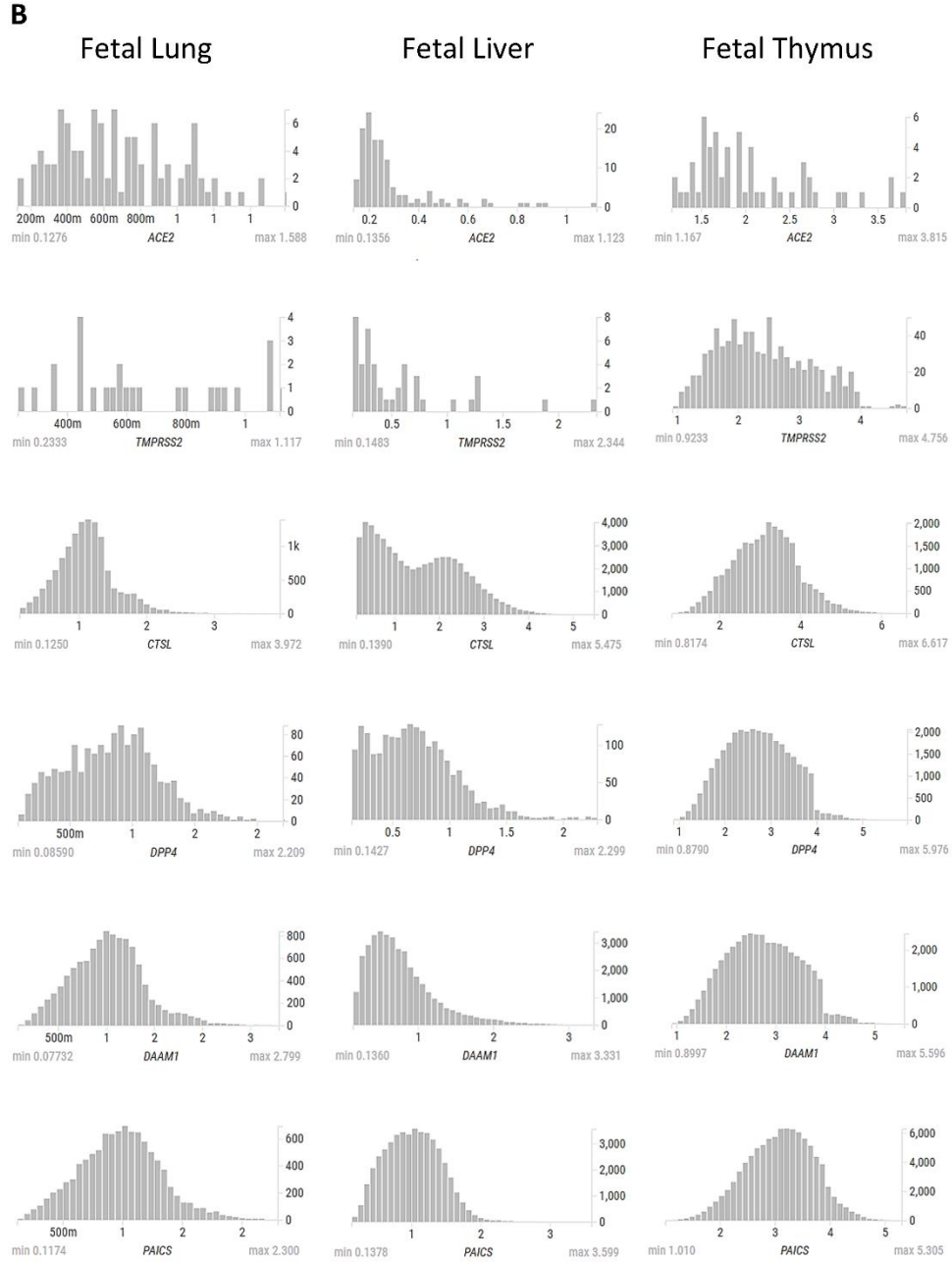
Fetal Lung
Fetal Liver
Fetal Thymus
min 0.1276 ACE2 max 1.588
min 0.1356 ACE2 max 1.123
min 1.167 ACE2 max 3.815
min 0.2333 TMPRSS2 max 1.117
min 0.1483 TMPRSS2 max 2.344
min 0.9233 TMPRSS2 max 4.756
min 0.1250 CTSL max 3.972
min 0.1390 CTSL max 5.475
min 0.8174 CTSL max 6.617
min 0.08590 DPP4 max 2.209
min 0.1427 DPP4 max 2.299
min 0.8790 DPP4 max 5.976
min 0.07732 DAAM1 max 2.799
min 0.1360 DAAM1 max 3.331
min 0.8997 DAAM1 max 5.596
min 0.1174 PAICS max 2.300
min 0.1378 PAICS max 3.599
min 1.010 PAICS max 5.305

Supplementary Figure 2. Gene expression of ACE2, TMPRSS2, CTSL, DPP4, DAAM1, and PAICS in scRNA-seq of fetal tissues. A. Bar plots representing the gene expression (log-transformed normalized counts) of *ACE2, TMPRSS2, CTSL, DPP4, DAAM1*, and *PAICS* in human placental tissues (Vento-Tormo et al., 2018). X-axis indicates log-transformed normalized counts while Y-axis indicates the amount of cell expressing the gene. B. Bar plots representing the gene expression (log-transformed normalized counts) of *ACE2, TMPRSS2, CTSL, DPP4, DAAM1*, and *PAICS* in human fetal lung (Miller et al., 2020), liver (Popescu et al., 2019), and thymus (Park et al., 2020). X-axis indicates log-transformed normalized counts while Y-axis indicates the amount of cell expressing the gene. The images were generated using COVID-19 Cell Atlas (https://www.covid19cellatlas.org) functionalities and the cells not expressing counts were omitted from the plot.

Supplementary Table 1. Differentially expressed genes in placenta tissue during the gestation (1º trimester x 2º trimester and 1º trimester x 2º trimester; Log2FC >= |0.5|; FDR< 0.05).

Supplementary Table 2. Functional enrichment analysis generated in the Metascape tool (https://metascape.org) [DOI: 10.1038/s41467-019-09234-6] for each cluster generate for placenta gene expression during gestation.

Supplementary Table 3. Functional enrichment analysis list generated in the Metascape tool (https://metascape.org) [DOI: 10.1038/s41467-019-09234-6] for DEGs in the placenta tissues (1º trimester x 2º trimester and 1º trimester x 2º trimester.

Supplementary Table 4. Human-SARS-CoV Interactome based on the in silico computational framework P-HIPSTer (http://phipster.org/).

Supplementary Table 5. Human-ZIKA Interactome based on the in silico computational framework P-HIPSTer (http://phipster.org/).

Supplementary Table 6. The Human-SARS-CoV interactome obtained in the P-HIPSTer (http://phipster.org/) for placenta.

Supplementary Table 7. The Human-ZIKA interactome obtained in the P-HIPSTer (http://phipster.org/) for placenta.

Supplementary table 8. Human-SARs Interactome based on literature.